Advances in High Energy Physics

Applications of the Holographic Duality to Strongly Coupled Quantum Systems

Lead Guest Editor: Li Li
Guest Editors: Hai-Qing Zhang, Song He, Zhang-Yu Nie, Yun-Long Zhang, and Bum-Hoon Lee

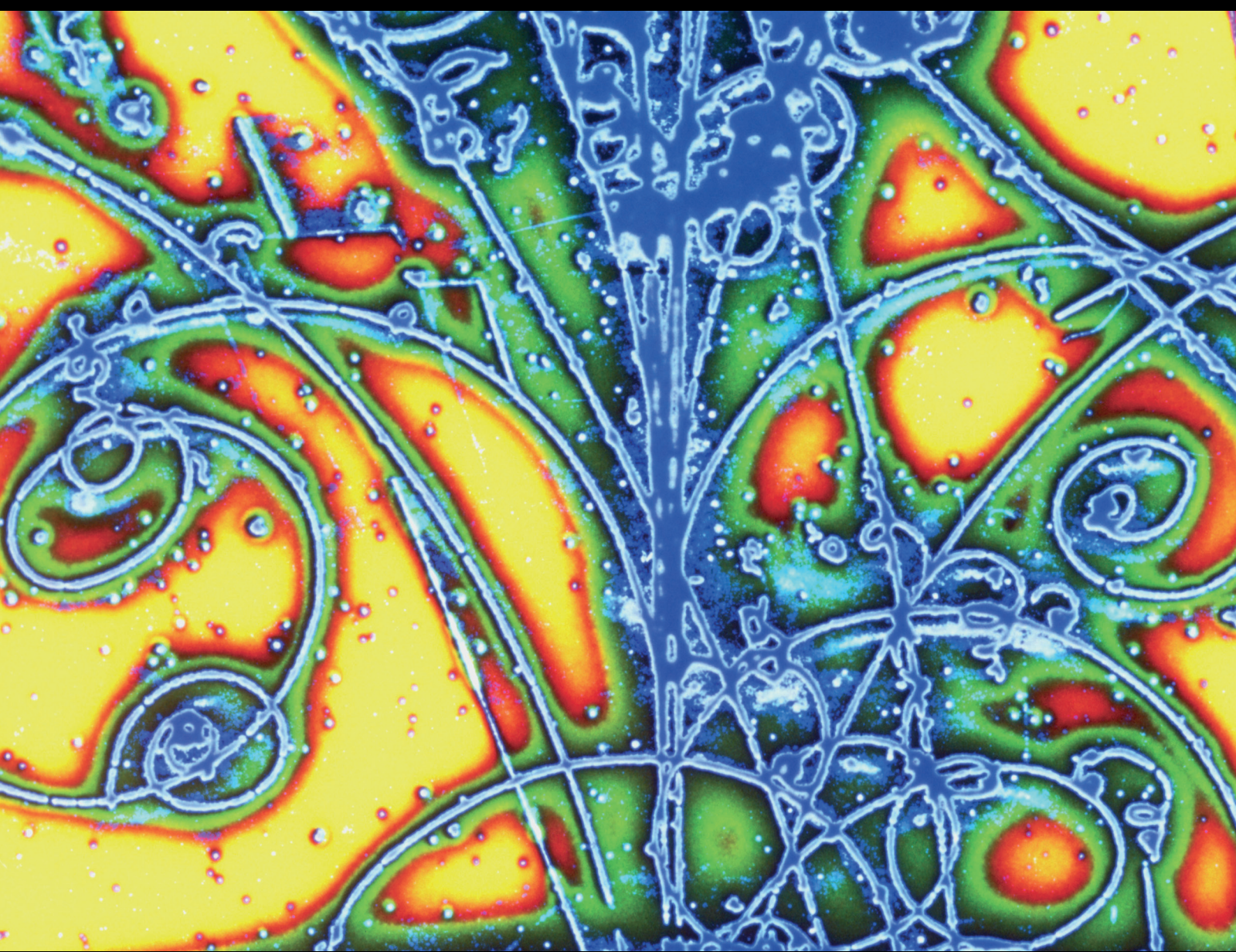

Applications of the Holographic Duality to Strongly Coupled Quantum Systems

Advances in High Energy Physics

Applications of the Holographic Duality to Strongly Coupled Quantum Systems

Lead Guest Editor: Li Li
Guest Editors: Hai-Qing Zhang, Song He, Zhang-Yu Nie, Yun-Long Zhang, and Bum-Hoon Lee

Copyright © 2017 Hindawi. All rights reserved.

This is a special issue published in "Advances in High Energy Physics." All articles are open access articles distributed under the Creative Commons Attribution License, which permits unrestricted use, distribution, and reproduction in any medium, provided the original work is properly cited.

Editorial Board

Luis A. Anchordoqui, USA
T. Asselmeyer-Maluga, Germany
Marco Battaglia, Switzerland
Lorenzo Bianchini, Switzerland
Burak Bilki, USA
Adrian Buzatu, UK
Rong-Gen Cai, China
Anna Cimmino, Belgium
Andrea Coccaro, Italy
Shi-Hai Dong, Mexico
Ricardo G. G. Felipe, Portugal
Chao-Qiang Geng, Taiwan
Philippe Gras, France
Xiaochun He, USA
Filipe R. Joaquim, Portugal
Aurelio Juste, Spain
Ming Liu, USA
Enrico Lunghi, USA
Grégory Moreau, France
Piero Nicolini, Germany
Sergio Palomares-Ruiz, Spain
Giovanni Pauletta, Italy
Yvonne Peters, UK
Anastasios Petkou, Greece
Alexey A. Petrov, USA
Thomas Rössler, Sweden
Juan José Sanz-Cillero, Spain
Edward Sarkisyan-Grinbaum, USA
Sally Seidel, USA
George Siopsis, USA
Luca Stanco, Italy
Mariam Tórtola, Spain
Smarajit Triambak, South Africa
Elias C. Vagenas, Kuwait
Yau W. Wah, USA

Contents

Applications of the Holographic Duality to Strongly Coupled Quantum Systems
Li Li, Hai-Qing Zhang, Song He, Zhang-Yu Nie, Yun-Long Zhang, and Bum-Hoon Lee
Volume 2017, Article ID 5972387, 2 pages

Reentrant Phase Transitions and Triple Points of Topological AdS Black Holes in Born-Infeld-Massive Gravity
Ming Zhang, De-Cheng Zou, and Rui-Hong Yue
Volume 2017, Article ID 3819246, 11 pages

AdS Black Hole with Phantom Scalar Field
Limei Zhang, Xiaoxiong Zeng, and Zhonghua Li
Volume 2017, Article ID 4940187, 7 pages

Note on Relation between Bottom-Up Holographic Models and Large-N_c QCD
S. S. Afonin
Volume 2017, Article ID 8358473, 6 pages

Bulk Local Operators, Conformal Descendants, and Radial Quantization
Zhao-Long Wang and Yi Yan
Volume 2017, Article ID 8185690, 11 pages

Van der Waals-Like Phase Transition from Holographic Entanglement Entropy in Lorentz Breaking Massive Gravity
Xian-Ming Liu, Hong-Bo Shao, and Xiao-Xiong Zeng
Volume 2017, Article ID 6402101, 8 pages

Holographic van der Waals Phase Transition for a Hairy Black Hole
Xiao-Xiong Zeng and Yi-Wen Han
Volume 2017, Article ID 2356174, 8 pages

Entropic Destruction of Heavy Quarkonium from a Deformed AdS_5 Model
Zi-qiang Zhang, Zhong-jie Luo, De-fu Hou, and Gang Chen
Volume 2017, Article ID 8910210, 6 pages

Heavy Quark Potential with Hyperscaling Violation
Zi-qiang Zhang, Chong Ma, De-fu Hou, and Gang Chen
Volume 2017, Article ID 8276534, 7 pages

Hindawi
Advances in High Energy Physics
Volume 2017, Article ID 5972387, 2 pages
https://doi.org/10.1155/2017/5972387

Editorial

Applications of the Holographic Duality to Strongly Coupled Quantum Systems

Li Li,[1] Hai-Qing Zhang,[2] Song He,[3] Zhang-Yu Nie,[4] Yun-Long Zhang,[5] and Bum-Hoon Lee[6]

[1]*Lehigh University, Bethlehem, PA, USA*
[2]*Utrecht University, Utrecht, Netherlands*
[3]*Max Planck Institute for Gravitational Physics, Golm, Germany*
[4]*Kunming University of Science and Technology, Kunming, Yunnan, China*
[5]*Asia Pacific Center for Theoretical Physics, Pohang, Republic of Korea*
[6]*Sogang University, Seoul, Republic of Korea*

Correspondence should be addressed to Li Li; lil416@lehigh.edu

Received 28 November 2017; Accepted 28 November 2017; Published 14 December 2017

Copyright © 2017 Li Li et al. This is an open access article distributed under the Creative Commons Attribution License, which permits unrestricted use, distribution, and reproduction in any medium, provided the original work is properly cited. The publication of this article was funded by SCOAP[3].

The holographic duality represents a major advance in our understanding of string theory and quantum gravity and also provides a powerful toolkit for studying strongly coupled quantum field theories. Thanks to this duality, challenging questions about dynamics in quantum phases of matter in strong coupling regime can be mapped to processes in theories of gravity which are tractable. It was proven to be very useful in describing unconventional physics in many fields, such as gauge theory, condensed matter, information theory, and systems described by hydrodynamics.

The selected contributions to this special issue are aimed at bringing together some of the latest developments in this field. The special issue covers several interesting topics, including novel black hole solutions, holographic QCD, entanglement entropy, and the construction of the bulk operators. The accepted articles are highlighted as follows.

The paper titled "Heavy Quark Potential with Hyperscaling Violation" by Z. Zhang et al. investigates the behavior of the heavy quark potential in the Lifshitz backgrounds with hyperscaling violation. It shows how the potential changes in the presence of the nonrelativistic parameters. The effect of a constant electric field on the potential is also investigated.

The paper titled "Holographic van der Waals Phase Transition for a Hairy Black Hole" by X.-X. Zeng and Y.-W. Han is devoted to studying the van der Waals phase transition in a hairy black hole by holography. The two-point correlation function is employed to probe the phase structure of the black hole, and some interesting behaviors are found in the temperature-thermal entropy plane.

The paper titled "Entropic Destruction of Heavy Quarkonium from a Deformed AdS_5 Model" by Z. Zhang et al. discusses the effects of the deformation parameter on the interdistance, the entropic force, and the quarkonium dissociation.

The paper by X.-M. Liu et al. is titled "Van der Waals-Like Phase Transition from Holographic Entanglement Entropy in Lorentz Breaking Massive Gravity." The authors use the entanglement entropy to probe the phase transition of AdS black holes in Lorentz breaking massive gravity. It suggests some potential relation between the entanglement entropy and the Bekenstein-Hawking entropy.

In the paper titled "Bulk Local Operators, Conformal Descendants, and Radial Quantization," Z.-L. Wang and Y. Yan establish a construction of the bulk local operators in AdS by considering CFT at finite energy scale. The authors also discuss a possible way of generalizing the construction beyond pure AdS.

The paper titled "Note on Relation between Bottom-Up Holographic Models and Large-N_c QCD" by S. S. Afonin

discusses a derivation of holographic actions quadratic in fields from general properties of the large-N_c limit in QCD.

The paper titled "AdS Black Hole with Phantom Scalar Field" by L. Zhang et al. deals with an AdS black hole solution with Ricci flat horizon in Einstein-phantom scalar theory. After discussing the thermodynamics of the phantom black hole, the authors present the behavior of the entanglement entropy for a strip geometry.

In the paper titled "Reentrant Phase Transitions and Triple Points of Topological AdS Black Holes in Born-Infeld-Massive Gravity" by M. Zhang et al., the authors study the critical behaviors of topological AdS black holes in the presence of Born-Infeld nonlinear electrodynamics in massive gravity. By considering the cosmological constant as a dynamical pressure of the system, some interesting phase structures are uncovered.

In summary, the holographic duality provides an invaluable source of physical intuition as well as computational power to deal with strongly coupled problems. Constructing, exploring, and categorizing the diverse states of matter through holography are a prominent theme in this special issue. We hope that this special issue will enrich readers with new investigations on the current related research areas and stimulate further studies.

Li Li
Hai-Qing Zhang
Song He
Zhang-Yu Nie
Yun-Long Zhang
Bum-Hoon Lee

Hindawi
Advances in High Energy Physics
Volume 2017, Article ID 3819246, 11 pages
https://doi.org/10.1155/2017/3819246

Research Article

Reentrant Phase Transitions and Triple Points of Topological AdS Black Holes in Born-Infeld-Massive Gravity

Ming Zhang,[1,2] De-Cheng Zou,[3] and Rui-Hong Yue[3]

[1]*Faculty of Science, Xi'an Aeronautical University, Xi'an 710077, China*
[2]*National Joint Engineering Research Center of Special Pump System Technology, Xi'an 710077, China*
[3]*Center for Gravitation and Cosmology, College of Physical Science and Technology, Yangzhou University, Yangzhou 225009, China*

Correspondence should be addressed to Ming Zhang; shakellar@126.com

Received 6 July 2017; Revised 13 September 2017; Accepted 12 October 2017; Published 6 November 2017

Academic Editor: Hai-Qing Zhang

Copyright © 2017 Ming Zhang et al. This is an open access article distributed under the Creative Commons Attribution License, which permits unrestricted use, distribution, and reproduction in any medium, provided the original work is properly cited. The publication of this article was funded by SCOAP[3].

Motivated by recent developments of black hole thermodynamics in de Rham, Gabadadze, and Tolley (dRGT) massive gravity, we study the critical behaviors of topological Anti-de Sitter (AdS) black holes in the presence of Born-Infeld nonlinear electrodynamics. Here the cosmological constant appears as a dynamical pressure of the system and its corresponding conjugate quantity is interpreted as thermodynamic volume. This shows that, besides the Van der Waals-like SBH/LBH phase transitions, the so-called reentrant phase transition (RPT) appears in four-dimensional space-time when the coupling coefficients $c_i m^2$ of massive potential and Born-Infeld parameter b satisfy some certain conditions. In addition, we also find the triple critical points and the small/intermediate/large black hole phase transitions for $d = 5$.

1. Introduction

Einstein's General Relativity (GR), which describes that the graviton is a massless spin-2 particle, helped us to understand the dynamics of the Universe [1–3]. However, there are some fundamental issues, such as the hierarchy problem in particle physics, the old cosmological constant problem, and the origin of late-time acceleration of the Universe, that still exist in GR [4]. One of the alternating theories of gravity is known as a massive gravity, where mass terms are added to the GR action. A graviton mass has the advantage to potentially provide a theory of dark energy which could explain the present day acceleration of our Universe [5]. On the other hand, since the quantum theory of massless gravitons is nonrenormalizable, a natural question is whether one can build a self-consistent gravity theory if the graviton is massive. The first attempt toward constructing the theory of massive gravity was done by Fierz and Pauli (FP) [6]. With the quadratic order, the FP mass term is the only ghost-free term describing a gravity theory with five degrees of freedom [7]. However, due to the existence of the van Dam-Veltman-Zakharov (vDVZ) discontinuity, this theory cannot recover linearized Einstein gravity in the limit of vanishing graviton mass [8, 9].

In particular, Vainshtein [10] proposed that the linear massive gravity can be recovered to GR through the "Vainshtein Mechanism" at small scales by including nonlinear terms in the massive gravity action. Nevertheless, it usually brings various instabilities for the gravitational theories on the nonlinear level by adding generic mass terms, since this model suffers from a pathology called a "Boulware-Deser" (BD) ghost. Later, a new nonlinear massive gravity theory was proposed by de Rham, Gabadadze, and Tolley (dRGT) [11–13], where the BD ghost [14] was eliminated by introducing higher order interaction terms in the action. Then, Vegh et al. [15, 16] constructed a nontrivial black hole solution with a Ricci flat horizon in four-dimensional dRGT massive gravity. The spherically symmetric solutions were also addressed in [17–19]; the corresponding charged black hole solution was found in [20, 21].

Recent development on the thermodynamics of black holes in extended phase space shows that the cosmological constant can be interpreted as the thermodynamic pressure

and treated as a thermodynamic variable in its own right [22, 23]:

$$P = -\frac{\Lambda}{8\pi} \tag{1}$$

in the geometric units $G_N = \hbar = c = 1$. Such operation assumes that gravitational theories including different values of the cosmological constants fall in the same class, with unified thermodynamic relations. For black hole thermodynamics, the variation of the cosmological constant ensures the consistency between the first law of black hole thermodynamics and the Smarr formula. Moreover, the classical theory of gravity may be an effective theory which follows from a yet unknown fundamental theory, in which all the presently "physical constants" are actually moduli parameters that can run from place to place in the moduli space of the fundamental theory. Since the fundamental theory is yet unknown, it is more reasonable to consider the extended thermodynamics of gravitational theories involving only a single action, and then all variables will appear in the thermodynamical relations. In the extended phase space, the charged AdS black hole black hole admits a more direct and precise coincidence between the first-order small/large black holes (SBH/LBH) phase transition and the Van der Waals liquid-gas phase transition, and both systems share the same critical exponents near the critical point [24]. More discussions in various gravity theories can be found in [25–46]. Recently, some investigations for thermodynamics of AdS black holes have been also generalized to the extended phase space in the dRGT massive gravity [47–50], which show the Van der Waals-like SBH/LBH phase transition in the charged topological AdS black holes. In addition, the deep relation between the dynamical perturbation and the Van der Waals-like SBH/LBH phase transition in the four-dimensional dRGT massive gravity has been also recovered in [51]. In particular, for neutral AdS black holes in all $d \geq 6$ dimensional space-time, there exist peculiar behaviors of intermediate/small/large black hole phase transitions reminiscent of reentrant phase transitions (RPTs) when the coupling coefficients $c_i m^2$ of massive potential satisfy some certain conditions [52]. A system undergoes an RPT if a monotonic variation of any thermodynamic quantity results in two (or more) phase transitions such that the final state is macroscopically similar to the initial state. The RPT is usually observed in multicomponent fluid systems, ferroelectrics, gels, liquid crystals, and binary gases [53].

In Maxwell's electromagnetic field theory, a point-like charge which allowed a singularity at the charge position usually brings about infinite self-energy. In order to overcome this problem, Born and Infeld [54] and Hoffmann [55] introduced Born-Infeld electromagnetic field to solve infinite self-energy problem by imposing a maximum strength of the electromagnetic field. In addition, BI type effective action arises in an open superstring theory and D-branes are free of physical singularities. In recent two decades, exact solutions of gravitating black objects in the presence of BI theory have been vastly investigated. In the extended phase space, [56, 57] recovered the RPT in the four-dimensional Einstein-Born-Infeld AdS black hole with spherical horizon. However, for the higher-dimensional Einstein-Born-Infeld AdS black holes, there is no RPT. What about AdS black holes in the Born-Infeld-massive gravity? In this paper, we will generalize the discussion to topological AdS black holes for $d = 4$ and 5 in the Born-Infeld-massive gravity.

This paper is organized as follows. In Section 2, we review the thermodynamics of Born-Infeld-massive black holes in the extended phase space. In Section 3, we study the critical behaviors of four- and five-dimensional topological AdS black holes in context of $P-V$ criticality and phase diagrams. We end the paper with conclusions and discussions in Section 4.

2. Thermodynamics of d-Dimensional Born-Infeld AdS Black Holes

We start with the action of d-dimensional massive gravity in presence of Born-Infeld field [58]:

$$\mathcal{I} = \frac{1}{16\pi}\int d^d x\sqrt{-g}\Big[R - 2\Lambda + \mathcal{L}(\mathcal{F}) + m^2\sum_{i=1}^{4} c_i \mathcal{U}_i(g, f)\Big], \tag{2}$$

where the last four terms are the massive potential associated with graviton mass, c_i are the negative constants [21], and f is a fixed rank-2 symmetric tensor. Moreover, $\mathcal{U}_i$ are symmetric polynomials of the eigenvalues of the $d \times d$ matrix $\mathcal{K}^\mu_\nu \equiv \sqrt{g^{\mu\alpha} f_{\alpha\nu}}$:

$$\begin{aligned}
\mathcal{U}_1 &= [\mathcal{K}], \\
\mathcal{U}_2 &= [\mathcal{K}]^2 - \left[\mathcal{K}^2\right], \\
\mathcal{U}_3 &= [\mathcal{K}]^3 - 3[\mathcal{K}]\left[\mathcal{K}^2\right] + 2\left[\mathcal{K}^3\right], \\
\mathcal{U}_4 &= [\mathcal{K}]^4 - 6\left[\mathcal{K}^2\right][\mathcal{K}]^2 + 8\left[\mathcal{K}^3\right][\mathcal{K}] + 3\left[\mathcal{K}^2\right]^2 \\
&\quad - 6\left[\mathcal{K}^4\right].
\end{aligned} \tag{3}$$

The square root in $\mathcal{K}$ is understood as the matrix square root, that is, $(\sqrt{A})^\mu{}_\nu(\sqrt{A})_\lambda{}^\nu = A^\mu{}_\lambda$, and the rectangular brackets denote traces $[\mathcal{K}] = \mathcal{K}^\mu{}_\mu$. In addition, b is the Born-Infeld parameter and $\mathcal{L}(\mathcal{F})$ with

$$\mathcal{L}(\mathcal{F}) = 4b^2\left(1 - \sqrt{1 + \frac{F^{\mu\nu}F_{\mu\nu}}{2b^2}}\right). \tag{4}$$

In the limit $b \to \infty$, it reduces to the standard Maxwell field $\mathcal{L}(\mathcal{F}) = -F^{\mu\nu}F_{\mu\nu} + \mathcal{O}(F^4)$. If taking $b = 0$, $\mathcal{L}(\mathcal{F})$ disappears.

Consider the metric of d-dimensional space-time in the following form:

$$ds^2 = -f(r)\,dt^2 + \frac{1}{f(r)}dr^2 + r^2 h_{ij}dx^i dx^j, \tag{5}$$

where $h_{ij}dx^i dx^j$ is the line element for an Einstein space with constant curvature $(d-2)(d-3)k$. The constant k

characterizes the geometric property of hypersurface, which takes values $k = 0$ for flat, $k = -1$ for negative curvature, and $k = 1$ for positive curvature, respectively.

By using the reference metric [21]

$$f_{\mu\nu} = \mathrm{diag}\left(0, 0, c_0^2 h_{ij}\right) \tag{6}$$

with a positive constant c_0, we can obtain

$$\begin{aligned}
\mathcal{U}_1 &= \frac{(d-2)\,c_0}{r}, \\
\mathcal{U}_2 &= \frac{(d-2)\,(d-3)\,c_0^2}{r^2}, \\
\mathcal{U}_3 &= \frac{(d-2)\,(d-3)\,(d-4)\,c_0^3}{r^3}, \\
\mathcal{U}_4 &= \frac{(d-2)\,(d-3)\,(d-4)\,(d-5)\,c_0^4}{r^4}.
\end{aligned} \tag{7}$$

Obviously, the terms related to c_3 and c_4 only appear in the black hole solutions for $d \geq 5$ and $d \geq 6$, respectively [21].

In addition, the electromagnetic field tensor in d-dimensions is given by $F_{\mathrm{tr}} = \sqrt{d_2 d_3/(1+\Gamma)}(q/r^{d_2})$, and the metric function $f(r)$ is obtained as follows [58]:

$$\begin{aligned}
f(r) = k &- \frac{m_0}{r^{d_3}} + \frac{\left(4b^2 - 2\Lambda\right)}{d_1 d_2} r^2 - \frac{4b^2 r^2}{d_1 d_2}\sqrt{1+\Gamma} \\
&+ \frac{4d_2 q^2}{d_1 r^{2d_3}}\mathscr{H} \\
&+ m^2 c_0 \left(\frac{c_1 r}{d_2} + c_0 c_2 + \frac{d_3 c_0^2 c_3}{r} + \frac{d_3 d_4 c_0^3 c_4}{r^2}\right),
\end{aligned} \tag{8}$$

where $d_i = d - i$ and

$$\begin{aligned}
\Gamma &= \frac{d_2 d_3 q^2}{b^2 r^{2d_2}}, \\
\mathscr{H} &= {}_2F_1\left[\frac{1}{2}, \frac{d_3}{2d_2}, \frac{3d_{7/3}}{2d_2}, -\Gamma\right].
\end{aligned} \tag{9}$$

Moreover, m_0 and q are related to the mass M and charge Q of black holes as

$$\begin{aligned}
Q &= \frac{\sqrt{d_2 d_3}\,\Sigma_k}{4\pi} q, \\
M &= \frac{d_2 \Sigma_k}{16\pi} m_0,
\end{aligned} \tag{10}$$

where Σ_k represents the volume of constant curvature hypersurface described by $h_{ij}dx^i dx^j$. The electromagnetic potential difference (Φ) between the horizon and infinity reads as $\Phi = \sqrt{d_2/d_3}(q/r_+^{d_3})\mathscr{H}_+$.

Then the mass M of the Born-Infeld AdS black hole for massive gravity is given by

$$\begin{aligned}
M = \frac{d_2 \Sigma_k r_+^{d_3}}{16\pi} \Bigg[& k + \frac{16\pi P}{d_1 d_2} r_+^2 + \frac{4b^2 r_+^2}{d_1 d_2}\left(1 - \sqrt{1+\Gamma_+}\right) \\
& + \frac{4d_2 q^2}{d_1 r_+^{2d_3}}\mathscr{H}_+ \\
& + m^2 \left(\frac{c_0 c_1 r_+}{d_2} + c_0^2 c_2 + \frac{d_3 c_0^3 c_3}{r_+} + \frac{d_3 d_4 c_0^4 c_4}{r_+^2}\right)\Bigg],
\end{aligned} \tag{11}$$

in terms of the horizon radius r_+. Due to existence of the pressure in obtained relation for total mass of the black holes, here the black hole mass M can be considered as the enthalpy H rather than the internal energy of the gravitational system [59].

In addition, the Hawking temperature which is related to the definition of surface gravity on the outer horizon r_+ can be obtained as

$$\begin{aligned}
T = & \frac{d_3 k}{4\pi r_+} + \frac{4r_+}{d_2} P + \frac{b^2 r_+}{d_2 \pi}\left(1 - \sqrt{1+\Gamma_+}\right) \\
& + \frac{m^2 c_0}{4\pi}\left(c_1 + \frac{d_3 c_0 c_2}{r_+} + \frac{d_3 d_4 c_0^2 c_3}{r_+^2} + \frac{d_3 d_4 d_5 c_0^3 c_4}{r_+^3}\right),
\end{aligned} \tag{12}$$

and the entropy S of the Born-Infeld AdS black hole reads as

$$S = \frac{\Sigma_k}{4} r_+^{d_2}. \tag{13}$$

It is easy to check that those thermodynamic quantities obey the (extended phase space) first law of black hole thermodynamics:

$$\begin{aligned}
dH = TdS + VdP + \mathfrak{B}db &+ \frac{c_0 m^2 \Sigma_k r_+^{d_2}}{16\pi} dc_1 \\
&+ \frac{d_2 c_0^2 m^2 \Sigma_k r_+^{d_3}}{16\pi} dc_2 + \frac{d_2 d_3 c_0^3 m^2 \Sigma_k r_+^{d_4}}{16\pi} dc_3 \\
&+ \frac{d_2 d_3 d_4 c_0^4 m^2 \Sigma_k r_+^{d_5}}{16\pi} dc_4,
\end{aligned} \tag{14}$$

where $\mathfrak{B}$, which is a quantity conjugate to b, is called the "Born-Infeld vacuum polarization":

$$\begin{aligned}
\mathfrak{B} &= \left(\frac{\partial H}{\partial b}\right)\Bigg|_{(S,P,c_1,c_2,c_3,c_4)} \\
&= \frac{\Sigma_k b r_+^{d_1}}{2d_1 \pi}\left(1 - \sqrt{1+\Gamma_+}\right) + \frac{d_2 d_3 \Sigma_k}{4\pi d_1 b}\frac{\mathscr{H}_+ q^2}{r_+^{d_3}},
\end{aligned} \tag{15}$$

and the thermodynamic volume V [60], which is the corresponding conjugate quantity of P, can be written as

$$V = \frac{\Sigma_k r_1^{d_1}}{d_1}. \tag{16}$$

The behavior of free energy G is important to determine the thermodynamic phase transition in the canonical ensemble. We can calculate the free energy from the thermodynamic relation:

$$\begin{aligned} G &= H - TS \\ &= \frac{r_+^{d_1}}{d_1 d_2}\left(P + \frac{b^2}{4\pi}\sqrt{1+\Gamma_+}\right) + \frac{d_2^2 q^2 \mathscr{H}_+}{2\pi d_1 r_+^{d_3}} + \frac{r_+^{d_3}}{16\pi} \\ &\quad + \frac{m^2 c_0^2 r_+^{d_5}}{16\pi}\left(c_2 r_+^2 + 2d_3 c_0 c_3 r_+ + 3d_3 d_4 c_0^2 c_4\right). \end{aligned} \tag{17}$$

3. Phase Transitions of Topological AdS Black Holes in Born-Infeld-Massive Gravity

For further convenience, we denote

$$\begin{aligned} \widehat{T} &= T - \frac{c_0 c_1 m^2}{4\pi}, \\ W_2 &= -\frac{k + c_0^2 c_2 m^2}{8\pi}, \\ W_3 &= -\frac{c_0^3 c_3 m^2}{8\pi}, \\ W_4 &= -\frac{c_0^4 c_4 m^2}{8\pi}, \end{aligned} \tag{18}$$

where $\widehat{T}$ denotes the shifted temperature and can be negative according to the value of $c_0 c_1 m^2$. Then, the equation of state of the black hole can be obtained from (12):

$$\begin{aligned} P = \frac{d_2}{4r_+}\Bigg[&\widehat{T} + \frac{2d_3 W_2}{r_+} + \frac{2d_3 d_4 W_3}{r_+^2} + \frac{2d_3 d_4 d_5 W_4}{r_+^3} \\ &- \frac{b^2 r_+}{d_2 \pi}\left(1 - \sqrt{1+\Gamma_+}\right)\Bigg]. \end{aligned} \tag{19}$$

To compare with the VdW fluid equation, we can translate the "geometric" equation of state to physical one by identifying the specific volume v of the fluid with the horizon radius of the black hole as $v = 4r_+/d_2$. Evidently, the specific volume v is proportional to the horizon radius r_+; therefore we will just use the horizon radius in the equation of state for the black hole hereafter in this paper.

We know that the critical point occurs when P has an inflection point:

$$\left.\frac{\partial P}{\partial r_+}\right|_{\widehat{T}=\widehat{T}_c, r_+=r_c} = \left.\frac{\partial^2 P}{\partial r_+^2}\right|_{\widehat{T}=\widehat{T}_c, r_+=r_c} = 0, \tag{20}$$

where the subscript stands for the quantities at the critical point. The critical shifted temperature is obtained as

$$\begin{aligned} \widehat{T}_c = &-\frac{2d_3}{r_c}\left(2w_2 + \frac{3d_4 W_3}{r_c} + \frac{4d_4 d_5 W_4}{r_c^2}\right) \\ &- \frac{d_2 d_3 q^2}{\pi r_c^{2d_{5/2}}}\left(1+\Gamma_+\right)^{-1/2}, \end{aligned} \tag{21}$$

and the equation for critical horizon radius r_c is given by

$$\begin{aligned} F(r_c) = &\, 6d_4 d_5 W_4 + 3d_4 W_3 r_c + W_2 r_c^2 \\ &+ \frac{d_{5/2} d_2 q^2}{2\pi r_c^{2d_4}}\left(1+\Gamma_+\right)^{-1/2} \\ &- \frac{d_3 d_2^3 q^4}{4\pi b^2 r_c^{4d_3}}\left(1+\Gamma_+\right)^{-3/2} = 0. \end{aligned} \tag{22}$$

For later discussions, it is convenient to rescale some quantities in the following way:

$$\begin{aligned} W_2 &= q^{2/(d-2)} \cdot b^{2(d-3)/(d-2)} w_2, \\ W_3 &= q^{3/(d-2)} \cdot b^{(2d-7)/(d-2)} w_3, \\ W_4 &= q^{4/(d-2)} \cdot b^{2(d-4)/(d-2)} w_4, \\ r_+ &= \left(\frac{q}{b}\right)^{1/(d-2)} \cdot x, \\ P &= b^2 \cdot p, \\ \widehat{T} &= q^{1/(d-2)} \cdot b^{(2d-5)/(d-2)} \cdot t, \\ G &= q^{(d-1)/(d-2)} \cdot b^{-2/(d-2)} \Sigma_k \cdot g. \end{aligned} \tag{23}$$

In terms of quantities above, (19), (21), and (22) can be written as

$$\begin{aligned} p = \frac{d_2}{4x}\Bigg[&t + \frac{2d_3 w_2}{x} + \frac{2d_3 d_4 w_3}{x^2} + \frac{2d_3 d_4 d_5 w_4}{x^3} \\ &- \frac{x}{d_2 \pi}\left(1 - \sqrt{1 + \frac{d_2 d_3}{x^{2d_2}}}\right)\Bigg], \end{aligned} \tag{24}$$

$$\begin{aligned} t_c = &-\frac{2d_3}{x_c}\left(2w_2 + \frac{3d_4 w_3}{x_c} + \frac{4d_4 d_5 w_4}{x_c^2}\right) - \frac{d_2 d_3}{\pi x_c^{2d_{5/2}}}\Bigg(1 \\ &+ \frac{d_2 d_3}{x_c^{2d_2}}\Bigg)^{-1/2}, \end{aligned} \tag{25}$$

$$\begin{aligned} F(x_c) = &\, 6d_4 d_5 w_4 + 3d_4 w_3 x_c + w_2 x_c^2 + \frac{d_2 d_{5/2}}{2\pi x_c^{2d_4}}\Bigg(1 \\ &+ \frac{d_2 d_3}{x_c^{2d_2}}\Bigg)^{-1/2} - \frac{d_3 d_2^3}{4\pi x_c^{4d_3}}\left(1 + \frac{d_2 d_3}{x_c^{2d_2}}\right)^{-3/2} = 0, \end{aligned} \tag{26}$$

where x_c denotes the critical value of x. For arbitrary parameter d, it is hard to obtain the exact solution of (26).

In what follows we shall specialize to $d = 4$ and 5 and then perform a detailed study of the thermodynamics of these black holes.

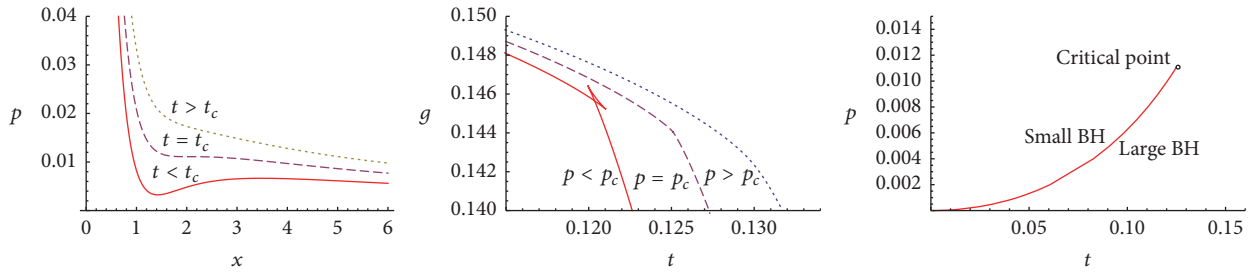

FIGURE 1: Born-Infeld AdS black holes for $d = 4$ and $w_2 = -0.1$. There is one critical point, which corresponds to VdW-like SBH/LBH phase transition when $t < t_c$. Here the critical pressure and temperature read $p = p_c \approx 0.011986$ and $t = t_c \approx 0.125087$, respectively.

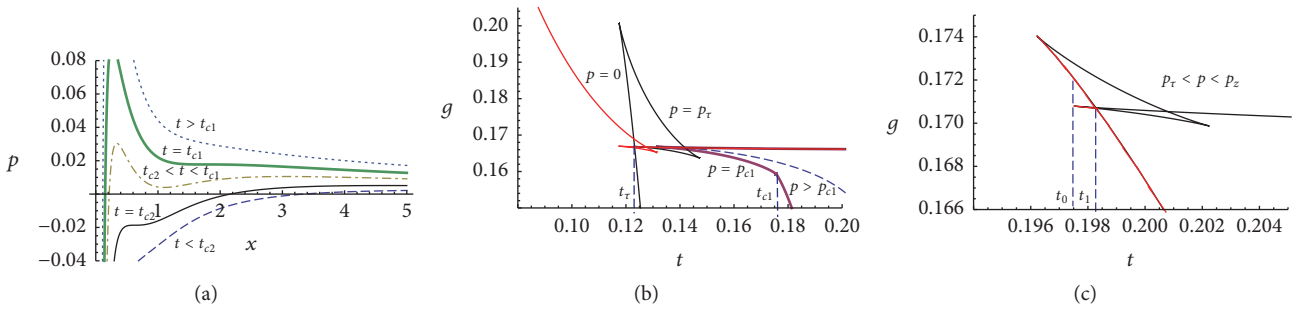

FIGURE 2: Born-Infeld AdS black holes for $d = 4$ and $w_2 = -0.124$. (a) The $p - x$ diagram shows the existence of two critical points, one at positive pressure $p_{c1} \approx 0.0177545$, the other at negative pressure $p_{c2} \approx -0.0084877$. (b) The Gibbs free energy shows one physical (with positive pressure) critical point and the corresponding first-order SBH/LBH phase transition, occurring for $t \in (t_\tau, t_{c1})$ and $p \in (p_\tau, p_{c1})$. (c) There is a *reentrant phase transition* (RPT) corresponding to the *zeroth-order phase transition* at $t = t_0$ followed by a first-order VdW-like SBH/LBH phase transition at the intersection $t = t_1$ with the swallowtail structure.

3.1. $P - V$ Criticality for $d = 4$. For $d = 4$, (26) will reduce to the cubic equation:

$$F(y) = y^3 - \frac{3y}{4} - \frac{\pi w_2}{2} = 0 \tag{27}$$

with $y = (x_c^4 + 2)^{-1/2}$.

Depending on different values of w_2, (27) admits one or more positive real roots for x, which can be also reflected by

$$\frac{\partial F(y)}{\partial y} = 3y^2 - \frac{3}{4}. \tag{28}$$

When $|w_2| \le 1/2\pi$, three real roots occur, which are given by

$$y_i = \cos\left(\frac{1}{3}\arccos(2\pi w_2) - \frac{2\pi i}{3}\right), \quad i = 0, 1, 2. \tag{29}$$

Moreover, in order that $x_c = (1/y^2 - 2)^{1/4}$ be positive, we require an additional constraint $|y| \le 1/\sqrt{2}$. Then, we have $y_0 > 0$ in case of $-1/2\pi \le w_2 \le -1/\sqrt{8}\pi$, and $y_1 > 0$ in the region of $-1/2\pi \le w_2 \le 0$, while the solution y_2 is always negative.

Now by inserting solutions of y_0 and y_1 into (24) and (25), we analyze the critical behaviors. Notice that analytic methods cannot be applied in our analysis because of the complexity of the Gibbs free energy and equation of state, we resort to graphical and numerical methods.

(1) $w_2 \in (-1/\sqrt{8}\pi, 0)$. As shown in Figure 1, the $p - x$ diagram displays that the dashed curve represents critical isotherm at $t = t_c$ and the dotted and solid curves correspond to $t > t_c$ and $t < t_c$, respectively. In the $g - t$ diagram, the solid curve represents $p < p_c$, the dotted curve correspond to $p > p_c$, and the dashed curve is for $p = p_c$. We observe standard swallowtail behavior. Moreover, the $p - t$ diagram shows the coexistence line of the first-order phase transition terminating at a critical point. These plots are analogous to typical behavior of the liquid-gas phase transition of the Van der Waals fluid.

(2) $w_2 \in (-0.132795, -1/\sqrt{8}\pi)$, there only exist one physical (with positive pressure) critical point and the corresponding VdW-like SBH/LBH phase transition, which occurs for the pressures $p \in (p_\tau, p_{c1})$ and temperatures $t \in (t_\tau, t_{c1})$; see Figure 2. For the $p - t$ diagram in Figure 3, three separate phases of black holes emerge in the region of $p_\tau < p \le p_z < p_{c1}$: intermediate black holes (IBH) (on the left), small (on the middle), and large (on the right), where small and large black holes are separated by the SBH/LBH phase transition, but the intermediate and small are separated by a finite jump in g, which is so-called *zeroth-order phase transition* [61].

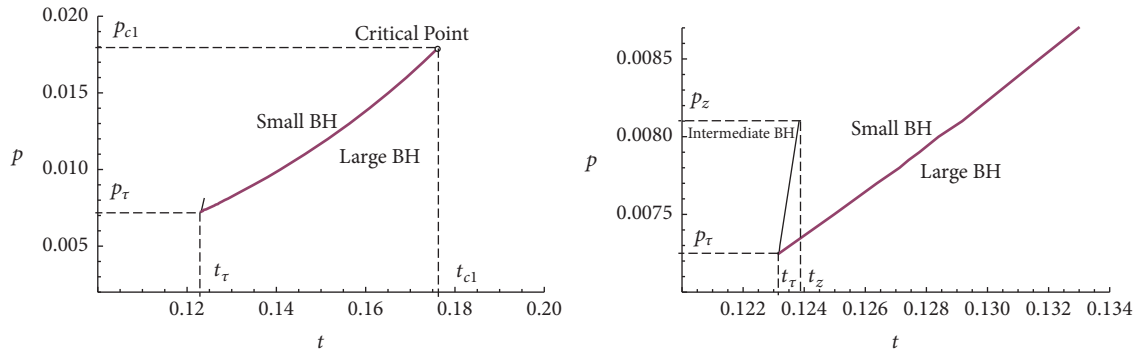

FIGURE 3: The coexistence line of the VdW-like SBH/LBH phase transition is depicted by a thick solid line. It initiates from the critical point (p_{c1}, t_{c1}) and terminates at (p_τ, t_τ). The solid line describes the "coexistence line" of small and intermediate black holes, separated by a finite gap in g, indicating the zeroth-order phase transition. It commences from (t_z, p_z) and terminates at (p_τ, t_τ).

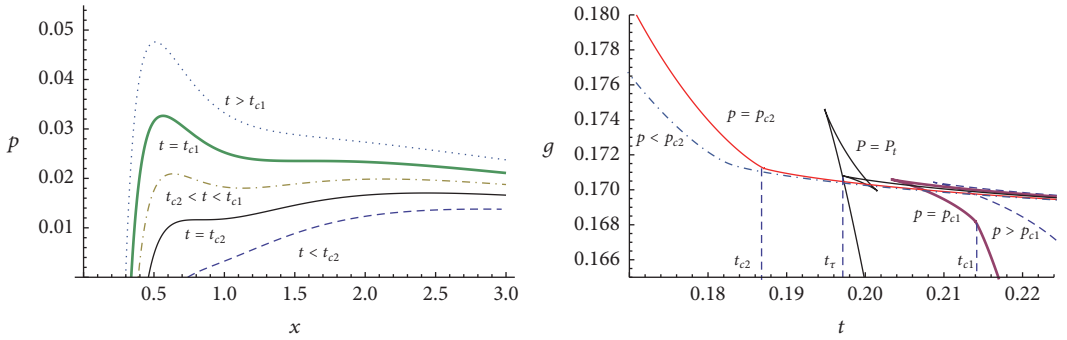

FIGURE 4: Born-Infeld AdS black holes for $d = 4$ and $w_2 = -0.14$. There are two critical points at positive pressure.

For $p < p_\tau$ only one phase of large black holes exists. When taking $w_2 = -0.124$, we obtain

$$\begin{aligned}(t_\tau, t_z, t_{c1}) &\approx (0.12316, 0.123825, 0.175593),\\ (p_\tau, p_z, p_{c1}) &\approx (0.0072472, 0.008104, 0.0177545).\end{aligned} \tag{30}$$

(3) $w_2 \in (-1/2\pi, -0.132795)$, there exist two critical points with positive pressure, and the similar RPT also occurs. As shown in Figure 4, we obtain

$$\begin{aligned}&(t_{c2}, t_\tau, t_z, t_{c1})\\ &\quad\approx (0.187113, 0.197121, 0.198064, 0.2139999),\\ &(p_{c2}, p_\tau, p_z, p_{c1})\\ &\quad\approx (0.0116313, 0.018695, 0.0194174, 0.0235228),\end{aligned} \tag{31}$$

when taking $w_2 = -0.14$.

With regard to $|w_2| > 1/2\pi$, the solution of (27) is given by

$$y_3 = -\cosh\left(\frac{1}{3}\arccos\left(-2\pi w_2\right)\right), \tag{32}$$

which violates the constraint condition $|y| \le 1/\sqrt{2}$.

All in all, when the parameter w_2 satisfies $-1/2\pi < w_2 < 0$, the Van der Waals-like SBH/LBH phase transition appears. In addition, the interesting RPT happens in case of $-1/2\pi < w_2 < -1/\sqrt{8}\pi$.

3.2. $P - V$ Criticality for $d = 5$. Then (26) can be rewritten as

$$\begin{aligned}F(x_c) = &\frac{1}{x_c}\left(x_c^6 + 6\right)^{-3/2} - \frac{5}{18x_c}\left(x_c^6 + 6\right)^{-1/2}\\ &- \frac{2\pi}{27}\left(w_2 + \frac{3w_3}{x_c}\right) = 0.\end{aligned} \tag{33}$$

Evidently, it is not possible to obtain analytic solution of above equation. To see more closely the phase transition of the Born-Infeld AdS black hole, here we analyze the asymptotic property of the function $F(x_c)$. In addition, the function $dF(x_c)/dx_c$ reads

$$\begin{aligned}\frac{dF(x_c)}{dx_c} = &72\left(1 - \frac{5x_c^6}{24}\right)^2 + \frac{135x_c^{12}}{8}\\ &+ 4\pi w_3\left(x_c^6 + 6\right)^{5/2}.\end{aligned} \tag{34}$$

Evidently, (33) has more than one real roots. For different values of w_2 and w_3, we will investigate the phase structure and criticality in the extended phase space.

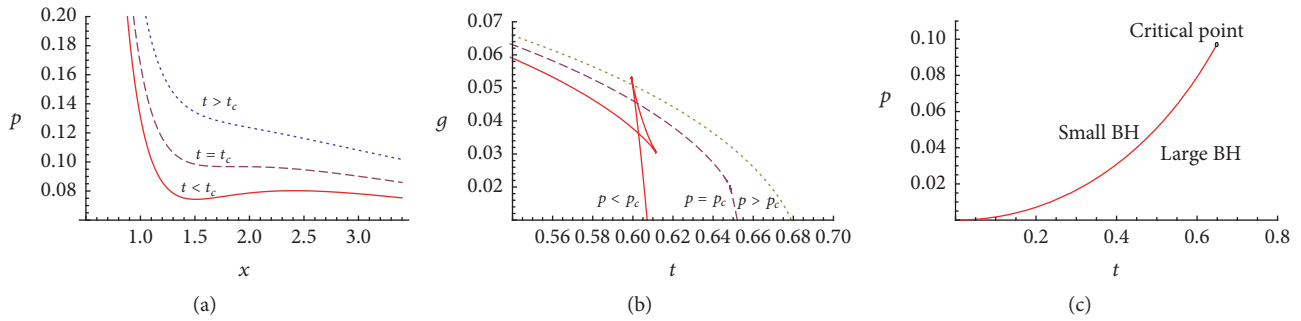

FIGURE 5: Born-Infeld AdS black holes for $d = 5$, $w_2 = -0.25$, and $w_3 = 0.1$. (a) The $p - x$ diagram. The dashed curve represents critical isotherm at $t = t_c$. The dotted and solid curves correspond to $t > t_c$ and $t < t_c$, respectively. (b) The $g - t$ diagram. The solid curve represents $p < p_c$, the dotted curve correspond to $p > p_c$, and the dashed curve is for $p = p_c$. We observe standard swallowtail behavior. (c) The $p - t$ diagram, showing the coexistence line of SBH/LBH phase transition terminating at a critical point. These plots are analogous to typical behavior of the liquid-gas phase transition of the VdW fluid.

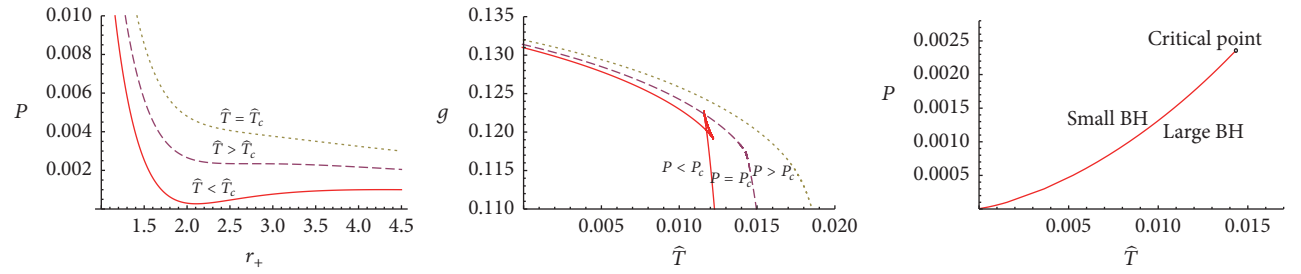

FIGURE 6: Born-Infeld AdS black holes for $d = 5$, $w_2 = 0.001$, and $w_3 = -0.02$.

3.2.1. $w_2 > 0$ *and* $w_3 > 0$. When $x_c \to +\infty$, $F(x_c)$ equals $-2\pi w_2/27$. Near the origin $x = 0$, we have

$$F(x_c) = -\frac{\left(\sqrt{6} + 12\pi w_3\right)}{54 x_c}; \tag{35}$$

namely, $F(x_c)$ approaches $-\infty$ on account of $w_3 > -1/2\sqrt{6}\pi$. Moreover, function $dF(x_c)/dx_c$ is always positive, so there is no real solution for x_+. Therefore, there is no critical point.

3.2.2. $w_2 < 0$ *and* $w_3 > 0$. Here we adopt similar discussions above. The function $F(x_c) = -2\pi w_2/27 > 0$ in case of $w_2 < 0$. However, $F(x_c)$ approaches $-\infty$ near the origin $x = 0$. Evidently, there is only one positive root of (33) on account of $dF(x_c)/dx_c > 0$. Then, a critical point occurs. In Figure 5, we display VdW-like small/large black hole phase transition in the system.

3.2.3. $w_2 > 0$ *and* $w_3 < 0$. In this case, it is hard work to discuss the asymptotic property of (33). Here we resort to graphical and numerical methods and also find the existence of VdW-like small/large black hole phase transition in the system; see Figure 6.

3.2.4. $w_2 < 0$ *and* $w_3 < 0$. In [58], Hendi et al. pointed out that the VdW-like SBH/LBH phase transition occurs when $w_2 < 0$ and $w_3 < 0$. Actually, there are some other interesting phase transitions.

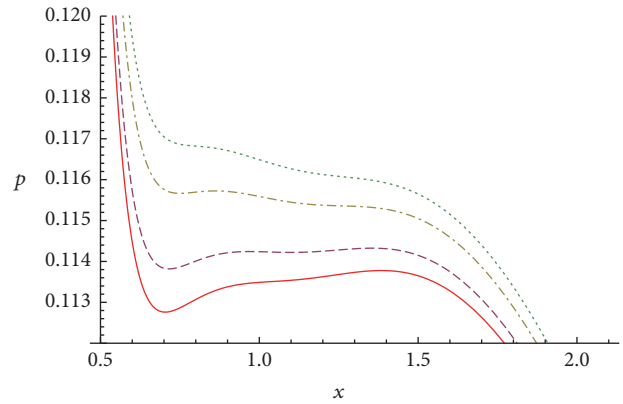

FIGURE 7: Behavior of p as a function of x for $t = 0.495, 0.497, 0.4988$, and 0.5 from bottom to top. For small pressure, one can see that there are stable SBH and LBH branches, which implies the occurrence of VdW-like phase transition. With the increasing of the temperature, there appears a new stable IBH branch. Further increasing the pressure, this branch disappears.

For the case of $w_2 = -0.084825$ and $w_3 = -0.045$, the pressure p has three critical points, that is, $(p_{c1}, p_{c2}, p_{c3}) = (0.113983, 0.115076, 0.116354)$ and $(t_{c1}, t_{c2}, t_{c3}) = (0.496659, 0.498326, 0.499503)$. We plot the pressure p as a function of x for $t = 0.48, 0.497, 0.4988$, and 0.51 (from bottom to top) in Figure 7. When $p < p_{c1}$, there exists a characteristic swallowtail behavior in the $g - t$ diagram, and

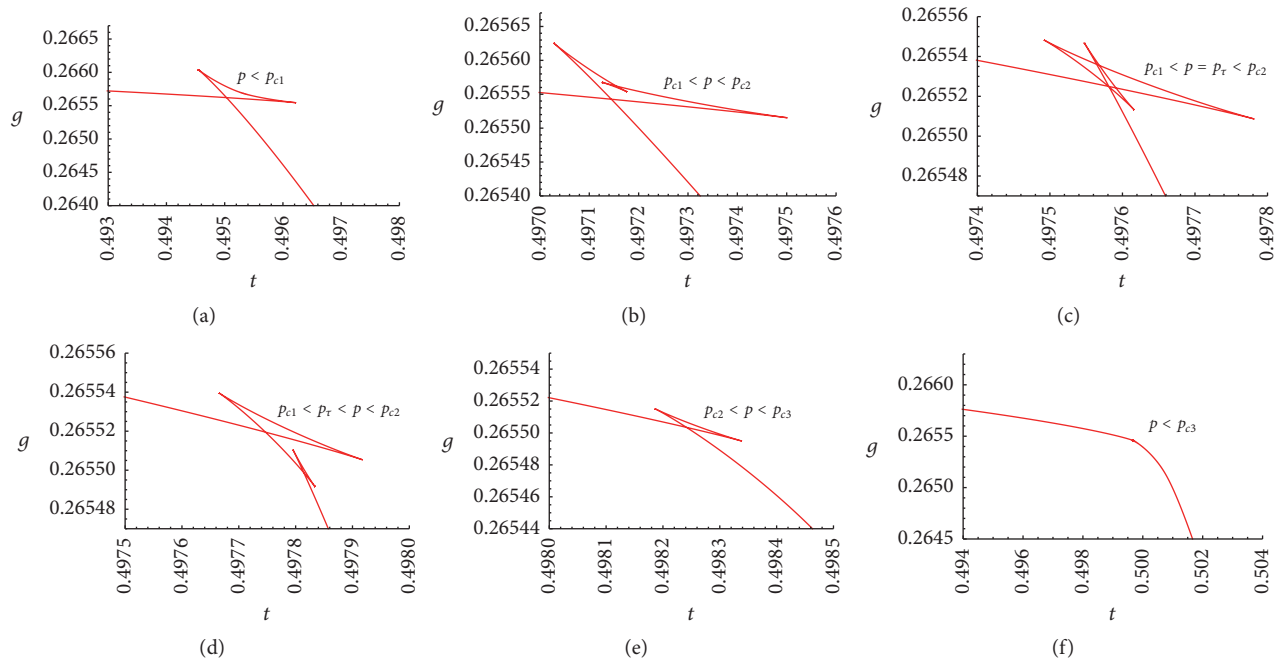

FIGURE 8: Gibbs free energy of five-dimensional AdS black holes for $w_2 = -0.084825$ and $w_3 = -0.045$.

a VdW-like SBH/LBH phase transition will occur. Further increasing p such that $p_{c1} < p < p_{c2}$, there appears a new stable IBH branch. For the corresponding Gibbs free energy in Figure 8, three black hole phases (i.e., small, large, and intermediate black holes) coexist together. Therefore, we observe a triple point characterized by $(p_\tau, t_\tau) = (0.01960, 0.11226)$. Slightly above this pressure, a standard SBH/IBH/LBH phase transition will appear in the system with the increase of t. And such phase transition disappears when p_{c2} is approached.

Further increasing p, the stable IBH branch vanishes in case of $p_{c2} < p < p_{c3}$. And only one stable branch survives when $p > p_{c3}$. In the ranges $p < p_{c1}$ and $p_{c2} < p < p_{c3}$, one characteristic swallowtail behavior is displayed in Figure 8. When $p > p_{c3}$, there is no such behavior.

4. Conclusions and Discussions

In the extended phase space, we have studied the phase transition and critical behavior of topological AdS black holes in the four- and five-dimensional Born-Infeld-massive gravity. For $d = 4$, we found that when the horizon topology is spherical ($k = 1$), Ricci flat ($k = 0$), or hyperbolic ($k = -1$), there always exist the Van der Waals-like SBH/LBH phase transitions when the coupling coefficients of massive potential are located in the region $-1/2\pi < w_2 < 0$. In addition, a monotonic lowering of the temperature yields a large-small-large black hole transition in the region $-1/2\pi < w_2 < -1/\sqrt{8}\pi$, where we refer to the former large state as an intermediate black hole (IBH), which is reminiscent of RPTs. Moreover, this process is also accompanied by a discontinuity in the global minimum of the Gibbs free energy, referred to as a zeroth-order phase transition.

In some range of the parameters, there are three critical points for five-dimensional Born-Infeld AdS black hole. In such range, the Gibbs free energy displays the behavior of two swallowtails. This phenomenon has been never recovered before.

Recent observations of gravitational waves have put an upper bound of 1.2×10^{-22} eV/c^2 on the graviton's mass [62]. We can find in 4-dimensional case; the interesting RPTs can always appear as long as the parameters q and b take the suitable values with the constant k taking the values ± 1. When the constant $k = 0$, the role of the graviton's mass is highlighted, the parameters q and b cannot take an acceptable range (means in the framework of the Born-Infeld theory) to make the parameter $w_2 \in (-1/2\pi, -1/\sqrt{8}\pi)$, which means only the VdW-like phase transitions might happen. In the 5-dimensional case, when the constant $k = 1$, this interesting phenomenon could appear as long as the parameters q and b take the suitable values. There are no three critical points when the constant k takes -1 or 0, because the parameter w_2 is always positive.

Reference [57] shows that the RPTs only exist in the 4-dimensional Born-Infeld AdS black hole with a spherical horizon and also gives the proof that there is no reentrant phase transition in the system of higher (≥5) dimensional Born-Infeld AdS black hole. Reference [48] demonstrated that there only exists the Van der Waals-like phase transition in the 4-dimensional AdS black hole in massive gravity with Maxwell's electromagnetic field theory. Our results reveal that the nonlinear electromagnetic field plays an important role in the phase transition of the 4-dimensional AdS black hole, and the massive gravity could bring richer phase structures and critical behavior (triple critical points) than that of the Born-Infeld term in the 5-dimensional AdS black hole.

Recently, the charged black hole [63], Born-Infeld black hole [64], and black hole in the Maxwell and Yang-Mills fields [65] have been constructed in Gauss-Bonnet-massive gravity. Only Van der Waals-like first-order SBH/LBH phase transition exists in these models. In addition, the RPT and triple points also occur in the higher-dimensional rotating AdS black holes [66, 67] and higher-dimensional Gauss-Bonnet AdS black hole [68–70]. It would be interesting to extend our discussion to these black holes in Gauss-Bonnet and 3rd-order Lovelock-massive gravity.

Conflicts of Interest

The authors declare that they have no conflicts of interest.

Acknowledgments

The work is supported by the National Natural Science Foundation of China under Grant nos. 11647050, 11605152, 11675139, and 51575420, Scientific Research Program Funded by Shaanxi Provincial Education Department under Program no. 16JK1394, and Natural Science Foundation of Jiangsu Province under Grant no. BK20160452.

References

[1] S. N. Gupta, "Gravitation and electromagnetism," *Physical Review A: Atomic, Molecular and Optical Physics*, vol. 96, no. 6, pp. 1683–1685, 1954.

[2] S. Weinberg, "Photons and gravitons in perturbation theory: Derivation of maxwell's and einstein's equations," *Physical Review A: Atomic, Molecular and Optical Physics*, vol. 138, no. 4B, pp. B988–B1002, 1965.

[3] R. P. Feynman, F. B. Morinigo, W. G. Wagner, and B. Hatfield, *Feynman lectures on gravitation*, Addison-Wesley, 1995.

[4] S. Capozziello and M. De Laurentis, "Extended theories of gravity," *Physics Reports*, vol. 509, no. 4-5, pp. 167–320, 2011.

[5] C. de Rham, "Massive gravity," *Living Reviews in Relativity*, vol. 17, no. 7, 2014.

[6] M. Fierz and W. Pauli, "On relativistic wave equations for particles of arbitrary spin in an electromagnetic field," *Proceedings of the Royal Society A Mathematical, Physical and Engineering Sciences*, vol. 173, no. 953, pp. 211–232, 1939.

[7] P. van Nieuwenhuizen, "On ghost-free tensor Lagrangians and linearized gravitation," *Nuclear Physics B*, vol. 60, no. C, pp. 478–492, 1973.

[8] H. van Dam and M. Veltman, "Massive and mass-less Yang-Mills and gravitational fields," *Nuclear Physics B*, vol. 22, no. 2, pp. 397–411, 1970.

[9] V. I. Zakharov, "Linearized gravitation theory and the graviton mass," *JETP Lett*, vol. 12, p. 312, 1970.

[10] A. I. Vainshtein, "To the problem of nonvanishing gravitation mass," *Physics Letters B*, vol. 39, no. 3, pp. 393-394, 1972.

[11] C. de Rham and G. Gabadadze, "Generalization of the Fierz-Pauli action," *Physical Review D: Particles, Fields, Gravitation and Cosmology*, vol. 82, Article ID 044020, 2010.

[12] C. de Rham, G. Gabadadze, and A. J. Tolley, "Resummation of massive gravity," *Physical Review Letters*, vol. 106, no. 23, Article ID 231101, 2011.

[13] K. Hinterbichler, "Theoretical aspects of massive gravity," *Reviews of Modern Physics*, vol. 84, no. 2, 2012.

[14] D. G. Boulware and S. Deser, "Can gravitation have a finite range?" *Physical Review D: Particles, Fields, Gravitation and Cosmology*, vol. 6, no. 12, pp. 3368–3382, 1972.

[15] D. Vegh, "Holography without translational symmetry," *High Energy Physics - Theory*, 2013.

[16] A. Adams, D. A. Roberts, and O. Saremi, "Hawking-Page transition in holographic massive gravity," *Physical Review D: Particles, Fields, Gravitation and Cosmology*, vol. 91, no. 4, 046003, 9 pages, 2015.

[17] T. M. Nieuwenhuizen, "Exact Schwarzschild-de Sitter black holes in a family of massive gravity models," *Physical Review D: Particles, Fields, Gravitation and Cosmology*, vol. 84, no. 2, Article ID 024038, 2011.

[18] R. Brito, V. Cardoso, and P. Pani, "Black holes with massive graviton hair," *Physical Review D: Particles, Fields, Gravitation and Cosmology*, vol. 88, no. 6, Article ID 064006, 2013.

[19] S. G. Ghosh, L. Tannukij, and P. Wongjun, "A class of black holes in dRGT massive gravity and their thermodynamical properties," *The European Physical Journal C*, vol. 76, no. 3, article no. 119, 2016.

[20] L. Berezhiani, G. Chkareuli, C. De Rham, G. Gabadadze, and A. J. Tolley, "On black holes in massive gravity," *Physical Review D: Particles, Fields, Gravitation and Cosmology*, vol. 85, no. 4, Article ID 044024, 2012.

[21] R.-G. Cai, Y.-P. Hu, Q.-Y. Pan, and Y.-L. Zhang, "Thermodynamics of black holes in massive gravity," *Physical Review D: Particles, Fields, Gravitation and Cosmology*, vol. 91, no. 2, 024032, 12 pages, 2015.

[22] B. P. Dolan, "Pressure and volume in the first law of black hole thermodynamics," *Classical and Quantum Gravity*, vol. 28, no. 23, Article ID 235017, 2011.

[23] B. P. Dolan, "The cosmological constant and black-hole thermodynamic potentials," *Classical and Quantum Gravity*, vol. 28, no. 12, Article ID 125020, 2011.

[24] D. Kubiznak and R. B. Mann, "P-V criticality of charged AdS black holes," *Journal of High Energy Physics*, vol. 1207, no. 33, 2012.

[25] D. Hansen, D. Kubiznak, and R. B. Mann, "Universality of $P-V$ criticality in horizon thermodynamics," *Journal of High Energy Physics*, vol. 1701, no. 47, 2017.

[26] R.-G. Cai, L.-M. Cao, L. Li, and R.-Q. Yang, "P-V criticality in the extended phase space of Gauss-Bonnet black holes in AdS space," *Journal of High Energy Physics*, vol. 2013, no. 9, article no. 005, 2013.

[27] S. Dutta, A. Jain, and R. Soni, "Dyonic black hole and holography," *Journal of High Energy Physics*, vol. 2013, no. 12, 2013.

[28] S. H. Hendi and M. H. Vahidinia, "Extended phase space thermodynamics and $P-V$ criticality of black holes with a nonlinear source," *Physical Review D: Particles, Fields, Gravitation and Cosmology*, vol. 88, no. 8, Article ID 084045, 11 pages, 2013.

[29] W. Xu, H. Xu, and L. Zhao, "Gauss-bonnet coupling constant as a free thermodynamical variable and the associated criticality," *The European Physical Journal C*, vol. 74, no. 7, article 2970, 2014.

[30] H.-H. Zhao, L.-C. Zhang, M.-S. Ma, and R. Zhao, "P-V criticality of higher dimensional charged topological dilaton de Sitter black holes," *Physical Review D: Particles, Fields, Gravitation and Cosmology*, vol. 90, no. 6, Article ID 064018, 2014.

[31] D. C. Zou, Y. Liu, and B. Wang, "Critical behavior of charged Gauss-Bonnet-AdS black holes in the grand canonical ensemble," *Physical Review D: Particles, Fields, Gravitation and Cosmology*, vol. 90, no. 4, Article ID 044063, 2014.

[32] H. Xu, W. Xu, and L. Zhao, "Extended phase space thermodynamics for third-order Lovelock black holes in diverse dimensions," *The European Physical Journal C*, vol. 74, article 3074, 2014.

[33] W. Xu and L. Zhao, "Critical phenomena of static charged AdS black holes in conformal gravity," *Physics Letters. B. Particle Physics, Nuclear Physics and Cosmology*, vol. 736, pp. 214–220, 2014.

[34] M. H. Dehghani, S. Kamrani, and A. Sheykhi, "P-V criticality of charged dilatonic black holes," *Physical Review D: Particles, Fields, Gravitation and Cosmology*, vol. 90, no. 10, Article ID 104020, 2014.

[35] C. O. Lee, "The extended thermodynamic properties of Taub-NUT/Bolt-AdS spaces," *Physics Letters. B. Particle Physics, Nuclear Physics and Cosmology*, vol. 738, pp. 294–300, 2014.

[36] J. L. Zhang, R. G. Cai, and H. Yu, "Phase transition and thermodynamical geometry for Schwarzschild AdS black hole in $AdS_5 \times S_5$ spacetime," *Journal of High Energy Physics*, vol. 2015, no. 2, article 143, 2015.

[37] M. Zhang, Z.-Y. Yang, D.-C. Zou, W. Xu, and R.-H. Yue, "$P - V$ criticality of AdS black hole in the Einstein-Maxwell-power-Yang-MILls gravity," *General Relativity and Gravitation*, vol. 47, no. 2, 2015.

[38] Y. Liu, D.-C. Zou, and B. Wang, "Signature of the Van der Waals like small-large charged AdS black hole phase transition in quasinormal modes," *Journal of High Energy Physics*, vol. 2014, no. 9, article no. 179, 2014.

[39] J. L. Zhang, R. G. Cai, and H. Yu, "Phase transition and thermodynamical geometry of Reissner-Nordström-AdS black holes in extended phase space," *Physical Review D: Particles, Fields, Gravitation and Cosmology*, vol. 91, no. 4, Article ID 044028, 14 pages, 2015.

[40] B. R. Majhi and S. Samanta, "P-V criticality of AdS black holes in a general framework," *Physics Letters. B. Particle Physics, Nuclear Physics and Cosmology*, vol. 773, pp. 203–207, 2017.

[41] S. H. Hendi, B. E. Panah, S. Panahiyan, and M. S. Talezadeh, "Geometrical thermodynamics and P–V criticality of the black holes with power-law Maxwell field," *The European Physical Journal C*, vol. 77, no. 2, article no. 133, 2017.

[42] S. H. Hendi, S. Panahiyan, B. Eslam Panah, M. Faizal, and M. Momennia, "Critical behavior of charged black holes in Gauss-Bonnet gravity's rainbow," *Physical Review D: Particles, Fields, Gravitation and Cosmology*, vol. 94, no. 2, Article ID 024028, 2016.

[43] D. Kubiznak, R. B. Mann, and M. Teo, "Black hole chemistry: thermodynamics with lambda," *Classical and Quantum Gravity*, vol. 34, no. 6, 2017.

[44] X. Kuang and O. Miskovic, "Thermal phase transitions of dimensionally continued AdS black holes," *Physical Review D: Particles, Fields, Gravitation and Cosmology*, vol. 95, no. 4, 2017.

[45] Y. G. Miao and Y. M. Wu, "Thermodynamics of the Schwarzschild-AdS black hole with a minimal length," *Advances in High Energy Physics*, vol. 2017, 14 pages, 2017.

[46] M. Cadoni, E. Franzin, and M. Tuveri, "Van der Waals-like behaviour of charged black holes and hysteresis in the dual QFTs," *Physics Letters. B. Particle Physics, Nuclear Physics and Cosmology*, vol. 768, pp. 393–396, 2017.

[47] S. H. Hendi, B. Eslam Panah, and S. Panahiyan, "Einstein-Born-Infeld-massive gravity: adS–black hole solutions and their thermodynamical properties," *Journal of High Energy Physics*, vol. 95, no. 11, 2015.

[48] J. Xu, L. M. Cao, and Y. P. Hu, "P-V criticality in the extended phase space of black holes in massive gravity," *Phys. Rev. D*, vol. 91, Article ID 124033, 2015.

[49] M. Zhang and W. B. Liu, "Coexistent physics of massive black holes in the phase transitions," *General Relativity and Quantum Cosmology*, 2016.

[50] S. H. Hendi, S. Panahiyan, B. Eslam Panah, and M. Momennia, "Phase transition of charged black holes in massive gravity through new methods," *Annalen der Physik*, vol. 528, no. 11-12, pp. 819–834, 2016.

[51] D. Zou, Y. Liu, and R. Yue, "Behavior of quasinormal modes and Van der Waals-like phase transition of charged AdS black holes in massive gravity," *The European Physical Journal C*, vol. 77, no. 6, 2017.

[52] D. Zou, R. Yue, and M. Zhang, "Reentrant phase transitions of higher-dimensional AdS black holes in dRGT massive gravity," *The European Physical Journal C*, vol. 77, no. 4, 2017.

[53] T. Narayanan and A. Kumar, "Reentrant phase transitions in multicomponent liquid mixtures," *Physics Reports*, vol. 249, no. 3, pp. 135–218, 1994.

[54] M. Born and L. Infeld, "Foundations of the new field theory," *Proceedings of the Royal Society A Mathematical, Physical and Engineering Sciences*, vol. 144, no. 852, pp. 425–451, 1934.

[55] B. Hoffmann, "Gravitational and electromagnetic mass in the born-infeld electrodynamics," *Physical Review A: Atomic, Molecular and Optical Physics*, vol. 47, no. 11, pp. 877–880, 1935.

[56] S. Gunasekaran, D. Kubiznak, and R. B. Mann, "Extended phase space thermodynamics for charged and rotating black holes and Born-Infeld vacuum polarization," *Journal of High Energy Physics*, vol. 2012, no. 11, article 110, 2012.

[57] D.-C. Zou, S.-J. Zhang, and B. Wang, "Critical behavior of Born-Infeld AdS black holes in the extended phase space thermodynamics," *Physical Review D: Particles, Fields, Gravitation and Cosmology*, vol. 89, Article ID 044002, 2014.

[58] S. H. Hendi, B. E. Panah, and S. Panahiyan, "Einstein-Born-Infeld-massive gravity: adS-black hole solutions and their thermodynamical properties," *Journal of High Energy Physics*, vol. 2015, no. 11, article no. 157, pp. 1–29, 2015.

[59] D. Kastor, S. Ray, and J. Traschen, "Enthalpy and the mechanics of AdS black holes," *Classical and Quantum Gravity*, vol. 26, no. 19, Article ID 195011, 195011, 16 pages, 2009.

[60] M. Cvetic, G. W. Gibbons, D. Kubiznak, and C. N. Pope, "Black Hole Enthalpy and an Entropy Inequality for the Thermodynamic Volume," *Phys. Rev. D*, vol. 84, Article ID 024037, 2011.

[61] V. P. Maslov, "Zeroth-order phase transitions," *Mathematical Notes*, vol. 76, no. 5-6, pp. 697–710, 2004.

[62] B. P. Abbott et al., "Observation of gravitational waves from a binary black hole merger," *Physical Review Letters*, vol. 116, no. 6, 2016.

[63] S. H. Hendi, S. Panahiyan, and B. E. Panah, "Charged black hole solutions in Gauss-Bonnet-massive gravity," *Journal of High Energy Physics*, vol. 2016, no. 1, article 129, pp. 1–35, 2016.

[64] S. H. Hendi, G.-Q. Li, J.-X. Mo, S. Panahiyan, and B. E. Panah, "New perspective for black hole thermodynamics in Gauss-Bonnet-Born-Infeld massive gravity," *The European Physical Journal C*, vol. 76, no. 10, article 571, 2016.

[65] K. Meng and J. Li, "Black hole solution of Gauss-Bonnet massive gravity coupled to Maxwell and Yang-Mills fields in five dimensions," *EPL (Europhysics Letters)*, vol. 116, no. 1, Article ID 10005, 2016.

[66] N. Altamirano, D. Kubiznak, and R. Mann, "Reentrant phase transitions in rotating AdS black holes," *Physical Review D: Particles, Fields, Gravitation and Cosmology*, vol. 88, no. 10, Article ID 101502, 5 pages, 2013.

[67] N. Altamirano, D. Kubiznak, R. B. Mann, and Z. Sherkatghanad, "Thermodynamics of rotating black holes and black rings: phase transitions and thermodynamic volume," *Galaxies*, vol. 2, no. 89, 2014.

[68] S.-W. Wei and Y.-X. Liu, "Triple points and phase diagrams in the extended phase space of charged Gauss-Bonnet black holes in AdS space," *Physical Review D: Particles, Fields, Gravitation and Cosmology*, vol. 90, no. 4, Article ID 044057, 2014.

[69] A. M. Frassino, D. Kubizňák, R. B. Mann, and F. Simovic, "Multiple reentrant phase transitions and triple points in Lovelock thermodynamics," *Journal of High Energy Physics*, vol. 2014, no. 9, article no. 80, pp. 1–47, 2014.

[70] R. A. Hennigar, E. Tjoa, and R. B. Mann, "Thermodynamics of hairy black holes in Lovelock gravity," *Journal of High Energy Physics*, vol. 2017, no. 2, article 70, 2017.

Hindawi
Advances in High Energy Physics
Volume 2017, Article ID 4940187, 7 pages
https://doi.org/10.1155/2017/4940187

Research Article

AdS Black Hole with Phantom Scalar Field

Limei Zhang,[1] Xiaoxiong Zeng,[2] and Zhonghua Li[3]

[1]*College of Physics and Space Science, China West Normal University, Nanchong, Sichuan 637002, China*
[2]*Institute of Theoretical Physics, Chinese Academy of Sciences, Beijing 100190, China*
[3]*Institute of Theoretical Physics, China West Normal University, Nanchong, Sichuan 637002, China*

Correspondence should be addressed to Zhonghua Li; sclzh888@163.com

Received 6 July 2017; Accepted 2 August 2017; Published 15 October 2017

Academic Editor: Li Li

Copyright © 2017 Limei Zhang et al. This is an open access article distributed under the Creative Commons Attribution License, which permits unrestricted use, distribution, and reproduction in any medium, provided the original work is properly cited. The publication of this article was funded by SCOAP[3].

We present an AdS black hole solution with Ricci flat horizon in Einstein-phantom scalar theory. The phantom scalar fields just depend on the transverse coordinates x and y, which are parameterized by the parameter α. We study the thermodynamics of the AdS phantom black hole. Although its horizon is a Ricci flat Euclidean space, we find that the thermodynamical properties of the black hole solution are qualitatively the same as those of AdS Schwarzschild black hole. Namely, there exists a minimal temperature and the large black hole is thermodynamically stable, while the smaller one is unstable, so there is a so-called Hawking-Page phase transition between the large black hole and the thermal gas solution in the AdS space-time in Poincare coordinates. We also calculate the entanglement entropy for a strip geometry dual to the AdS phantom black holes and find that the behavior of the entanglement entropy is qualitatively the same as that of the black hole thermodynamical entropy.

1. Introduction

Due to its confined boundary of anti-de Sitter (AdS) space-time, thermodynamics of black hole in AdS space and those in flat or de Sitter space-time are very different. For example, for a Schwarzschild AdS black hole, it is stable if its horizon is larger than a certain value, while, for a small black hole, the effect of cosmological constant can be neglected, the black hole behaves just like a Schwarzschild black hole in flat space, and it is thermodynamically unstable. In addition, it is found that there is an AdS black hole only when the temperature of black hole is larger than a critical value, while there is only a thermal gas solution when its temperature is less than the value. The first-order phase transition which occurs between the black hole solution and the thermal gas solution in the AdS space-time is named Hawking-Page phase transition [1]. The phase transition gets its interpretation following the AdS/CFT correspondence [2–5].

Another big difference between black holes in AdS space and flat or de Sitter space-time is that the horizon of black holes in flat or de Sitter space must have a spherical structure, while the horizon topology of black holes in AdS space-time could be a zero or negative constant curvature surface, except for the case with a positive constant curvature surface. These kinds of black holes with zero or negative constant curvature horizon have been studied in the literature [6–19]: they are usually called topological AdS black holes. Particularly, we find that these so-called topological AdS black holes are always thermodynamically stable, and there do not exist Hawking-Page phase transitions related to those topological black holes [18]. Of course, we should mention here that if one of spatial coordinates is compacted for the Ricci flat AdS black holes, then the AdS space-time in Poincare coordinates is no longer a ground state with respect to the black hole solutions, instead the so-called AdS soliton has more low energy and then there is a Hawking-Page phase transition between the Ricci flat black hole and AdS soliton [20–22]. The Ricci flat black holes mean zero curvature horizon black holes.

On the other hand, since people discovered the phenomenon of accelerated expansion of the universe at the end of last century, there have been a lot of proposals to explain the cause of this phenomenon. One way is so-called phantom dark energy with state equation, $p = \omega\rho$, where the state parameter satisfies $\omega < -1$, and p and ρ represent the pressure and energy density of phantom dark energy, respectively. To realize phantom dark energy, one can alter

the mark in front of the kinetic term of a scalar field [23]. This is called phantom scalar field. Except for various studies in cosmology, the influence of phantom scalar field in black hole physics has also been extensively investigated. For instance, the destiny of a black hole owing to accretion of phantom dark energy has been studied in [24]. Thermodynamics of spherically symmetric black holes and critical phenomenon with phantom Maxwell field and phantom scalar field have been discussed in [25]. Very recently, people have studied thermodynamical geometry of AdS charged black holes with spherical horizon in [26].

In this study, we consider Einstein gravity theory with a negative cosmological constant and massless phantom scalar field. The black hole will have a Ricci flat horizon and phantom scalar fields only linearly depend on transverse coordinates. The thermodynamics of AdS phantom black hole are studied, and we find that although its horizon is Ricci flat and infinitely extended, the thermodynamical properties of the black hole and AdS Schwarzschild spherically symmetric black hole are qualitatively the same. In particular, Hawking-Page phase transition can emerge between phantom black hole and the thermal gas solution in AdS space-time in Poincare coordinates. Further, we will calculate holographic entanglement entropy of a strip geometry which is dual to the AdS phantom black hole boundary following the proposal made by Ryu and Takayanagi in [27]. In recent papers on holographic superconductor models, it has been found that entanglement entropy plays a good probe role in revealing phase structure and phase transition in those systems. It can indicate the appearance of a new phase and gives the order of phase transition based on the behavior of entanglement entropy [28–33]. Very recently holographic entanglement entropy dual to a spherically symmetric AdS charged black hole has been calculated by Johnson [34]. It was found that the entanglement entropy can characterize the related phase transition for a charged AdS black hole. Further studies on holographic entanglement entropy and its relation to phase transition have been done for various AdS black holes in [35–38]. For the AdS phantom black hole presented in this paper, we will further show such a relation which keeps valid even for the case with the Ricci flat horizon black hole.

2. Phantom AdS Black Hole Solution

We first consider a Einstein-Hilbert action with phantom massless scalar fields and a negative cosmological constant as

$$S = \frac{1}{16\pi G}\int d^4x\sqrt{-g}\left[R - 2\Lambda + \frac{1}{2}\sum_{i=1}^{2}\left(\partial\phi_i\right)^2\right]. \quad (1)$$

In the above formula, G is the Newtonian gravitational constant and ϕ_i stands for massless phantom scalar fields. In four dimensions, the relationship between the negative cosmological constant Λ and the AdS curvature radius l can be as follows:

$$\Lambda = -\frac{3}{l^2}. \quad (2)$$

The Einstein's field equations corresponding with action (1) read

$$R_{\mu\nu} - \frac{1}{2}g^{\mu\nu}R + \Lambda g^{\mu\nu} = T_{\mu\nu}, \quad (3)$$

where the energy momentum tensor is

$$T_{\mu\nu} = \sum_{i=1}^{2}\left[-\nabla_\mu\phi_i\nabla_\nu\phi_i + \frac{1}{2}g_{\mu\nu}\left(\nabla\phi_i\right)^2\right]. \quad (4)$$

The motion equation of the phantom scalar field is

$$\nabla^2\phi_i = 0. \quad (5)$$

Now we consider a black hole solution which has a Ricci flat horizon in this system with the metric ansatz as

$$ds^2 = -f(r)\,dt^2 + \frac{1}{f(r)}dr^2 + r^2\left(dx^2 + dy^2\right). \quad (6)$$

With this metric, one has the nonzero part of Ricci tensor as follows [18]:

$$\begin{aligned} R_{tt} &= \frac{1}{2}ff'' + \frac{1}{r}ff', \\ R_{rr} &= -\frac{1}{2}\frac{f''}{f} - \frac{1}{r}\frac{f'}{f}, \\ R_{xx} &= R_{yy} = -\left(f + rf'\right), \end{aligned} \quad (7)$$

where $f' = df/dr$ and $f'' = d^2f/d^2r$. The Ricci scalar can be written as follows:

$$R = g^{tt}R_{tt} + g^{rr}R_{rr} + g^{ij}R_{ij} = -f'' - \frac{4}{r}f' - \frac{2f}{r^2}. \quad (8)$$

We take the scalar fields to be functions of transverse coordinates as follows:

$$\begin{aligned} \phi_1 &= \alpha x, \\ \phi_2 &= \alpha y, \end{aligned} \quad (9)$$

where α is a constant; then it is found that the equations of motions for both gravitational field and matter field are satisfied if $f(r)$ takes the following form:

$$f(r) = \alpha^2 + \frac{r^2}{l^2} - \frac{2M}{r}, \quad (10)$$

in which M is a parameter relating to the mass of the solution. In fact, this solution describes an AdS black hole with a Ricci flat horizon. As we can see that the influence of the phantom scalar in the solution is manifested by parameter α. In addition, note that the scalar field enters the action only through its derivative and therefore enjoys a shift symmetry. These scalar fields are only determined up to a constant. When the phantom scalar fields are absent, the solution reduces to the AdS black hole solution with Ricci flat horizon in Einstein gravity. In that case, one has $\alpha = 0$. A natural generalization of solution (10) is to include electric and

magnetic charge from Maxwell field. Namely if a Maxwell field appears in action (1), then one has a dynamic phantom AdS black hole solution as

$$f(r) = \alpha^2 + \frac{r^2}{l^2} - \frac{2M}{r} + \frac{e^2 + g^2}{r^2}, \tag{11}$$

where e and g are electric charge and magnetic charge of the solution, respectively. Here we mention that one can easily generalize these black hole solutions (10) and (11) to higher dimensional ($d > 4$) cases. Finally we should stress that if the scalar fields are the usual canonical ones in (1), namely, the sign of the kinetic term in the scalar fields formula is negative, this AdS black hole solution was first found in [39] with the metric function:

$$f(r) = -\alpha^2 + \frac{r^2}{l^2} - \frac{2M}{r}. \tag{12}$$

In that case, the thermodynamical properties of solution (12) and the topological black hole with a horizon of negative constant curvature space are qualitatively the same in AdS space-time [18].

3. Thermodynamics of the Phantom AdS Black Hole

In this section, the thermodynamics of this AdS black hole solution are discussed. Here we are discussing the case where the transverse coordinates x and y are infinitely extended. In other words, the directions spanned by x and y are not compacted. In that case, precisely speaking, what we are discussing is not a black hole, but a black brane. And the vacuum of the system is no longer the AdS solution, but an AdS space in Poincare coordinates with metric function:

$$f(r) = \frac{r^2}{l^2}. \tag{13}$$

On the other hand, let us note that when $\alpha^2 = 1$, the metric function in (10) is nothing, but the one for a Schwarzschild AdS black hole is with a spherical horizon. Thus one may expect that the thermodynamic properties of the black hole solution (10) are essentially the same as those of AdS Schwarzschild black holes. Here we will show this indeed holds. To make qualitative comparison, we take that the area spanned by x and y is 4π. So parameter M in (10) is just the mass of the solution with respect to the AdS vacuum in Poincare coordinates. In this paper we take the units with $G = c = h = k_b = 1$.

The horizon of the black hole is given by $f(r)|_{r=r_+} = 0$. Thus the black hole mass can be expressed in terms of the horizon radius r_+ as

$$M = \frac{\alpha^2}{2} r_+ + \frac{r_+^3}{2l^2}. \tag{14}$$

As a function of the horizon radius r_+, M is a monotonically increasing function. In other words, this equation shows that for any positive value of M there is a corresponding horizon. And only when the case $r_+ \to 0$, $M \to 0$. The Hawking temperature T_H of the black hole can be obtained in several ways. One way is that the Euclidean time of the black hole solution should take a period so that the potential conical singularity can be avoided at the horizon of the black hole and the inverse of the period just gives the Hawking temperature. In this way, one has the Hawking temperature of the black hole as

$$T = \frac{1}{4\pi r_+}\left(\alpha^2 + \frac{3r_+^2}{l^2}\right). \tag{15}$$

In Einstein's gravity theory, the entropy of black hole obeys the well-known Bekenstein-Hawking area formula. In our case, the entropy of black hole can be expressed as follows:

$$S = \pi r_+^2. \tag{16}$$

Substituting (16) into (15) and eliminating r_+, T is given by

$$T = \frac{\alpha^2 + 3S/\pi l^2}{4\sqrt{\pi}\sqrt{S}}. \tag{17}$$

It is easy to show that the mass, entropy, and the temperature of the black hole obey the first law of black hole thermodynamics:

$$dM = TdS. \tag{18}$$

To study the thermodynamical stability of the black hole, let us calculate the heat capacity:

$$C = T\frac{\partial S}{\partial T} = \frac{\partial M}{\partial T} = \frac{2l^2\pi r_+^2\left(3r_+^2/l^2 + \alpha^2\right)}{3r_+^2 - l^2\alpha^2}. \tag{19}$$

We can see that the heat capacity is positive when $r_+ > l\alpha/\sqrt{3}$, negative when $r_+ < l\alpha/\sqrt{3}$, and divergent when $r_+ = l\alpha/\sqrt{3}$. This means that the black hole is locally thermodynamically unstable for small horizons with $r_+ < l\alpha/\sqrt{3}$, while it is locally thermodynamically stable for large horizons with $r_+ > l\alpha/\sqrt{3}$. Figure 1 shows the temperature-entropy relation. And it is easy to see that the small entropy is thermodynamically unstable, while the large entropy is thermodynamically stable.

The Hawking temperature (15) can be reexpressed as

$$\frac{3}{l^2}r_+^2 - 4\pi k_B T r_+ + \alpha^2 = 0. \tag{20}$$

Through this relation, we can see that there exists a minimal temperature as

$$T_{\min} = \frac{\alpha\sqrt{3}}{2\pi l}. \tag{21}$$

In that case, corresponding horizon radius is given by

$$r_0 = \frac{\alpha l}{\sqrt{3}}. \tag{22}$$

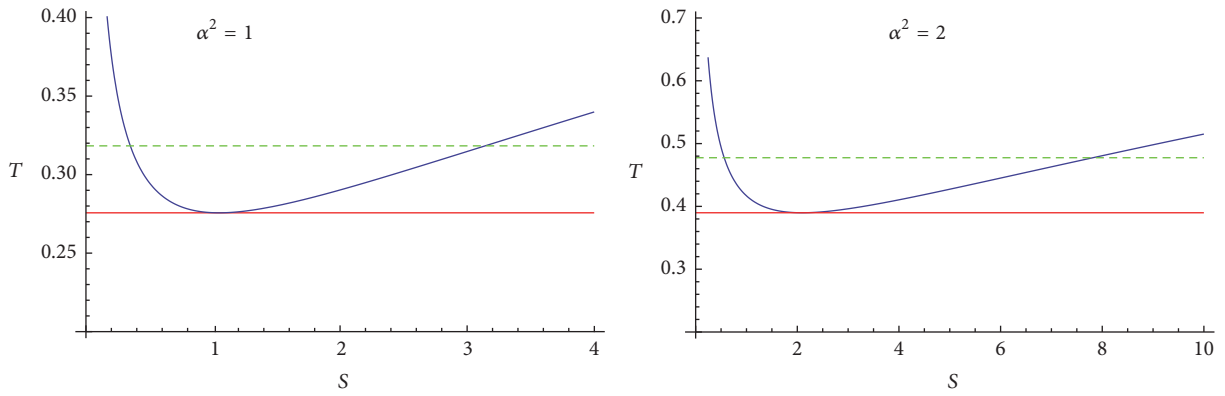

FIGURE 1: The black hole temperature in terms of entropy. The dashed green line represents the Hawking-Page transition temperature, while the solid red line stands for T_{min}. When $T < T_{min}$, there is only a thermal gas solution in the AdS space. When $T > T_{min}$, for a given temperature T, there exist two black hole solutions given by (23). The one with large horizon is stable, while it is thermodynamically unstable for the smaller one.

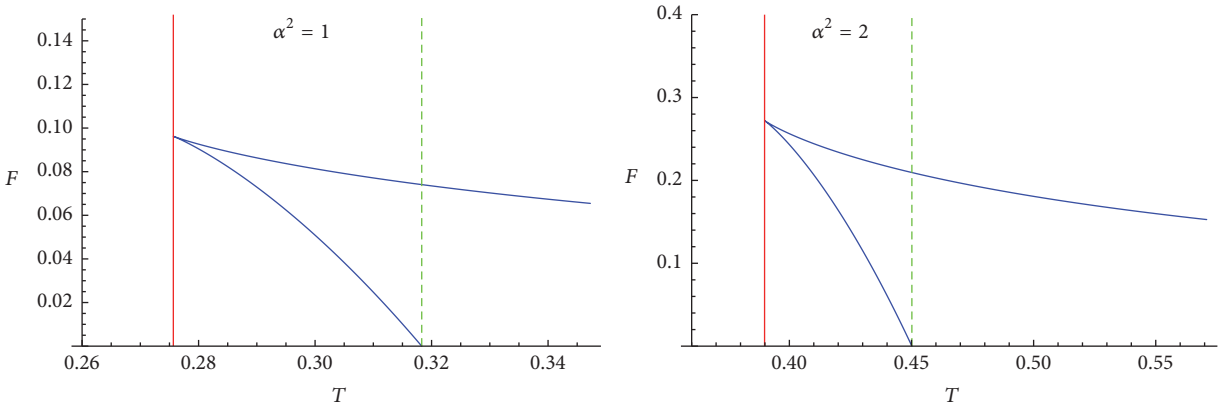

FIGURE 2: The Helmholtz free energy of the black hole as a function of temperature T. The dashed green line stands for the Hawking-Page transition temperature, while the solid red line represents the minimal temperature.

When $T > T_{min}$, for a given temperature, there are two black hole horizons:

$$r_{l,s} = \frac{\alpha^2 T}{2\pi T_{min}^2}\left(1 + \sqrt{1 - \frac{T_{min}^2}{T^2}}\right). \tag{23}$$

The small black hole with negative heat capacity is thermodynamically unstable, while the larger one with positive heat capacity is thermodynamically stable.

With the mass, entropy, and temperature, the Helmholtz free energy is easily calculated as

$$F = M - TS = \frac{1}{4} r_+ \left(-\frac{r_+^2}{l^2} + \alpha^2\right). \tag{24}$$

According to the above, we can easily see that the free energy is equivalent to the Euclidean action by setting the pure AdS vacuum in Poincare coordinates as a ground state. We can see from the free energy that the free energy is positive when $r_+ < l\alpha$, while it is negative when $r_+ > l\alpha$. It implies that the black hole is globally thermodynamically unstable when $r_+ < l\alpha$, while it is globally thermodynamically stable when $r_+ > l\alpha$. Namely, there is a Hawking-Page phase transition when the free energy vanishes and $r_+ = l\alpha$. The Hawking-Page transition temperature is given by

$$T_{HP} = \frac{\alpha}{\pi l}. \tag{25}$$

When $T > T_{HP}$, the system is dominated by the black hole solution; while it is dominated by a thermal gas solution as $T < T_{HP}$. When $T = T_{HP}$, the Hawking-Page transition happens between the black hole phase and thermal gas phase.

From (21) and (25), we can see that the phantom scalar field has some effect on the thermodynamic stability and the Hawking-Page transition temperature through the parameter α. But the ratio between these two temperatures,

$$D = \frac{T_{HP}}{T_{min}} = \frac{2\sqrt{3}}{3}, \tag{26}$$

is independent of the parameter α. The ratio is the same as the one for the case of the AdS Schwarzschild black hole. We show the free energy of the black hole as a function of temperature in Figure 2.

4. Entanglement Entropy and Hawking-Page Transition

For a quantum mechanical system with many degrees of freedom, we separate the total system into two subsystems A and B. The Hilbert space of the total system can be expressed by the direct product of the two subsystems A and B as $H_{\text{total}} = H_A \bigotimes H_B$. For the observer who is only accessible to subsystem A, because the information of B cannot be directly observed, the total system is described by reduced density matrix ρ_A:

$$\rho_A = \text{tr}_B \rho_{\text{total}}, \tag{27}$$

where the trace is taken only over the Hilbert space of subsystem B. The entanglement entropy of the subsystem A is defined as

$$S_A = -\text{tr}_A \rho_A \log \rho_A. \tag{28}$$

Usually it is very difficult to calculate entanglement entropy in quantum field theory. However, the AdS/CFT correspondence provides a powerful tool to calculate the entanglement entropy for a strong coupling conformal field theory in a simple way. Suppose that the boundary of the subsystem A is ∂A in the boundary of the AdS space-time. The entanglement entropy of the subsystem A is given by the following formula [27]:

$$S_A = \frac{\text{Area}\,(\gamma_A)}{4G}, \tag{29}$$

where G is the Newton gravitational constant in the AdS bulk and γ is the minimal surface extended into the bulk with boundary $\partial\gamma = \partial A$.

Now we will take formula (29) to calculate the entanglement entropy of the conformal field theory dual to the AdS black hole solution given by (10). To study the entanglement entropy, we should choose a proper region for A. Here we consider a rectangular strip parameterized by the boundary coordinates x and y, and we assume y-direction is infinitely extended and direction x has width ℓ. Thus we can use x to parameterize the minimal surface.

With the help of (6) and (29), we can obtain the area of the minimal surface for the strip geometry as follows:

$$\text{Area}\,(\gamma_A) = L \int_{-\ell/2}^{\ell/2} dx \sqrt{\frac{\left(r'\right)^2}{f\,(r)} + r}, \tag{30}$$

where $r' = dr/dx$ and L is the length along y-direction, which will be set to be unity in what follows. Note that the integrand in (30) does not depend explicitly on x. We can derive the equation of motion of $r(x)$ as

$$\begin{aligned} &4r\,(x)^2\, f\,(r)^2 - 2f\,(r)\, r'\,(x)^2 + r\,(x)\, r'\,(x)^2\, f'\,(r) \\ &\quad - 2f\,(r)\, r r''\,(x) = 0. \end{aligned} \tag{31}$$

Due to the symmetry of the minimal surface, obviously we have

$$\begin{aligned} r\,(0) &= r_0, \\ r'\,(0) &= 0, \end{aligned} \tag{32}$$

at the returning point $r = r_0$ where $x = 0$. With condition (32), we can solve (31) numerically and obtain function $r(x)$. Then substituting $r(x)$ into (30), we can get the entanglement entropy. It is found that the entanglement entropy is always divergent. In order to get more meaningful physically results, we introduce an ultraviolet cut-off. Here we are interested in the regularized entropy $\delta S = S - S_0$, where S_0 is the entanglement entropy for the same geometry, but the bulk is the pure AdS space in Poincare coordinates, which is also calculated with numerical method. In Figure 3, as typical examples, we plot the regularized entanglement entropy versus the temperature of the black hole in the cases $\ell = 0.6$, $\ell = 1.2$ and $\alpha^2 = 1$, $\alpha^2 = 2$, the corresponding ultraviolet cut-off is set to be $r(0.59)$, $r(1.19)$. Comparing Figure 3 with Figure 1, we find that the behavior of the entanglement entropy is quite similar to that of the black hole entropy, and the corresponding minimal temperatures T_{min}, which is shown by solid red line in Figure 3, are the same as those in Figure 1.

In Figure 3, we also show the Hawking-Page transition temperature with dashed green line. With (26), it shows that the ratio between the minimal temperature and Hawking-Page transition temperature also keeps valid in the behavior of the entanglement entropy. In addition, we notice that, with the change of the width ℓ, the entanglement entropy changes consequently, but the phase structure of the entanglement entropy does not changes and the minimal temperature does not change. We can therefore conclude that the entanglement entropy can indeed reveal the phase structure of the AdS phantom black hole.

5. Discussion and Conclusions

Black hole physics is one of important topics in general relativity and quantum gravity. Thermodynamics, quantum mechanics, statistical physics, and information theory are entangled with each other in black hole thermodynamics. It is generally believed that to completely understand black hole thermodynamics will be greatly helpful to establish a self-consistent quantum gravity theory. In this respect, the AdS black hole might play a central role since the AdS/CFT correspondence relates a quantum gravity in AdS space-time to a conformal field theory in the AdS boundary. In this paper, we have presented an AdS black hole solution with Ricci flat horizon in Einstein-phantom scalar theory. The phantom scalar fields only depend on the transverse coordinates x and y and are parameterized by the parameter α (see (9)). However, we noticed that the parameter α can be renormalized to be one by the following rescaling:

$$\begin{aligned} t &\longrightarrow \frac{t}{\alpha}, \\ r &\longrightarrow \alpha r, \\ (x, y) &\longrightarrow \frac{(x, y)}{\alpha}, \\ M &\longrightarrow \alpha^3 M. \end{aligned} \tag{33}$$

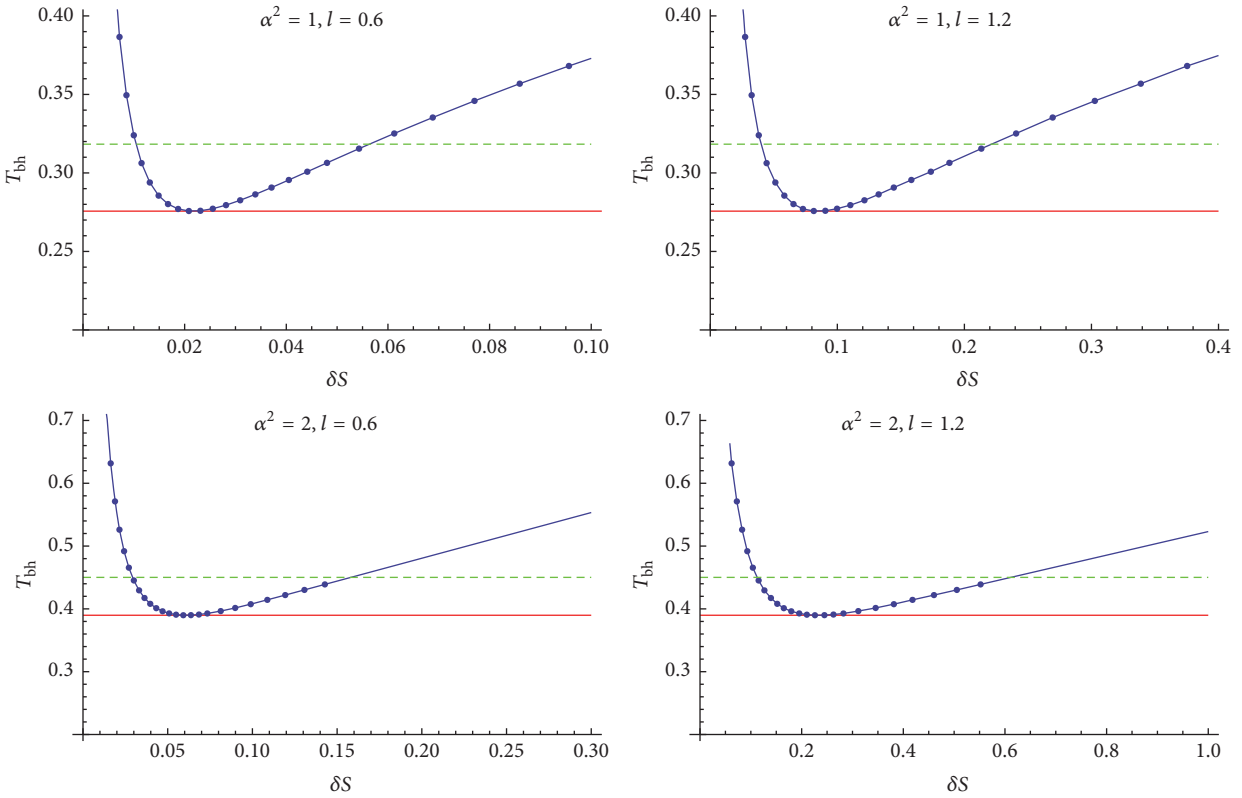

FIGURE 3: The regularized entanglement entropy versus the black hole temperature. The dashed green line represents the Hawking-Page transition temperature, while the solid red line stands for the minimal temperature.

With the rescaling (33), the black hole solution can be rewritten as

$$ds^2 = -g(r)\,dt^2 + g^{-1}(r)\,dr^2 + r^2\left(dx^2 + dy^2\right), \quad (34)$$

with

$$g(r) = 1 + \frac{r^2}{l^2} - \frac{2M}{r}. \quad (35)$$

Comparing this black hole solution with the AdS Schwarzschild black hole,

$$ds^2 = -g(r)\,dt^2 + g^{-1}(r)\,dr^2 + r^2\left(d\theta^2 + \sin^2\theta d\varphi^2\right), \quad (36)$$

we note that the only difference is the replacement of the 2-dimensional Euclidean space R^2 by the 2-dimensional sphere S^2.

Indeed we have found that although its horizon structure is Ricci flat, the AdS black hole with phantom scalar has qualitatively same thermodynamic properties as those of AdS Schwarzschild black hole: there exists a minimal temperature and small black hole is thermodynamically unstable, while large black hole is thermodynamically stable. And in particular, the Hawking-Page phase transition can happen between the AdS phantom black hole and the thermal gas solution in AdS space-time in Poincare coordinate.

Further we have calculated the entanglement entropy of dual conformal field theory for a strip geometry in the AdS boundary by the Ryu-Takayanagi proposal. It was found that the behavior of the entanglement entropy is also qualitatively the same as that of the thermodynamical entropy of the black hole. This example further supports that the black hole entropy might indeed be interpreted as entanglement entropy. On the other hand, it also indicates entanglement entropy is indeed a good probe to phase structure and phase transition in black hole thermodynamics.

Conflicts of Interest

The authors declare that they have no conflicts of interest.

Acknowledgments

This work is supported by Meritocracy Research Funds (463508) of China West Normal University and the authors thank R. G. Cai for helpful suggestions and discussions.

References

[1] S. W. Hawking and D. N. Page, "Thermodynamics of black holes in anti-de Sitter space," *Communications in Mathematical Physics*, vol. 87, no. 4, pp. 577–588, 1983.

[2] J. Maldacena, "The large-N limit of superconformal field theories and supergravity," *International Journal of Theoretical Physics*, vol. 38, no. 4, pp. 1113–1133, 1999.

[3] S. S. Gubser, I. R. Klebanov, and A. M. Polyakov, "Gauge theory correlators from non-critical string theory," *Physics Letters B*, vol. 428, no. 1-2, pp. 105–114, 1998.

[4] E. Witten, "Anti de Sitter space and holography," *Advances in Theoretical and Mathematical Physics*, vol. 2, no. 2, pp. 253–291, 1998.

[5] E. Witten, "Anti-de Sitter space, thermal phase transition, and confinement in gauge theories," *Advances in Theoretical and Mathematical Physics*, vol. 2, no. 3, pp. 505–532, 1998.

[6] J. P. Lemos, "Two-dimensional black holes and planar general relativity," *Classical and Quantum Gravity*, vol. 12, no. 4, pp. 1081–1086, 1995.

[7] J. P. S. Lemos, "Cylindrical black hole in general relativity," *Physics Letters B*, vol. 353, pp. 46–51, 1994.

[8] C. G. Huang and C. B. Liang, "A torus-like black hole," *Physics Letters A*, vol. 201, no. 1, pp. 27–32, 1995.

[9] J. P. Lemos and V. T. Zanchin, "Rotating charged black strings and three-dimensional black holes," *Physical Review D*, vol. 54, no. 6, pp. 3840–3853, 1996.

[10] R.-G. Cai and Y.-Z. Zhang, "Black plane solutions in four-dimensional spacetimes," *Physical Review D*, vol. 54, no. 8, pp. 4891–4898, 1996.

[11] R.-G. Cai, J.-Y. Ji, and K.-S. Soh, "Topological dilaton black holes," *Physical Review D*, vol. 57, no. 10, pp. 6547–6550, 1998.

[12] S. Åminneborg, I. Bengtsson, S. Holst, and P. Peldán, "Making anti-de Sitter black holes," *Classical and Quantum Gravity*, vol. 13, no. 10, pp. 2707–2714, 1996.

[13] R. B. Mann, "Pair production of topological anti-de Sitter black holes," *Classical and Quantum Gravity*, vol. 14, no. 5, pp. L109–L114, 1997.

[14] L. Vanzo, "Black holes with unusual topology," *Physical Review D*, vol. 56, no. 10, pp. 6475–6483, 1997.

[15] D. R. Brill, J. Louko, and P. Peldán, "Thermodynamics of (3 + 1)-dimensional black holes with toroidal or higher genus horizons," *Physical Review D*, vol. 56, no. 6, pp. 3600–3610, 1997.

[16] D. Klemm, V. Moretti, and L. Vanzo, "Rotating topological black holes," *Physical REView D*, vol. 57, pp. 6127–6137, 1998.

[17] R.-G. Cai and K.-S. Soh, "Topological black holes in the dimensionally continued gravity," *Physical Review D*, vol. 59, no. 4, Article ID 044013, 1999.

[18] D. Birmingham, "Topological black holes in anti-de Sitter space," *Classical and Quantum Gravity*, vol. 16, no. 4, pp. 1197–1205, 1999.

[19] R.-G. Cai, "Gauss-Bonnet black holes in AdS spaces," *Physical Review D*, vol. 65, Article ID 084014, 2002.

[20] S. Surya, K. Schleich, and D. M. Witt, "Phase transitions for flat AdS black holes," *Physical Review Letters*, vol. 86, no. 23, pp. 5231–5234, 2001.

[21] R.-G. Cai, S. P. Kim, and B. Wang, "Ricci flat black holes and Hawking-Page phase transition in Gauss-Bonnet gravity and dilaton gravity," *Physical Review D*, vol. 76, no. 2, Article ID 024011, 2007.

[22] A. Anabalón, D. Astefanesei, and D. Choque, "Hairy AdS solitons," *Physics Letters B*, vol. 762, pp. 80–85, 2016.

[23] R. R. Caldwell, "A phantom menace? Cosmological consequences of a dark energy component with super-negative equation of state," *Physics Letters B*, vol. 545, no. 1-2, pp. 23–29, 2002.

[24] E. Babichev, V. Dokuchaev, and Y. Eroshenko, "Black hole mass decreasing due to phantom energy accretion," *Physical Review Letters*, vol. 93, no. 2, Article ID 021102, 2004.

[25] M. Azreg-Aïnou, G. T. Marques, and M. E. Rodrigues, "Phantom black holes and critical phenomena," *Journal of Cosmology and Astroparticle Physics*, vol. 2014, no. 7, article 36, 2014.

[26] H. Quevedo, M. N. Quevedo, and A. Sánchez, "Geometrothermodynamics of phantom AdS black holes," *European Physical Journal C*, vol. 76, no. 3, article 110, 2016.

[27] S. Ryu and T. Takayanagi, "Holographic derivation of entanglement entropy from AdS/CFT," *Physical Review Letters*, vol. 96, Article ID 181602, 2006.

[28] T. Albash and C. V. Johnson, "Holographic studies of entanglement entropy in superconductors," *Journal of High Energy Physics*, vol. 2012, no. 5, article 79, pp. 1–21, 2012.

[29] R.-G. Cai, S. He, L. Li, and Y.-L. Zhang, "Holographic entanglement entropy in P-wave superconductor phase transition," *Journal of High Energy Physics*, vol. 2012, no. 7, article 27, 2012.

[30] R. G. Cai, S. He, L. Li, and L. F. Li, "Entanglement entropy and Wilson loop in Stückelberg holographic insulator/superconductor model," *Journal of High Energy Physics*, vol. 2012, no. 10, article 107, 2012.

[31] R. G. Cai, L. Li, L. F. Li, and R. K. Su, "Entanglement entropy in holographic P-wave superconductor/insulator model," *Journal of High Energy Physics*, vol. 2013, article 63, 2013.

[32] R.-G. Cai, S. He, L. Li, and Y.-L. Zhang, "Holographic entanglement entropy in insulator/superconductor transition," *Journal of High Energy Physics*, vol. 2012, no. 7, article 88, 2012.

[33] L.-F. Li, R.-G. Cai, L. Li, and C. Shen, "Entanglement entropy in a holographic p-wave superconductor model," *Nuclear Physics B*, vol. 894, pp. 15–28, 2015.

[34] C. V. Johnson, "Large N phase transitions, finite volume, and entanglement entropy," *Journal of High Energy Physics*, vol. 2014, article 47, 2014.

[35] X. X. Zeng, H. Zhang, and L. F. Li, "Phase transition of holographic entanglement entropy in massive gravity," *Physics Letters B*, vol. 756, pp. 170–179, 2016.

[36] X.-X. Zeng, X.-M. Liu, and L.-F. Li, "Phase structure of the Born–Infeld–anti-de Sitter black holes probed by non-local observables," *European Physical Journal C*, vol. 76, no. 11, article 616, 2016.

[37] X. X. Zeng and L. F. Li, "Van der waals phase transition in the framework of holography," *Physics Letters B*, vol. 764, pp. 100–108, 2017.

[38] A. Dey, S. Mahapatra, and T. Sarkar, "Thermodynamics and entanglement entropy with Weyl corrections," *Physical Review D*, vol. 94, no. 4, Article ID 026006, 2016.

[39] Y. Bardoux, M. M. Caldarelli, and C. Charmousis, "Shaping black holes with free fields," *Journal of High Energy Physics*, vol. 2012, article 54, 2012.

Hindawi
Advances in High Energy Physics
Volume 2017, Article ID 8358473, 6 pages
https://doi.org/10.1155/2017/8358473

Research Article

Note on Relation between Bottom-Up Holographic Models and Large-N_c QCD

S. S. Afonin

Saint Petersburg State University, 7/9 Universitetskaya nab., St. Petersburg 199034, Russia

Correspondence should be addressed to S. S. Afonin; afonin24@mail.ru

Received 27 June 2017; Revised 23 August 2017; Accepted 27 August 2017; Published 2 October 2017

Academic Editor: Song He

Copyright © 2017 S. S. Afonin. This is an open access article distributed under the Creative Commons Attribution License, which permits unrestricted use, distribution, and reproduction in any medium, provided the original work is properly cited. The publication of this article was funded by SCOAP^3.

We discuss a derivation of the quadratic in fields part of action of bottom-up holographic models from some general properties of the large-N_c limit in QCD. The importance of rescaling of five-dimensional fields is emphasized using the soft wall model as an example.

1. Introduction

The physics of hadrons composed of light quarks are highly nonperturbative as these hadrons represent strongly coupled systems. Some time ago, an interesting proposal of analytical approach to the strongly coupled gauge theories came from the string theory, the hypothesis of AdS/CFT correspondence [1] (also referred to as gauge/gravity duality or holographic duality). It turns out that a description of certain strongly coupled gauge theories can be given in terms of weakly coupled higher-dimensional gravitational theories. The holographic ideas have penetrated into many branches of modern theoretical physics. In the hadron spectroscopy, these ideas are challenging, since the AdS/CFT correspondence provides a practical recipe for calculation of correlation functions in strongly coupled gauge theories. The calculation is performed via the semiclassical expansion of the action of higher-dimensional dual theories [2]. This can have a direct application to the hadron spectroscopy: the masses of hadron states appear as poles of correlation functions of QCD currents interpolating those states.

The concrete holographic prescription is as follows [2]. All correlation functions of a 4D field theory can be obtained from the generating functional of the connected correlators $W_{4D}[\varphi_0(x)]$ which depends on the sources $\varphi_0(x)$ for the 4D field theory operators. If we know the action S_{5D} of dual theory, the holographic correspondence postulates the identification:

$$W_{4D}\left[\varphi_0\left(x\right)\right] = S_{5D}\left[\varphi\left(x,\epsilon\right)\right]. \tag{1}$$

By assumption, the 5D dual theory is in the weakly coupled regime. This implies an important consequence: as the first approximation, one may consider only the quadratic terms in S_{5D} and use the semiclassical analysis. The calculation of n-point correlators consists thus in evaluation of S_{5D} on a solution of equation of motion and subsequent differentiation n times with respect to boundary values of 5D fields.

The bottom-up holographic approach represents an attempt to apply the holographic ideas to QCD. The corresponding models try to describe the nonperturbative dynamics of strong interactions in terms of a putative semiclassical five-dimensional theory. The first versions of bottom-up models, the so-called Hard Wall (HW) models [3, 4], had a problem with description of linear Regge and radial spectrum ($m_n \sim n$ instead of the behavior $m_n^2 \sim n$ expected in the phenomenology and on some theoretical grounds). The construction of the soft wall (SW) holographic model [5] solved this problem.

There is still no consensus on why the bottom-up holographic models turned out to be unexpectedly successful in the phenomenology. This success looks surprising and a bit enigmatic. An inherent property of the holographic duality

is the large-N_c (planar) limit of gauge theories [6, 7]. It is believed therefore that all AdS/QCD models are models for the planar QCD, where mesons represent stable and freely propagating particles (their interactions and decays are suppressed by powers of $1/N_c$ [6, 7]). Within a hypothetical dual theory, the corresponding mass spectrum should emerge in the weak coupling regime; that is, in the first approximation, it must be determined by a quadratic in fields part of action.

The purpose of this work is to demonstrate explicitly that the quadratic in fields parts of actions of typical bottom-up holographic models follows directly from some general expectations about the behavior of correlation functions in the large-N_c limit of QCD. Partly, this analysis was done in [8]. But the derivation in [8] did not take into account the fact that, in general case, one must use rescaled (with respect to the holographic coordinate) fields in order to have finite sources. This is especially important for the scalar and tensor mesons, since it leads to different mass spectra. In the present work, we fix this drawback and provide more justified expressions for meson spectra of SW model. As a byproduct, we also demonstrate the importance of "weak gravity" approximation which allows replacing the covariant derivatives by the usual ones and using an important relation for the 5D mass as a function of spin.

2. The Large-N_c QCD as a Kaluza-Klein Reduction

We recall some general results from the analysis of QCD in the limit of large number of colors N_c [6, 7]. The meson masses scale as $m \sim N_c^0$ and their full decay widths do as $\Gamma \sim N_c^{-1}$. The decay widths thus disappear in the limit of large N_c. Since the meson masses vary slightly with N_c, this limit is often useful in the meson spectroscopy. In the extreme case $N_c \to \infty$, the mesons are infinitely narrow and noninteracting; in addition, an infinite number of states emerge for each set of quantum numbers. Such an infinite tower of resonance poles saturates completely the two-point correlation function of quark currents with quantum numbers $I^G(J^{PC})$ corresponding to the given tower:

$$\left\langle \mathcal{O}_J(q)\, \mathcal{O}_J(-q) \right\rangle \sim \sum_{n=0}^{\infty} \frac{\left(F_n^{(J)}\right)^2}{q^2 - m_{n,J}^2 + i\varepsilon}. \tag{2}$$

With the help of functional integral formalism, this is described by the following action with source terms:

$$I_{[\mathcal{O}_J]} = (-1)^J \int d^4x \sum_{n=0}^{\infty} \left(\partial_\mu \phi_J^{(n)} \partial^\mu \phi_{(n)}^J - m_{n,J}^2 \phi_J^{(n)} \phi_{(n)}^J + \cdots + \phi_{(n)}^J \mathcal{O}_J^{(n)} \right). \tag{3}$$

Here, $\phi_J \doteq \phi_{\mu_1\mu_2\cdots\mu_J}$, $\mu_i = 0, 1, 2, 3$ (the sign convention is $(+---)$), corresponds to a meson field of spin J and the other quantum numbers are unspecified. The tensor ϕ_J is symmetric and traceless, $\phi^\mu_{\mu\cdots} = 0$ (to provide the irreducible $(J/2, J/2)$ representation of the homogeneous Lorentz group), and satisfies the auxiliary condition $\partial^\mu \phi_{\mu\cdots} = 0$ (to give the required $2J + 1$ physical degrees of freedom). The dots denote additional derivative terms appearing in description of free higher spin fields. The auxiliary conditions can be chosen in such a way that they do not make a contribution (to be discussed below). The tensor structure in the right-hand side of representation (2) depends on the structure of derivative terms. The sources $\mathcal{O}_J^{(n)}$ can be represented as

$$\mathcal{O}_J^{(n)} = F_n^{(J)} \mathcal{O}_J, \tag{4}$$

where the constants $F_n^{(J)}$ are defined by

$$\left\langle 0 \left| \mathcal{O}_J^{(n)} \right| \phi_J^{(n)} \right\rangle = F_n^{(J)} \varepsilon_J \tag{5}$$

for a meson $\phi_J^{(n)}$ with "polarization" ε_J and $\mathcal{O}_J$ is a common source to which the states $\phi_{(n)}^J$ are coupled with a "coupling" $F_n^{(J)}$. Representation (4) follows from the requirement to get the standard form for two-point correlators: integrating over the field ϕ_J in the generating functional

$$Z[\mathcal{O}_J] = \int \mathrm{D}\phi_J e^{I_{[\mathcal{O}_J]}}, \tag{6}$$

and differentiating twice with respect to $\mathcal{O}_J$ at $\mathcal{O}_J = 0$, one arrives at the sum over meson poles (2).

Our task is to rewrite expression (3) as a Kaluza-Klein reduction of action of some free 5D theory. We will look for the corresponding 5D actions in the form

$$S_{5D} = (-1)^J \cdot \int d^4x\, dz\, f_1(z) \left(\partial_M \varphi_J \partial^M \varphi^J - m_J^2 f_2(z) \varphi_J \varphi^J \right), \tag{7}$$

where $M = 0, 1, 2, 3, 4$, $\varphi_J = \varphi_{M_1 M_2 \cdots M_J}(x, z)$, and $f_1(z)$ and $f_2(z)$ are yet unknown functions of the fifth (space-like) coordinate z. We start from a flat 5D space having boundaries in the fifth coordinate, $z_{\min} \le z \le z_{\max}$. Action (7) contains a z-dependent background that is different for the kinetic and mass terms.

We will imply the following condition for the physical components of 5D fields,

$$\varphi_{z\cdots} = 0. \tag{8}$$

With this condition, no additional quadratic terms appear in description of free higher spin mesons [5, 9, 10].

The equation of motion for action (7) with condition (8) is

$$-\partial_z \left[f_1(z)\, \partial_z \varphi_n^{(J)}(z) \right] + f_1(z)\, f_2(z)\, m_J^2 \varphi_n^{(J)}(z) = m_{n,J}^2 f_1(z)\, \varphi_n^{(J)}(z), \tag{9}$$

where we used the usual plane-wave ansatz for the physical 4D particles carrying the 4D momentum q_n:

$$\varphi(x, z) = e^{iq_n x} \varphi_n(z), \qquad q_n^2 = m_n^2. \tag{10}$$

After imposing boundary conditions on the fields, (9) represents a classical Sturm-Liouville (SL) problem. Consider the following mathematical problem: given a spectrum $m_{n,J}^2$ in (3), find the functions $f_1(z)$ and $f_2(z)$ which, being inserted in (9), would lead to eigenvalues $m_{n,J}^2$. The solution of this "inverse" SL problem constitutes the main intermediate step in rewriting action (3) with sources as some free 5D field theory.

First, we recall briefly the main results of the SL theory. The SL equation is

$$-\partial_z \left[p(z)\,\partial_z\varphi\right] + q(z)\,\varphi = \lambda\omega(z)\,\varphi. \tag{11}$$

Here the function $p(z) > 0$ has a continuous derivative; the functions $q(z) > 0$ and $\omega(z) > 0$ are continuous on the finite closed interval $[z_{\min}, z_{\max}]$. The SL problem consists in finding the values of λ for which there exists a nontrivial solution of (11) satisfying certain boundary conditions. Under the assumptions that $p(z)^{-1}$, $q(z)$, and $\omega(z)$ are real-valued integrable functions over the interval $[z_{\min}, z_{\max}]$, with the boundary conditions of the form

$$\varphi(z_{\min})\cos\alpha - p(z_{\min})\,\varphi'(z_{\min})\sin\alpha = 0, \tag{12}$$

$$\varphi(z_{\max})\cos\beta - p(z_{\max})\,\varphi'(z_{\max})\sin\beta = 0, \tag{13}$$

where $\alpha, \beta \in [0, \pi)$ and prime means derivative, the SL theorem states that (i) there is an infinite discrete set of real eigenvalues λ_n, $n = 0, 1, 2, \ldots$, (ii) up to a normalization constant, there is a unique eigenfunction $\varphi_n(z)$ corresponding to each eigenvalue λ_n and this eigenfunction has exactly $n-1$ zeros in $[z_{\min}, z_{\max}]$, and (iii) the normalized eigenfunctions form an orthonormal basis:

$$\int_{z_{\min}}^{z_{\max}} \varphi_m(z)\,\varphi_n(z)\,\omega(z)\,dz = \delta_{mn}. \tag{14}$$

Thus the solutions of the SL problem form a complete set of functions in the interval $[z_{\min}, z_{\max}]$ which can be used for expansion of arbitrary (but sufficiently smooth) functions in that interval.

Under these conditions, the SL problem (9) has solutions $\varphi_n^{(J)}(z)$ which are normalized as

$$\int_{z_{\min}}^{z_{\max}} f_1(z)\,\varphi_m^{(J)}(z)\,\varphi_n^{(J)}(z)\,dz = \delta_{mn} \tag{15}$$

and form a complete set of functions. The function $\varphi_J(x,z)$ in (7) can be expanded in the 4D harmonics:

$$\varphi_J(x,z) = \sum_{n=0}^{\infty} \phi_J^{(n)}(x)\,\varphi_n^{(J)}(z). \tag{16}$$

Now we substitute expansion (16) into action (7):

$$\begin{aligned} S_{5D} = (-1)^J \int d^4x\,dz\,f_1(z) \sum_{m,n=0}^{\infty} \Big\{ & \varphi_m^{(J)}\varphi_n^{(J)}\partial_\mu\phi_J^{(m)}\partial_\mu\phi_J^{(n)} \\ & - \phi_J^{(m)}\phi_J^{(n)}\partial_z\varphi_m^{(J)}\partial_z\varphi_n^{(J)} \\ & - m_J^2 f_2(z)\,\varphi_m^{(J)}\varphi_n^{(J)}\phi_J^{(m)}\phi_J^{(n)}\Big\}. \end{aligned} \tag{17}$$

Integrating by parts and making use of (9), the second term in action (17) can be rewritten as (dropping the general factor $-\phi_J^{(m)}\phi_J^{(n)}$)

$$\begin{aligned} & \int_{z_{\min}}^{z_{\max}} dz\,f_1(z)\,\partial_z\varphi_m^{(J)}\partial_z\varphi_n^{(J)} \\ & \quad = \varphi_m^{(J)} f_1(z)\,\partial_z\varphi_n^{(J)}\Big|_{z_{\min}}^{z_{\max}} \\ & \qquad + \int_{z_{\min}}^{z_{\max}} dz\,\varphi_m^{(J)}\varphi_n^{(J)} g_J(z)\left(m_{n,J}^2 - f_2(z)\,m_J^2\right). \end{aligned} \tag{18}$$

Integrating over z in action (17) with the help of (15) and (18), we obtain

$$\begin{aligned} S_{5D} = (-1)^J \int d^4x \sum_{n=0}^{\infty} \Big\{ & \left(\partial^\mu\phi_{(n)}^J\right)^2 - m_{n,J}^2\left(\phi_{(n)}^J\right)^2 \\ & - \phi_{(n)}^J f_1(z)\,\partial_z\varphi_n^{(J)}\varphi_J(x,z)\Big|_{z_{\min}}^{z_{\max}}\Big\}, \end{aligned} \tag{19}$$

with $\varphi_J(x,z)$ given by (16). Action (19) has the form of (3) if we identify

$$\mathcal{O}_J^{(n)} = -\,f_1(z)\,\partial_z\varphi_n^{(J)}\varphi_J(x,z)\Big|_{z_{\min}}^{z_{\max}}. \tag{20}$$

The classical Kaluza-Klein reduction corresponds to $\mathcal{O}_J^{(n)} = 0$. But the case $\mathcal{O}_J^{(n)} \neq 0$ is possible as well. And this very possibility turns out to be equivalent to the holographic prescription for obtaining 4D Green's functions.

Choosing $\beta = 0$ or $\beta = \pi/2$ in the boundary condition (13), we can nullify the term at $z = z_{\max}$ in (20). Note in passing that for the vector mesons the first possibility is actually realized in the SW holographic models [5], where $z_{\max} \to \infty$, while the second one is realized in the HW models [3, 4], where $z_{\max}$ is the infrared cutoff. Thus,

$$\mathcal{O}_J^{(n)} = \lim_{z \to z_{\min}+0} f_1(z)\,\partial_z\varphi_n^{(J)}(z)\,\varphi_J(x,z). \tag{21}$$

3. From Large-N_c QCD to Bottom-up Holographic Models

Action (7) can be rewritten as a "weakly coupled" 5D gravitational theory of free field φ_J with the metric

$$ds^2 = f_2(z)\left(dx_\mu dx^\mu - dz^2\right), \tag{22}$$

which dictates the corresponding metric tensor G_{MN} and the background function $f_1(z)$:

$$f_1(z) = \sqrt{\left|\det G_{MN}\right|} = f_2^{5/2}(z). \tag{23}$$

We must impose the covariant rule for contraction of indices:

$$\begin{aligned} & \partial_M\varphi_J\partial^M\varphi^J \\ & \quad = \partial_M\varphi_{M_1\cdots M_J}\partial_{M'}\varphi_{M_1'\cdots M_J'}G^{MM'}G^{M_1M_1'}\cdots G^{M_JM_J'}, \end{aligned} \tag{24}$$

where

$$G^{MN} = G^{-1}_{MN} = f_2^{-1}(z)\,\eta^{MN}. \tag{25}$$

This can be achieved only if the function $f_1(z)$ in (23) is replaced by the J-dependent background:

$$f_1^{(J)}(z) = f_2^{(3/2)-J}(z). \tag{26}$$

All this just rearranges the notations but does not change our discussions above.

The choice

$$f_2(z) = \frac{R^2}{z^2}, \quad 0 \le z < \infty \tag{27}$$

in (22) corresponds to the AdS space of radius R. This choice will be exploited in what follows to find connections with the holographic approach.

Now we should identify the general source $\mathcal{O}_J$. The identification must provide finite and nonzero values for constants $F_n^{(J)}$ in representation (4). Our prescription is

$$\mathcal{O}_J = \frac{z f_1^{(J)} \varphi_J}{c} \sim \frac{z^{2(J-1)} \varphi_J}{c}, \tag{28}$$

$$F_n^{(J)} = \lim_{z\to+0} c \frac{\partial_z \varphi_n^{(J)}(z)}{z}. \tag{29}$$

The eigenfunctions $\varphi_n^{(J)}(z)$ in the AdS space behave as z^2 at small z for the twist-2 operators, that is, when relation (36) holds [8]. This ensures constant values for $F_n^{(J)}$ in (29). The appearance of factor c is due to freedom to redefine $F_n \to cF_n$ and $\mathcal{O} \to \mathcal{O}/c$, where the parameter c can be fixed by matching to the high energy asymptotics of the corresponding QCD correlators. For the case of vector mesons, our way of getting relation (29) is alternative (up to a general factor depending on normalization of fields) to the derivation of [3].

Relation (28) shows that if we want, following the AdS/CFT prescriptions, to interpret the source as a finite boundary value of a 5D field, $\varphi_J(x, +0) = \mathcal{O}_J$, we must rescale the higher spin ($J > 1$) fields:

$$\varphi_J = z^{2(1-J)} \widetilde{\varphi}_J. \tag{30}$$

In this sense, the physical tensor field is the rescaled one, $\widetilde{\varphi}_J$. This statement was obtained in [9] using a different approach.

Now we see that the holographic prescription for calculation of correlation functions in a 4D theory from a "dual" 5D theory is completely reconstructed on the level of quadratic in fields actions. The higher vertices (describing meson decays and scattering) are suppressed in the large-N_c limit and we therefore do not consider them.

Some clarifying remarks should be made. Since the AdS space is not flat, the usual derivatives must be replaced by the covariant ones in the case of tensor mesons. However, the holographic duality for strongly coupled 4D theories works only if the dual 5D theories are weakly coupled. This means that we should use the "weak gravity" limit (very large AdS radius) as the first approximation. In this limit, the affine connections are neglected as the AdS space locally is almost flat. This justifies the use of usual derivatives for higher spin mesons in our analysis.

The second remark concerns the standard statement that the spectrum of the HW model depends on the boundary conditions. Indeed, the Dirichlet boundary conditions that have been used since the pioneering papers [3, 4] correspond to the choice $\beta = \pi/2$ in (13) and seemingly one could use any other choice for β. There is, however, a subtle point here. With other choices, generally speaking, the boundary contribution at $z = z_{\max}$ is not zero. This means the appearance of the second source that would look strange for the standard functional technics (the existence of two sources is not necessarily senseless in the real strong interactions, where the physical degrees of freedom at low and high energies are different (pseudo-Goldstone bosons versus quarks and gluons). For instance, the quark vector current $\vec{q}\vec{\tau}\gamma_\mu q$ interpolates the ρ-meson at high enough energies, where the current quarks are well defined. At low enough energies, the ρ-meson could be considered as a two-pion state interpolated by the current $\pi^a \overrightarrow{\tau} \overleftrightarrow{\partial_\mu} \pi^b$. The ultraviolet and infrared sources should be then different as long as the physical degrees of freedom are different. As far as we know, this possibility was not exploited in the bottom-up approach).

The last remark concerns the choice of background in the 5D action. It can be shown that if we want to reproduce the linear Regge spectrum and simultaneously the correct analytical structure of the operator product expansion of the two-point correlators, the background is fixed unambiguously; it corresponds to nothing but the SW model to be discussed in the next section. The corresponding analysis is presented in detail in [8].

4. Spectrum of the Soft Wall Model

An attractive feature of the SW holographic models is the Regge spectrum for meson masses [5]. The original derivation of [5] was based on gauge higher spin fields. Condition (8) was interpreted as a gauge choice. A residual invariance after imposing (8) (that canceled the additional derivative terms) allowed eliminating the mass term for the rescaled fields (30). Below we reproduce the Regge spectrum of [5] using the massive higher spin fields and our discussions above.

The action of SW model is a particular case of (7) written in the AdS space:

$$S_{5D} = (-1)^J \cdot \int d^4x\, dz \sqrt{|\det G|}\, e^{az^2} \left(\partial_M \varphi_J \partial^M \varphi^J - m_J^2 \varphi_J \varphi^J\right), \tag{31}$$

where the dilaton background e^{az^2} was introduced to get the Regge spectrum. Substituting the rescaled field (30) and lowering all indices, we find

$$S_{5D} = (-1)^J R^{2J-1} \int d^4x\, dz\, e^{az^2} \left\{ \left(\partial_M \widetilde{\varphi}_J\right)^2 z^{1-2J} - \left((2-2J)^2 + m_J^2 R^2\right) z^{-1-2J} \widetilde{\varphi}_J^2 - 4\,(1-J)\, z^{-2J} \widetilde{\varphi}_J \partial_z \widetilde{\varphi}_J \right\}. \tag{32}$$

The corresponding equation of motion for physical modes (10) reads

$$-\partial_z \left[\frac{e^{az^2}}{z^{2J-1}} \partial_z \widetilde{\varphi}_{n,J} \right] + \frac{m_J^2 R^2 - 4\,(J-1)}{z^{2J+1}} e^{az^2} \widetilde{\varphi}_{n,J} = m_{n,J}^2 \frac{e^{az^2}}{z^{2J-1}} \widetilde{\varphi}_{n,J}. \tag{33}$$

The SL equation (33) has the following discrete spectrum:

$$m_{n,J}^2 = 2\,|a| \cdot \left[2n + 1 + \frac{a}{|a|}\,(1-J) + \sqrt{J^2 + m_J^2 R^2 - 4\,(J-1)} \right]. \tag{34}$$

This spectrum depends on the 5D mass m_J. The free p-form fields in the AdS_5 space have masses $m_p^2 R^2 = (\Delta - p)(\Delta + p - 4)$. As was shown in [10], condition (8) leads to decoupling of kinematical aspects and the symmetric tensors of rank p (describing mesons of spin p) obey the same equation as the p-form fields. In the "weak gravity" approximation, this results in the following 5D mass of higher spin fields propagating in the AdS_5 space [10, 11]:

$$m_J^2 R^2 = (\Delta - J)\,(\Delta + J - 4), \tag{35}$$

where Δ is the canonical dimension of operator in a 4D field theory. This operator is regarded as being dual to a corresponding 5D field on the AdS boundary.

The spectrum of the original SW model [5] corresponds to the operators of twist-2; that is, $\Delta = J + 2$. Substituting this dimension into (35), we have

$$m_J^2 R^2\big|_{\Delta = J+2} = 4\,(J-1). \tag{36}$$

Spectrum (34) reduces then to the spectrum of [5]:

$$m_{n,J}^2 = 2\,|a| \left[2n + J + 1 + \frac{a}{|a|}\,(1-J) \right]. \tag{37}$$

As was noticed in [5], the spectrum does not depend on spin if $a > 0$. The standard SW model has $a < 0$ and this choice dictates a remarkably simple Regge spectrum $m_{n,J}^2 = 4|a|(n + J)$ which coincides with the spectrum of poles of the Veneziano amplitude.

In fact, only the 5D mass (36) is to be substituted into (34) because if the twist is different from 2, then prescriptions (28) and (29) must be changed since a constant value of the source on the boundary $z = 0$ is provided by a different rescaling rule. This becomes especially important in the scalar sector. The case $J = 0$ in (37) formally corresponds to the spectrum of mesons interpolated by a scalar operator of canonical dimension $\Delta = 2$. But such a gauge-invariant operator cannot be constructed in QCD, where the simplest scalar operator is the twist-3 quark bilinear $\overline{q}q$. The corresponding 5D mass for $\Delta = 3$ is $m_J^2 R^2 = -3$ and the constant boundary value of the scalar source requires rescaling $\varphi \to z\widetilde{\varphi}$ [3]. It can be easily checked that the scalar spectrum coincides then with the vector one in (37):

$$m_{n,0}^2\big|_{\Delta=3} = 4\,|a|\,(n+1). \tag{38}$$

A 5D field dual on the boundary $z = 0$ to a scalar operator of twist-4 (such as the gluon operator $\alpha_s G_{\mu\nu}^2$) does not require rescaling; the corresponding mass spectrum is known to be

$$m_{n,0}^2\big|_{\Delta=4} = 2\,|a| \left[2n + 3 - \frac{a}{|a|} \right]. \tag{39}$$

The phenomenology again favors the choice of negative dilaton background: $a < 0$.

For the purposes of phenomenological applications, it can be interesting to construct an extension of the SW model which leads to a shifted Regge spectrum, $m_{n,J}^2 = 4|a|(n + J + b)$, where b is a phenomenological parameter regulating the intercept of Regge and radial trajectories. Such an extension was constructed in [12] for the vector case. The method of [12] can be generalized to higher spins. We will not display the derivation in detail and will just give the final answer that can be checked by a direct calculation: the dilaton background e^{az^2} must be replaced by

$$e^{az^2} \longrightarrow e^{az^2} U^2\left(b, -|J-1|; |a|\,z^2\right), \tag{40}$$

where U is Tricomi's hypergeometric function.

5. Conclusion

In essence, we tried to demonstrate that the bottom-up holographic approach to QCD represents nothing but a five-dimensional language for expressing some general expectations from the large-N_c limit in QCD. This interpretation is valid only for holographic actions quadratic in fields.

We emphasized the importance of rescaling of five-dimensional fields for correct derivation of meson spectra. The simplest SW holographic model was used as a typical example. The action of SW model is purely phenomenological and is constructed with the aim of getting the linear Regge spectrum. It is not known which 5D dynamical model results in the background e^{az^2} as a solution of 5D Einstein equations. An "intermediate" dynamical model that leads to such a background could look as follows:

$$S = \int d^4x\, dz \sqrt{g} \left(\partial_M \phi \partial^M \phi - m^2 \phi^2 + e^{\phi} \mathscr{L} \right), \tag{41}$$

where the action is written in the AdS_5 space and $\mathscr{L}$ represents a Lagrangian density for the meson sector. The

dilaton coupling in the form $e^{\phi}\mathscr{L}$ is typical in the string theory. If the 5D mass squared m^2 of the dilaton field ϕ takes the minimal value permitted in the AdS_5 space, $m^2R^2 = -4$ (the Breitenlohner-Freedman stability bound [13]) and one neglects back-reaction from $\mathscr{L}$; then the equation of motion for ϕ will have a solution $\phi = az^2$. This solution leads to the z-dependent background of SW model. One may speculate that the dilaton field ϕ in (41) mimics the nonperturbative gluodynamics. In the large-N_c limit, the gluon sector dominates. For instance, the probability of creation of glueballs scales as $\mathcal{O}(N_c^2)$, while that of mesons scales as $\mathcal{O}(N_c)$ [6, 7]. We do not see an abundant production of glueballs in the real world just because we cannot create experimentally the corresponding gluon currents. But theoretically the scaling $\mathcal{O}(N_c^2)$ of gluon sector justifies neglecting back-reaction from $\mathscr{L}$ in the first approximation. In any case, the simplest SW model should be viewed as an approximation in which a dynamical dilaton field is replaced by a static dilaton background dictated by the phenomenology.

The use of the bottom-up models is much broader than just modelling the hadron spectra; it includes description of the spontaneous chiral symmetry breaking in QCD, hadron form factors, QCD phase diagram, and so forth. The corresponding applications usually contain certain extensions of simple bottom-up models that go beyond the large-N_c limit or have no clear connections with the planar QCD. Establishing these connections is an open problem.

Conflicts of Interest

The author declares that there are no conflicts of interest.

References

[1] J. Maldacena, "The large N limit of superconformal field theories and supergravity," *Advances in Theoretical and Mathematical Physics*, vol. 2, no. 2, pp. 231–252, 1998.

[2] E. Witten, "Anti de Sitter space and holography," *Advances in Theoretical and Mathematical Physics*, vol. 2, no. 2, pp. 253–291, 1998.

[3] J. Erlich, E. Katz, D. T. Son, and M. A. Stephanov, "QCD and a holographic model of hadrons," *Physical Review Letters*, vol. 95, no. 26, Article ID 261602, 2005.

[4] L. Da Rold and A. Pomarol, "Chiral symmetry breaking from five-dimensional spaces," *Nuclear Physics B*, vol. 721, no. 1–3, pp. 79–97, 2005.

[5] A. Karch, E. Katz, D. T. Son, and M. A. Stephanov, "Linear confinement and AdS/QCD," *Physical Review D*, vol. 74, no. 1, Article ID 015005, 2006.

[6] G. t Hooft, "A planar diagram theory for strong interactions," *Nuclear Physics B*, vol. 72, p. 461, 1974.

[7] E. Witten, "Baryons in the 1/n expansion," *Nuclear Physics B*, vol. 160, p. 57, 1979.

[8] S. S. Afonin, "Holographic like models as a five-dimensional rewriting of large-Nc QCD," *International Journal of Modern Physics A*, vol. 25, p. 5683, 2010.

[9] E. Katz, A. Lewandowski, and M. D. Schwartz, "Tensor mesons in AdS/QCD," *Physical Review D*, vol. 74, no. 8, Article ID 086004, 2006.

[10] G. F. de Téramond and S. J. Brodsky, "Light-Front Holography: A First Approximation to QCD," *Physical Review Letters*, vol. 102, no. 8, 2009.

[11] T. Gutsche, V. E. Lyubovitskij, I. Schmidt, and A. Vega, "Dilaton in a soft-wall holographic approach to mesons and baryons," *Physical Review D*, vol. 85, Article ID 076003, 2012.

[12] S. S. Afonin, "Generalized soft wall model," *Physics Letters B*, vol. 719, no. 4-5, pp. 399–403, 2013.

[13] P. Breitenlohner and D. Z. Freedman, "Stability in gauged extended supergravity," *Annals of Physics*, vol. 144, no. 2, pp. 249–281, 1982.

Hindawi
Advances in High Energy Physics
Volume 2017, Article ID 8185690, 11 pages
https://doi.org/10.1155/2017/8185690

Research Article

Bulk Local Operators, Conformal Descendants, and Radial Quantization

Zhao-Long Wang[1,2] and Yi Yan[1,2]

[1] *Institute of Modern Physics, Northwest University, Xi'an 710069, China*
[2] *Shaanxi Key Laboratory for Theoretical Physics Frontiers, Xi'an 710069, China*

Correspondence should be addressed to Zhao-Long Wang; zlwang4@gmail.com

Received 5 July 2017; Accepted 13 August 2017; Published 2 October 2017

Academic Editor: Zhang-Yu Nie

Copyright © 2017 Zhao-Long Wang and Yi Yan. This is an open access article distributed under the Creative Commons Attribution License, which permits unrestricted use, distribution, and reproduction in any medium, provided the original work is properly cited. The publication of this article was funded by SCOAP[3].

We establish a construction of the bulk local operators in AdS by considering CFT at finite energy scale. Without assuming any prior knowledge about the bulk, the solution to the bulk free field equation automatically appears in the field theory arguments. In the radial quantization formalism, we find a properly regularized version of our initial construction. Possible generalizations beyond pure AdS are also discussed.

1. Introduction

The AdS/CFT correspondence [1–4] implies a duality between the quantum gravity in $d+1$-dimensional anti-de Sitter space and the d-dimensional conformal field theory which is defined on the boundary of AdS_{d+1}. The AdS metric in the Poincaré patch is given by

$$\mathrm{d}s^2 = \frac{1}{z^2}\left(\mathrm{d}z^2 + \eta_{\mu\nu}\mathrm{d}x^\mu \mathrm{d}x^\nu\right), \tag{1}$$

where the boundary is the d-dimensional flat space at $z = 0$. The relations between the boundary data of AdS and the CFT quantities have been well established in [4] by the field-operator correspondence. That is, the correlators of a conformal primary operator $\mathcal{O}(x)$ in the CFT are reproduced by the asymptotical data of a bulk field ϕ near the boundary. However, the explicit CFT construction of the bulk local degree of freedoms $\phi(x,z)$ inside the AdS space is not well understood yet. The earlier attempts [5–7] suggested to reconstruct $\phi(x,z)$ by propagating the bulk modes from the bulk to the boundary, and then [8–10] showed that it is equivalent to the smearing operator construction. In this letter, we suggest a different construction based on almost purely CFT arguments. In Section 2.1, we establish the construction by considering CFT at finite energy scale. The possible divergence and the prescription of regulator are discussed in Section 2.2. Then in Section 3, we find that our construction can get improved in the radial quantization formalism. We summarize our main results in Section 4, and a possible way of generalizing the construction beyond pure AdS is also proposed there.

2. CFT Construction of Bulk Local Operators

2.1. Renormalized Primary at Finite Energy Scale. It has been pointed out qualitatively [1–4, 11] that the bulk radial direction z is related to the energy scale in the dual field theory. In order to reconstruct $\phi(x,z)$, the first candidate is to consider in CFT the renormalized primary operator $\mathcal{O}(x,\mu)$ which is defined at a finite energy scale μ. On the other hand, the behaviors of a primary operator under the conformal transformation have already been encoded in its conformal family. Thus it is natural to expect, at least in the leading order, that the renormalization of the primary operator at a finite energy scale will lead to a mixing between the primary operator and its descendants

$$\mathcal{O}(x,\mu) = Z(\mu,\partial)\,\mathcal{O}(x). \tag{2}$$

For simplicity, we will only consider the scalar operator from now on. It is also natural to require that the renormalized

primary operator recovers the Lorentz properties and the scaling dimension of the original primary. Then we find it can only be in the following form:

$$\mathcal{O}(x,\mu) = Z\left(\mu^{-2}\Box\right)\mathcal{O}(x). \tag{3}$$

Is it possible to fix the explicit form of $Z(\mu^{-2}\Box)$ by imposing certain renormalization condition? The idea is to give the word "primary" a renormalized meaning. In the usual CFT language, the definition of a primary operator is equivalent to requiring that it transforms as a tensor under conformal transformations. We also notice that the renormalization scale μ will transform nontrivially under conformal transformations. Thus a direct guess is that the proper renormalization condition should be the following.

The renormalized primary transforms as a tensor under the generalized conformal transformations including the energy scale.

To address the generalized conformal transformations including the energy scale, let us firstly review the realization of conformal algebra on the x-space. Acting on the coordinates x^μ, the conformal generator can be expressed as follows:

$$\begin{aligned} P_\mu\circ &= -i\partial_\mu, \\ M_{\mu\nu}\circ &= -i\left(x_\mu\partial_\nu - x_\nu\partial_\mu\right), \\ D\circ &= -ix^\mu\partial_\mu, \\ K_\mu\circ &= -i\left(x^2\partial_\mu - 2x_\mu x^\nu\partial_\nu\right). \end{aligned} \tag{4}$$

It implies the standard conformal algebra

$$\begin{aligned} &\left[P_\mu, P_\nu\right] = 0, \\ &\left[M_{\mu\nu}, M_{\rho\sigma}\right] \\ &\quad = i\left(\eta_{\mu\rho}M_{\nu\sigma} + \eta_{\nu\sigma}M_{\mu\rho} - \eta_{\nu\rho}M_{\mu\sigma} - \eta_{\mu\sigma}M_{\nu\rho}\right), \\ &\left[M_{\mu\nu}, P_\rho\right] = i\left(\eta_{\mu\rho}P_\nu - \eta_{\nu\rho}P_\mu\right), \\ &\left[M_{\mu\nu}, K_\rho\right] = i\left(\eta_{\mu\rho}K_\nu - \eta_{\nu\rho}K_\mu\right), \\ &\left[D, M_{\mu\nu}\right] = 0, \\ &\left[D, K_\mu\right] = -iK_\mu, \\ &\left[D, P_\mu\right] = iP_\mu, \\ &\left[K_\mu, K_\nu\right] = 0, \\ &\left[K_\mu, P_\nu\right] = -2iM_{\mu\nu} - 2i\eta_{\mu\nu}D. \end{aligned} \tag{5}$$

To include the energy scale (for different approaches of introducing the finite energy scale, see [12, 13].), a straightforward way is to add ∂/∂_μ as well as μ-dependent coefficients into the realization (4). For latter convenience, we define $z \equiv 1/\mu$ and equivalently consider z instead. From the fact that the energy scale is Poincaré invariant, we conclude that the forms of P_μ and $M_{\mu\nu}$ remain intact. The scaling dimension of energy scale is obviously 1; thus we can easily write down the following generalized form of dilatation D:

$$D\circ = -i\left(z\partial_z + x^\mu\partial_\mu\right). \tag{6}$$

For the special conformal generator, the strategy is to take its most general ansatz

$$K_\mu\circ = -i\left[x^2\delta_\mu^\nu - 2x_\mu x^\nu + f_\mu{}^\nu(z,x)\right]\partial_\nu - ig_\mu(z,x)\partial_z \tag{7}$$

and then try to find the explicit form which satisfies the conformal algebra.

From $[K_\mu, P_\nu] = -2iM_{\mu\nu} - 2i\eta_{\mu\nu}D$, we get

$$2\eta_{\mu\nu}z\partial_z = -\partial_\nu f_\mu{}^\rho(z,x)\partial_\rho - \partial_\nu g_\mu(z,x)\partial_z. \tag{8}$$

It implies that

$$\begin{aligned} f_\mu{}^\nu(z,x) &= \delta_\mu^\nu f(z), \\ g_\mu(z,x) &= -2x_\mu z. \end{aligned} \tag{9}$$

From $[D, K_\mu] = -iK_\mu$, we further get

$$f(z) = \alpha z^2, \tag{10}$$

where α is an arbitrary constant. Finally, we can check that the above results satisfy $[K_\mu, K_\nu] = 0$. In conclusion, we have

$$\begin{aligned} P_\mu\circ &= -i\partial_\mu, \\ M_{\mu\nu}\circ &= -i\left(x_\mu\partial_\nu - x_\nu\partial_\mu\right), \\ D\circ &= -i\left(z\partial_z + x^\mu\partial_\mu\right), \\ K_\mu\circ &= -i\left[\left(x^2 + \alpha z^2\right)\partial_\mu - 2x_\mu x^\rho\partial_\rho - 2x_\mu z\partial_z\right]. \end{aligned} \tag{11}$$

In fact, this is exactly the isometry generator of the AdS space when $\alpha > 0$ and it suggests to identify $\sqrt{\alpha}z$ here with the standard AdS radial coordinate. We also notice that it corresponds to dS_{d+1} when α is negative, but we will only concentrate on the AdS case in this paper.

Given the generalized conformal transformation including the energy scale (11), we can try to decide the form of $Z(z^2\Box)$ by our renormalization condition on primary. For a scalar in the $\{x, z\}$ space, we can expand it by powers of z

$$\Phi(z,x) = z^\Delta\sum_{n=0}^{\infty} z^n\Phi_n(x). \tag{12}$$

The scalar transformation rule

$$\widetilde{\Phi}(\widetilde{z},\widetilde{x}) = \Phi(z,x) \tag{13}$$

implies that the terms appearing in the power expansion should transform as follows:

$$\begin{aligned}
&\left[P_\mu, \Phi_n(x)\right] = i\partial_\mu \Phi_n(x),\\
&\left[M_{\mu\nu}, \Phi_n(x)\right] = i\left(x_\mu\partial_\nu - x_\nu\partial_\mu\right)\Phi_n(x),\\
&\left[D, \Phi_n(x)\right] = i\left(\Delta + n + x^\mu\partial_\mu\right)\Phi_n(x),\\
&\left[K_\mu, \Phi_0(x)\right] = i\left[x^2\partial_\mu - 2x_\mu x^\nu\partial_\nu - 2x_\mu\Delta\right]\Phi_0(x),\\
&\left[K_\mu, \Phi_1(x)\right]\\
&\quad = i\left[x^2\partial_\mu - 2x_\mu x^\nu\partial_\nu - 2x_\mu(\Delta+1)\right]\Phi_1(x),\\
&\left[K_\mu, \Phi_n(x)\right]\\
&\quad = i\alpha\partial_\mu\Phi_{n-2}(x)\\
&\qquad + i\left[x^2\partial_\mu - 2x_\mu x^\nu\partial_\nu - 2x_\mu(\Delta+n)\right]\Phi_n(x)\\
&\qquad\qquad (n>1).
\end{aligned} \tag{14}$$

Now the task is to construct $\Phi_n(x)$ by the primary $\mathcal{O}$ and its scalar descendants $\Box^m\mathcal{O}$. From the conformal transformation rules of the primary we can deduce that

$$\begin{aligned}
&\left[P_\mu, \Box^n\mathcal{O}(x)\right] = i\partial_\mu\Box^n\mathcal{O}(x),\\
&\left[M_{\mu\nu}, \Box^n\mathcal{O}(x)\right] = \left[i\left(x_\mu\partial_\nu - x_\nu\partial_\mu\right) + \Sigma^{(\mathcal{O})}_{\nu\rho}\right]\Box^n\mathcal{O}(x),\\
&\left[D, \Box^n\mathcal{O}(x)\right] = i\left(\Delta + 2n + x^\mu\partial_\mu\right)\Box^n\mathcal{O}(x),\\
&\left[K_\mu, \mathcal{O}(x)\right] = \left[i\left(x^2\partial_\mu - 2x_\mu x^\nu\partial_\nu - 2x_\mu\Delta\right) - 2x^\nu\Sigma^{(\mathcal{O})}_{\mu\nu}\right]\\
&\quad\cdot\mathcal{O}(x),\\
&\left[K_\mu, \Box^n\mathcal{O}(x)\right] = 2n\left[d - 2(\Delta+n)\right]i\partial_\mu\Box^{n-1}\mathcal{O}(x)\\
&\quad - 4n\Sigma^{(\mathcal{O})}_{\mu\nu}\partial^\nu\Box^{n-1}\mathcal{O}(x)\\
&\quad + \left[i\left(x^2\partial_\mu - 2x_\mu x^\rho\partial_\rho - 2x_\mu(\Delta+2n)\right) - 2x^\rho\Sigma^{(\mathcal{O})}_{\mu\rho}\right]\\
&\quad\cdot\Box^n\mathcal{O}(x)\\
&\qquad\qquad (n\geq 1).
\end{aligned} \tag{15}$$

Comparing with (14), it implies the unique identification

$$\begin{aligned}
\Phi_{2n+1} &= 0,\\
\Phi_{2n} &= \frac{(-1)^n\alpha^n\Gamma(\Delta - d/2 + 1)}{4^n n!\Gamma(\Delta - d/2 + n + 1)}\Box^n\mathcal{O}.
\end{aligned} \tag{16}$$

In conclusion, up to an overall constant, our arguments show that the renormalized primary at energy scale $\mu = 1/z$ is given by

$$\begin{aligned}
\mathcal{O}(x,z) &= Z\left(z^2\Box\right)\mathcal{O}(x)\\
&= {}_0F_1\left(;\Delta - \frac{d}{2} + 1; -\frac{\alpha z^2}{4}\Box\right)\mathcal{O}(x),
\end{aligned} \tag{17}$$

and $z^\Delta\mathcal{O}(x,z)$ corresponds to a bulk scalar field $\phi(x,z)$. In the $\alpha = 0$ limit, it actually comes back to the usual language of CFT.

We notice that $Z(z^2\Box)$ obtained in (17) is nothing but the Fourier transformation of the solutions to the bulk free field equation with $\Phi(z\to 0)\sim z^\Delta$ behavior at the boundary. This construction is different from the one suggested in [5–10]. The approach there encountered only the $k^2 = \vec{k}^2 - w^2 < 0$ part of the bulk $\Phi(z\to 0)\sim z^\Delta$ modes, and thus it cannot be generalized to the Euclidean AdS case. Instead, our construction encounters all the bulk $\Phi(z\to 0)\sim z^\Delta$ modes since it is the honest Fourier transformation. Obviously, (17) is applicable for both signatures.

2.2. Two-Point Correlators: The Divergent Regime and the Regulator. As a consistency check, let us use (17) to recover the well-known bulk-boundary propagator. We find

$$\begin{aligned}
&z^\Delta\left\langle\mathcal{O}(z,x)\,\mathcal{O}\left(x'\right)\right\rangle\\
&\quad = \left\langle z^\Delta\,{}_0F_1\left(;\Delta - \frac{d}{2} + 1; -\frac{\alpha z^2}{4}\Box\right)\mathcal{O}(x)\,\mathcal{O}\left(x'\right)\right\rangle\\
&\quad = \frac{z^\Delta}{\left(x - x'\right)^{2\Delta}}\sum_{n=0}^{\infty}\frac{\Delta(\Delta+1)\cdots(\Delta+n-1)}{n!}\\
&\quad\cdot\left(\frac{-\alpha z^2}{\left(x-x'\right)^2}\right)^n.
\end{aligned} \tag{18}$$

In the regime $|x-x'|^2 > \alpha z^2$, the series is convergent and gives rise to the expected form of the bulk-boundary propagator

$$K\left(x,z;x'\right) = \left(\frac{z}{\alpha z^2 + \left(x-x'\right)^2}\right)^\Delta. \tag{19}$$

However, in the regime $|x-x'|^2 < \alpha z^2$, the series (18) is divergent. In fact, this result is not surprising. The $Z(z^2\Box)$ given in (17) is just the $\Phi(z\to 0)\sim z^\Delta$ modes of the bulk solution, while the Fourier transformation of (19) is a linear combination of the $\Phi(z\to 0)\sim z^\Delta$ modes and the $\Phi(z\to 0)\sim z^{d-\Delta}$ modes [14] which regulate the divergence of (18). The existence of the $\Phi(z\to 0)\sim z^{d-\Delta}$ constituent in (19) can be easily seen from the $z\to 0$ limit [15]

$$\lim_{z\to 0}\left(\frac{z}{\alpha z^2 + \left(x-x'\right)^2}\right)^\Delta \sim z^{d-\Delta}\delta\left(x-x'\right). \tag{20}$$

Although both the $\Phi(z\to 0)\sim z^\Delta$ and $\Phi(z\to 0)\sim z^{d-\Delta}$ modes diverge exponentially as $z\to\infty$, the combination is well-behaved in the interior since the two divergences cancel with each other. The explicit computation of the corresponding Fourier transformations is performed in Appendix.

In order to understand the above issue better, let us recall a simple fact in field theory. That is, the correlation function for composite operators always has zeroth-order UV divergence due to its composite natural. For example,

consider the composite operator $\mathcal{O} =: \phi_a \phi^a :$. The two-point correlator $\langle \mathcal{O}\mathcal{O} \rangle$ receives zeroth-order UV divergence from the following loop diagram even in the free theory.

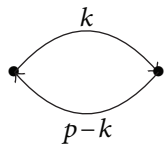

In the coordinate space, the corresponding divergence takes the following form:

$$f\left(\Lambda, \mu, \Box\right) \delta^d \left(x - x'\right), \tag{21}$$

where μ is the renormalization scale and Λ is the cut-off scale. This divergence cannot be canceled by any local counterterm in the original action. Instead, we need to define the regularized two-point function directly and remove it by hand. Or equivalently speaking, we need to add a local counterterm in the free energy $W[J]$

$$\begin{aligned} e^{W[J]} &= \left\langle e^{J\mathcal{O}} \right\rangle, \\ W\left[J\right] &\longrightarrow W_R\left[J\right] \\ &= W\left[J\right] - \int \mathrm{d}^d x \int \mathrm{d}^d x' c\left(x - x'\right) J\left(x\right) J\left(x'\right), \end{aligned} \tag{22}$$

where $c(x - x') = c(\Lambda, \mu, \Box)\delta^d(x - x')$. In principle, after the cancelation of the divergent part, a possible remnant term in the form $R(\mu, \Box)\delta^d(x - x')$ would still be there, and its explicit form depends on the prescription of the regularization.

We notice that the $\Phi(z \to 0) \sim z^{d-\Delta}$ modes of (19) in the coordinate space are given by

$$z^{d-\Delta}\, {}_0F_1\left(; \frac{d}{2} - \Delta + 1; -\frac{\alpha z^2}{4}\Box\right) \delta^d \left(x - x'\right). \tag{23}$$

It is right in the form of $R(\mu, \Box)\delta^d(x - x')$ appearing above. This fact suggests that one can understand it as the possible remnant term. The only special point is that there is an infinite order derivative operator acting on $\delta^d(x - x')$. Thus it is no longer a local function but a quasi-local term which is identically vanishing in the outer region $|x - x'|^2 > \alpha z^2$. Adding such a term does not affect the result (18) in the region $|x - x'|^2 > \alpha z^2$, and it is possible to cancel the divergence in the region $|x - x'|^2 < \alpha z^2$. If we take the continuity at $|x - x'|^2 = \alpha z^2$ as the prescription of the regularization of the two-point function, it will pick the correct ratio between the $\Phi(z \to 0) \sim z^{\Delta}$ modes and the $\Phi(z \to 0) \sim z^{d-\Delta}$ modes and then recovers (19) everywhere. This prescription is equivalent to the momentum space IR regularity condition used in the literatures [14]. Since it is natural to expect that effective operators defined at finite energy scale have some ambiguity in probing the distance shorter than its typical scale, the dependence on the prescription of regularization above is actually acceptable.

One can also check that the bulk-bulk propagator can be recovered by computing

$$z^{\Delta} z'^{\Delta} \left\langle \mathcal{O}\left(z, x\right) \mathcal{O}\left(z', x'\right) \right\rangle. \tag{24}$$

Again, there is a divergent regime at short distance. If the continuity prescription is imposed, it implies that one should take the following regulator:

$$\begin{aligned} & z_M^{d-\Delta} z_m^{\Delta}\, {}_0F_1\left(; \frac{d}{2} - \Delta + 1; -\frac{\alpha z_M^2}{4}\Box\right) \\ & \cdot\, {}_0F_1\left(; \Delta - \frac{d}{2} + 1; -\frac{\alpha z_m^2}{4}\Box\right) \delta^d \left(x - x'\right), \end{aligned} \tag{25}$$

where $z_M = \max\{z, z'\}$ and $z_m = \min\{z, z'\}$.

3. Radial Quantization

3.1. Radial Quantization in CFT. In Section 2, we have constructed the bulk local operator and also explained its divergent regime with the regularization prescription there. However, the present formula is not convenient in discussing the bulk physics since the regulator should always be added by hand. It will be pretty nice if one can find a smart formula in which the regulator has been automatically built in. To achieve such a formula, let us discuss the radial quantization in usual CFT language firstly.

The radial quantization for CFT was detailedly reviewed in [16, 17]. We will equivalently reexpress the results there by introducing the radial expansion for the operators. Again, we will just consider scalar primary here. The radial expansion of a scalar primary operator $\mathcal{O}(x)$ is given by

$$\begin{aligned} \mathcal{O}\left(x\right) = & \sum_{m=0}^{\infty} \frac{1}{m!} x^{\mu_1} \cdots x^{\mu_m} O_{\mu_1 \cdots \mu_m} \\ & + \sum_{n=0}^{\infty} \frac{1}{n!} \check{x}^{2\Delta} \check{x}^{\nu_1} \cdots \check{x}^{\nu_n} \check{O}_{\nu_1 \cdots \nu_n}, \end{aligned} \tag{26}$$

where $\check{x}$ is the inversion of x

$$\check{x}^{\mu} = \mathcal{I} \circ x^{\mu} = \frac{x^{\mu}}{x^2}. \tag{27}$$

In a unitary theory, its Hermitian conjugation is induced by the inversion

$$\begin{aligned} \mathcal{O}^{\dagger}\left(x\right) &= \check{O}\left(-x\right) = \frac{1}{x^{2\Delta}} \mathcal{O}\left(-\check{x}\right) \\ &= \sum_{n=0}^{\infty} \frac{(-1)^n}{n!} x^{\nu_1} \cdots x^{\nu_n} \check{O}_{\nu_1 \cdots \nu_n} \\ &\quad + \sum_{m=0}^{\infty} \frac{(-1)^m}{m!} \check{x}^{2\Delta} \check{x}^{\mu_1} \cdots \check{x}^{\mu_m} O_{\mu_1 \cdots \mu_m}. \end{aligned} \tag{28}$$

In terms of the component operators, it is given by

$$\begin{aligned} O^{\dagger}_{\mu_1 \cdots \mu_n} &= (-1)^n \check{O}_{\mu_1 \cdots \mu_n}, \\ \check{O}^{\dagger}_{\mu_1 \cdots \mu_n} &= (-1)^n O_{\mu_1 \cdots \mu_n}. \end{aligned} \tag{29}$$

The vacuum $|1\rangle$ is defined by

$$\begin{aligned} \check{O}_{\nu_1\cdots\nu_n}|1\rangle &= 0, \\ \langle 1|O_{\mu_1\cdots\mu_m} &= 0. \end{aligned} \tag{30}$$

It is equivalent to requiring that the state $\mathcal{O}(x)|1\rangle$ and all its descendants are regular at $x = 0$, while the conjugated state $\langle 1|\check{O}(x)$ and all its descendants are also regular at $x = 0$. One can check that the vacuum $|1\rangle$ defined in (30) is actually conformal invariant. The conformal transformation rules of the component operators can be deduced from the standard rules for primary $\mathcal{O}(x)$. We find

$$\begin{aligned} &\left[P_\mu, O_{\mu_1\cdots\mu_m}\right] = iO_{\mu\mu_1\cdots\mu_m}, \\ &\left[P_\mu, \check{O}_{\nu_1\cdots\nu_n}\right] = i\left[n(n-1)\eta_{(\nu_1\nu_2}\check{O}_{\nu_3\cdots\nu_n)\mu}\right. \\ &\quad \left. - 2n(\Delta+n-1)\eta_{\mu(\nu_1}\check{O}_{\nu_2\cdots\nu_n)}\right], \\ &\left[M_{\mu\nu}, O_{\mu_1\cdots\mu_m}\right] = im\left[\eta_{\mu(\mu_1}O_{\mu_2\cdots\mu_m)\nu} - \eta_{\nu(\mu_1}O_{\mu_2\cdots\mu_m)\mu}\right], \\ &\left[M_{\mu\nu}, \check{O}_{\nu_1\cdots\nu_n}\right] = in\left[\eta_{\mu(\nu_1}\check{O}_{\nu_2\cdots\nu_n)\nu} - \eta_{\nu(\nu_1}\check{O}_{\nu_2\cdots\nu_m)\mu}\right], \\ &\left[D, O_{\mu_1\cdots\mu_m}\right] = i(\Delta+m)O_{\mu_1\cdots\mu_m}, \\ &\left[D, \check{O}_{\nu_1\cdots\nu_n}\right] = -i(\Delta+m)\check{O}_{\nu_1\cdots\nu_n}, \\ &\left[K_\mu, O_{\mu_1\cdots\mu_m}\right] = i\left[m(m-1)\eta_{(\mu_1\mu_2}O_{\mu_3\cdots\mu_m)\mu}\right. \\ &\quad \left. - 2m(\Delta+m-1)\eta_{\mu(\mu_1}O_{\mu_2\cdots\mu_m)}\right], \\ &\left[K_\mu, \check{O}_{\nu_1\cdots\nu_n}\right] = i\check{O}_{\mu\nu_1\cdots\nu_n}. \end{aligned} \tag{31}$$

Given the input data

$$\left\langle \mathcal{O}'(0) \mid \mathcal{O}(0)\right\rangle = \langle 1|\check{O}'_0 O_0|1\rangle = C_{\mathcal{O}'\mathcal{O}}, \tag{32}$$

one can decide the inner product between the states $|\partial_{\mu_n}\cdots\partial_{\mu_1}\mathcal{O}(0)\rangle = O_{\mu_1\cdots\mu_n}|1\rangle$ by using (31) and the conformal invariance of the vacuum. The result is

$$\begin{aligned} &\langle 1|\check{O}'_{\nu_n\cdots\nu_1}O^{\mu_1\cdots\mu_m}|1\rangle \\ &= \delta_{mn}C_{\mathcal{O}'\mathcal{O}}\sum_{k=0}^{\lfloor n/2\rfloor}\frac{(-1)^{n-k}2^n(n!)^2\Gamma(\Delta+n-k)}{(n-2k)!k!(2!)^{2k}\Gamma(\Delta)}\delta^{(\mu_1}_{(\nu_1} \\ &\cdots\delta^{\mu_{n-2k}}_{\nu_{n-2k}}\eta_{\nu_{n-2k+1}\nu_{n-2k+2}}\cdots\eta_{\nu_{n-1}\nu_n)}\eta^{\mu_{n-2k+1}\mu_{n-2k+2}} \\ &\cdots\eta^{\mu_{n-1}\mu_n)}. \end{aligned} \tag{33}$$

Now we can reproduce the well-known two-point correlator by the "silly" computation

$$\begin{aligned} &\langle 1|\mathcal{O}(x)\mathcal{O}'\left(x'\right)|1\rangle = \sum_{m=0}^{\infty}\sum_{n=0}^{\infty}\frac{1}{m!n!} \\ &\cdot\frac{x^{\mu_1}\cdots x^{\mu_m}x'^{\nu_1}\cdots x'^{\nu_n}}{x^{2(\Delta+m)}}\langle 1|\check{O}_{\mu_1\cdots\mu_m}O'_{\nu_1\cdots\nu_n}|1\rangle \\ &= C_{\mathcal{O}'\mathcal{O}}\sum_{\widehat{n}=0}^{\infty}\sum_{k=0}^{\infty}\frac{(-1)^{\widehat{n}+k}2^{\widehat{n}}\Gamma(\Delta+\widehat{n}+k)}{\widehat{n}!k!\Gamma(\Delta)} \\ &\cdot\frac{\left(x\cdot x'\right)^{\widehat{n}}x'^{2k}}{x^{2(\Delta+\widehat{n}+k)}}. \end{aligned} \tag{34}$$

The convergence of the series requires that $|x| > |x'|$. (Strictly speaking, the convergence argument is accurate only for the Euclidean case. For the Lorentzian case, proper analytical continuations are needed as what usually happened in the quantum field theory computations.) It means that the usual CFT correlator is reproduced by the radial ordered function $\langle 1|\widehat{\mathcal{R}}\mathcal{O}(x)\mathcal{O}'(x')|1\rangle$. In the radial quantization where the dilatation operator D is treated as the Hamiltonian, the radial ordered function is the natural analogy of the time ordered function in the usual quantum field theory.

3.2. Radial Quantization at Finite Energy Scale. Now let us consider the CFT radial quantization in the presence of the finite energy scale μ. A direct idea is acting upon the radial expansion (26) with the $Z(\mu^{-2}\Box)$ in (17). We get

$$\begin{aligned} &{}_0F_1\left(;\Delta-\frac{d}{2}+1;-\frac{\alpha z^2}{4}\Box\right)\mathcal{O}(x) \\ &= \sum_{s=0}^{\infty}\sum_{k=0}^{\infty}\frac{\left(-\alpha z^2\right)^k\Gamma(\Delta-d/2+1)}{2^{2k}k!s!\Gamma(\Delta-d/2+k+1)} \\ &\cdot x^{\nu_1}\cdots x^{\nu_s}O_{\mu_1\cdots\mu_k}{}^{\mu_1\cdots\mu_k}{}_{\nu_1\cdots\nu_s} \\ &+ \sum_{s=0}^{\infty}\sum_{l=0}^{\infty}\frac{\left(-\alpha z^2\right)^l\Gamma(\Delta-d/2+1)}{2^{2l}l!s!\Gamma(\Delta-d/2+l+1)} \\ &\cdot {}_1F_0\left(\Delta+2l+s;;-\frac{\alpha z^2}{x^2}\right)\frac{x^{\nu_1}\cdots x^{\nu_s}}{x^{2(\Delta+2l+s)}} \\ &\cdot\check{O}_{\mu_1\cdots\mu_l}{}^{\mu_1\cdots\mu_l}{}_{\nu_1\cdots\nu_s}. \end{aligned} \tag{35}$$

We notice that when $|x|^2 > \alpha z^2$

$$\begin{aligned} &\frac{1}{x^{2(\Delta+2l+s)}}{}_1F_0\left(\Delta+2l+s;;-\frac{\alpha z^2}{x^2}\right) \\ &= \frac{1}{\left(x^2+\alpha z^2\right)^{\Delta+2l+s}}, \end{aligned} \tag{36}$$

and it is divergent in the regime $|x|^2 < \alpha z^2$. The structure of the divergent regime is quite similar to what we have seen

in Section 2. Thus it is natural to expect the following as the regularized radial expansion at finite energy scale

$$\begin{aligned}\mathcal{O}(x,z) &= \sum_{m=0}^{\infty}\frac{1}{m!}x^{\mu_1}\cdots x^{\mu_m}O_{\mu_1\cdots\mu_m}(z)\\ &\quad+\sum_{n=0}^{\infty}\frac{1}{n!}\frac{x^{\nu_1}\cdots x^{\nu_n}}{\left(x^2+\alpha z^2\right)^{\Delta+n}}\check{O}_{\nu_1\cdots\nu_n}(\check{z}),\end{aligned} \tag{37}$$

where the component operator at finite energy scale is a linear combination of the original ones

$$\begin{aligned}&O_{\mu_1\cdots\mu_m}(z)\\ &\quad=\sum_{k=0}^{\infty}\frac{\left(-\alpha z^2\right)^k\Gamma(\Delta-d/2+1)}{2^{2k}k!\Gamma(\Delta-d/2+k+1)}O_{\nu_1\cdots\nu_k}{}^{\nu_1\cdots\nu_k}{}_{\mu_1\cdots\mu_m},\\ &\check{O}_{\mu_1\cdots\mu_m}(\check{z})\\ &\quad=\sum_{k=0}^{\infty}\frac{\left(-\alpha\check{z}^2\right)^k\Gamma(\Delta-d/2+1)}{2^{2k}k!\Gamma(\Delta-d/2+k+1)}\check{O}_{\nu_1\cdots\nu_k}{}^{\nu_1\cdots\nu_k}{}_{\mu_1\cdots\mu_m},\end{aligned} \tag{38}$$

and the inversion of x and z in the generalized scene is given by

$$\begin{aligned}\check{x}^{\mu}&=\mathcal{J}\circ x^{\mu}=\frac{x^{\mu}}{x^2+\alpha z^2},\\ \check{z}&=\mathcal{J}\circ z=\frac{z}{x^2+\alpha z^2}.\end{aligned} \tag{39}$$

Correspondingly, the inversion of $\mathcal{O}(x,z)$ is

$$\begin{aligned}\check{O}(x,z)&=\frac{1}{\left(x^2+\alpha z^2\right)^{\Delta}}\mathcal{O}(\check{x};\check{z})\\ &=\sum_{n=0}^{\infty}\frac{1}{n!}x^{\nu_1}\cdots x^{\nu_n}\check{O}_{\nu_1\cdots\nu_n}(z)\\ &\quad+\sum_{m=0}^{\infty}\frac{1}{m!}\frac{x^{\mu_1}\cdots x^{\mu_m}}{\left(x^2+\alpha z^2\right)^{\Delta+n}}O_{\mu_1\cdots\mu_m}(\check{z}).\end{aligned} \tag{40}$$

From (29), we can see that the Hermitian conjugation relation keeps intact at finite energy scale

$$\mathcal{O}^{\dagger}(x,z)=\check{O}(-x,z). \tag{41}$$

Simply by using (31), one can write down the conformal transformation rule for the component fields at finite energy scale directly as follows:

$$\begin{aligned}&\left[P_{\mu},O_{\mu_1\cdots\mu_m}(z)\right]=iO_{\mu\mu_1\cdots\mu_m}(z),\\ &\left[P_{\mu},\check{O}_{\mu_1\cdots\mu_m}(z)\right]=i\left[\alpha z^2\check{O}_{\mu_1\cdots\mu_m\mu}(z)\right.\\ &\quad+m(m-1)\eta_{(\mu_1\mu_2}\check{O}_{\mu_3\cdots\mu_m)\mu}(z)\\ &\quad\left.-2m\left(\Delta+m-1+z\partial_z\right)\eta_{\mu(\mu_1}\check{O}_{\mu_2\cdots\mu_m)}(z)\right],\\ &\left[M_{\mu\nu},O_{\mu_1\cdots\mu_m}(z)\right]=im\left[\eta_{\mu(\mu_1}O_{\mu_2\cdots\mu_m)\nu}(z)\right.\\ &\quad\left.-\eta_{\nu(\mu_1}O_{\mu_2\cdots\mu_m)\mu}(z)\right],\\ &\left[M_{\mu\nu},\check{O}_{\mu_1\cdots\mu_m}(z)\right]=im\left[\eta_{\mu(\nu_1}\check{O}_{\nu_2\cdots\nu_m)\nu}(z)\right.\\ &\quad\left.-\eta_{\nu(\nu_1}\check{O}_{\nu_2\cdots\nu_m)\mu}(z)\right],\\ &\left[D,O_{\mu_1\cdots\mu_m}(z)\right]=i\left(\Delta+m+z\partial_z\right)O_{\mu_1\cdots\mu_m}(z),\\ &\left[D,\check{O}_{\mu_1\cdots\mu_m}(z)\right]=-i\left(\Delta+m+z\partial_z\right)\check{O}_{\mu_1\cdots\mu_m}(z),\\ &\left[K_{\mu},O_{\mu_1\cdots\mu_m}(z)\right]=i\left[\alpha z^2O_{\mu_1\cdots\mu_m\mu}(z)\right.\\ &\quad+m(m-1)\eta_{(\mu_1\mu_2}O_{\mu_3\cdots\mu_m)\mu}(z)\\ &\quad\left.-2m\left(\Delta+m-1+z\partial_z\right)\eta_{\mu(\mu_1}O_{\mu_2\cdots\mu_m)}(z)\right],\\ &\left[K_{\mu},\check{O}_{\mu_1\cdots\mu_m}(z)\right]=i\check{O}_{\mu\mu_1\cdots\mu_m}(z).\end{aligned} \tag{42}$$

Similar to the arguments in Section 2.1, we can show that a bulk scalar field $\Phi(x,z)$ expanded as

$$\begin{aligned}\Phi(x,z)&=\sum_{m=0}^{\infty}\frac{z^{\Delta}}{m!}x^{\mu_1}\cdots x^{\mu_m}\Phi_{\mu_1\cdots\mu_m}(z)\\ &\quad+\sum_{n=0}^{\infty}\frac{1}{n!}\frac{z^{\Delta}x^{\nu_1}\cdots x^{\nu_n}}{\left(x^2+\alpha z^2\right)^{\Delta+n}}\check{\Phi}_{\nu_1\cdots\nu_n}(\check{z})\end{aligned} \tag{43}$$

indeed requires the transformation rules (42) for its components. Thus, the regularized version (37) of primary at finite energy scale satisfies our basic renormalization condition for primary operators.

Parallel with (34), the standard bulk-boundary as well as bulk-bulk propagator can be reproduced by computing the radial ordered function $\langle 1|\widehat{\mathcal{R}}O(x,z)\mathcal{O}'(x',z')|1\rangle$. In our present case where energy scales are introduced, the radial order is defined by $x^2+\alpha z^2$. Providing this radial order, there is no ambiguity everywhere in reproducing the bulk-boundary and bulk-bulk propagator. Therefore, (37) is indeed the smart formula which we are looking for.

Since our construction directly comes back to the standard CFT language in the $\alpha\to 0$ limit, it is possible that (37) will not suffer from the problem about bulk locality appearing in the smearing operator construction [18]. In order to address it properly, one should generalize the standard results

about OPE to the cases with finite energy scales. We hope to report on this issue in a future work.

Formula (37) also suggests that one could define the finite energy scale effective Hilbert space $\mathscr{H}_z$ by acting on the vacuum $|1\rangle$ with $O_{\mu_1\cdots\mu_m}(z)$. An interesting observation is that $\mathscr{H}_z$ actually contains less information than the UV Hilbert space $\mathscr{H} = \mathscr{H}_{z=0}$. For example, considering the scalar sector, one can construct the following state:

$$|\lambda\rangle = \sum_{n=0}^{\infty} \frac{\lambda^n \Gamma(\Delta)\,\Gamma(\Delta - d/2 + 1)\,\Gamma(d/2)}{2^{4n} n!\,\Gamma(\Delta + n)\,\Gamma(\Delta - d/2 + n + 1)\,\Gamma(n + d/2)} \cdot O_n |1\rangle, \tag{44}$$

where we denote $O_n(z) = O_{\nu_1\cdots\nu_n}{}^{\nu_1\cdots\nu_n}(z)$. It is a well-defined state in $\mathscr{H}$ since the norm is finite

$$\langle\lambda \mid \lambda\rangle = C_{\mathcal{O}} \sum_{n=0}^{\infty} \frac{\lambda^n \Gamma(\Delta)\,\Gamma(\Delta - d/2 + 1)\,\Gamma(d/2)}{2^{4n} n!\,\Gamma(\Delta + n)\,\Gamma(\Delta - d/2 + n + 1)\,\Gamma(n + d/2)}. \tag{45}$$

The inner product between the state $|\lambda\rangle$ and the states in $\mathscr{H}_z$ is given by

$$\langle\lambda| O_m(z) |1\rangle = C_{\mathcal{O}} \lambda^m \sum_{k=0}^{\infty} \frac{\left(-\alpha\lambda z^2\right)^k \Gamma(\Delta - d/2 + 1)}{2^{2k} k!\,\Gamma(\Delta - d/2 + k + 1)}. \tag{46}$$

Since the ${}_0F_1$ function has infinite number of zeros, the inner product will be zero for infinite many λ's providing $z \neq 0$. Therefore, there are an infinite number of states in $\mathscr{H}$ perpendicular to the finite energy scale effective Hilbert space $\mathscr{H}_{z\neq 0}$. Although this observation is something one could expect for effective descriptions at finite energy scale, it may have some possible advantages in discussing the c-theorem and the entanglement entropy.

4. Discussions

In the previous sections, we suggest a CFT construction of the bulk local operators in pure AdS space. The construction is based on considering CFT at finite energy scale. The basic result is that bulk operator is given by acting upon the original CFT primary with an infinite order differential operator $Z_{\text{AdS}}(\mu, \partial)$. Although we do not assume any knowledge about the bulk in advance, our arguments automatically show that $Z_{\text{AdS}}(\mu, \partial)$ should be the Fourier transformation of the $\Phi(z \to 0) \sim z^{\Delta}$ solution to the bulk free field equation. We also discuss the relation between the regulator of the two-point function and the $\Phi(z \to 0) \sim z^{d-\Delta}$ modes. In Section 3, based on the radial quantization in CFT, we find an improved formula of our construction in which the regulator is automatically built in.

The next challenge is how to generalize our construction to geometries beyond pure AdS. A naive guess is that the bulk local operator is also effectively given by acting upon the original CFT primary with the infinite order differential operator $Z_{\text{Geom}}(\mu, \partial)$, which is the Fourier transformation of the bulk $\Phi(z \to 0) \sim z^{\Delta}$ modes in the corresponding geometry. On the other hand, our CFT arguments in Section 2.1 seem state independent. Thus, it suggests that the bulk local operator should always be given by $Z_{\text{AdS}}(\mu, \partial)$ for all asymptotic AdS geometries which are basically very heavy excited states in the CFT. We conjecture that these two possibilities are actually complementary to each other. The explicit proposal [19] for the underlying mechanism can be summarized as the following.

Bulk geometries are actually dual to the coherent states $|\text{Geom}\rangle = F(T_{\mu\nu})|1\rangle$ which is created by acting on the vacuum $|1\rangle$ with certain function $F(T_{\mu\nu})$ of stress tensor and its descendants.

The bulk correlators of the dual field $\phi(x, z)$ can be reproduced by computing

$$\langle\text{Geom}| \cdots Z_{\text{AdS}}(\mu, \partial)\, \mathcal{O}(x) \cdots |\text{Geom}\rangle = \langle 1| F^{\dagger}\left(T_{\mu\nu}\right) \cdots Z_{\text{AdS}}(\mu, \partial)\, \mathcal{O}(x) \cdots F\left(T_{\mu\nu}\right) |1\rangle. \tag{47}$$

On the other hand, by using the local conformal Ward identity [20–22], one may convert (at least in the two-dimensional CFT) the effects of $F(T_{\mu\nu})$ to a differential operator $\widehat{\mathscr{F}}[F]$ acting on the operator $Z_{\text{AdS}}(\mu, \partial)\mathcal{O}(x)$ as follows:

$$\langle 1| F^{\dagger}\left(T_{\mu\nu}\right) \cdots Z_{\text{AdS}}(\mu, \partial)\, \mathcal{O}(x) \cdots F\left(T_{\mu\nu}\right) |1\rangle = \langle 1| \cdots \widehat{\mathscr{F}}[F]\, Z_{\text{AdS}}(\mu, \partial)\, \mathcal{O}(x) \cdots |1\rangle. \tag{48}$$

The new differential operator $\widehat{\mathscr{F}}[F] Z_{\text{AdS}}(\mu, \partial)$ is expected to be exactly $Z_{\text{Geom}}(\mu, \partial)$ of the corresponding geometry. For the black hole geometry, the horizon is the position where the series in $Z_{\text{Geom}}(\mu, \partial)$ becomes ill-defined. However, everything could be still well defined after coming back to the $|\text{Geom}\rangle$ description and one can explore the black hole interior in this formalism.

Finally, it is also possible that multiple states with different $F(T_{\mu\nu})$ give rise to the same differential operator $Z_{\text{Geom}}(\mu, \partial)$. Thus it could be a dual CFT way to explain the entropy of AdS black hole. If indeed so, it means that all the black hole microstates should correspond exactly to the same geometry, and thus one does not need to take any average over different microgeometries. This picture seems different from what people usually expected for quantum gravity and may offer new possibilities to the discussions of the black hole firewall problem [23, 24].

As the early version of this work was drawing a conclusion, [25] appeared with results which partially overlap with Section 2.1 in this manuscript. We also realized that the two-dimensional version of their results has already appeared in [26].

Appendix

A. The Momentum Space Formula

In the momentum space, the general solutions to the bulk free scalar equation are given by the linear combination of the $\Phi(z \to 0) \sim z^{\Delta}$ modes

$$z^{\Delta} k^{2\Delta-d}\, {}_0F_1\left(;\Delta-\frac{d}{2}+1;\frac{z^2k^2}{4}\right) = \Gamma\left(\Delta-\frac{d}{2}+1\right) z^{d/2}\,(2k)^{\Delta-d/2}\, I_{\Delta-d/2}, \tag{A.1}$$

as well as the $\Phi(z \to 0) \sim z^{d-\Delta}$ modes

$$z^{d-\Delta}\, {}_0F_1\left(;\frac{d}{2}-\Delta+1;\frac{z^2k^2}{4}\right) = \Gamma\left(\frac{d}{2}-\Delta+1\right) z^{d/2}\left(\frac{k}{2}\right)^{\Delta-d/2} I_{d/2-\Delta}. \tag{A.2}$$

In the following, let us derive the Fourier transformation of them, respectively.

A.1. $\Phi(z \to 0) \sim z^{\Delta}$ *Modes.* The Fourier transformation of the $\Phi(z \to 0) \sim z^{\Delta}$ mode is

$$\begin{aligned}
&\lim_{\Lambda\to\infty} \frac{z^{d/2}}{(2\pi)^d} \int \mathrm{d}^d k \mathrm{e}^{-(zk)^2/\Lambda^2} I_{\Delta-d/2}(zk)\, k^{\Delta-d/2} \mathrm{e}^{ik(x-x')} \\
&= \lim_{\Lambda\to\infty} \frac{z^{d/2}}{(2\pi)^d} \frac{2\pi^{(d-1)/2}}{\Gamma((d-1)/2)} \frac{\sqrt{\pi}\Gamma((d-1)/2)}{\Gamma(d/2)} \\
&\cdot \int_0^{\infty} \mathrm{d}k \mathrm{e}^{-(zk)^2/\Lambda^2} I_{\Delta-d/2}(zk) \\
&\cdot k^{\Delta+d/2-1}\, {}_0F_1\left(;\frac{d}{2};-\frac{k^2r^2}{4}\right) = \lim_{\Lambda\to\infty} \frac{z^{d/2}}{(2\pi)^d} \\
&\cdot \frac{2\pi^{(d-1)/2}}{\Gamma((d-1)/2)} \frac{\sqrt{\pi}\Gamma((d-1)/2)}{\Gamma(d/2)} \\
&\cdot \sum_{m=0}^{\infty} \frac{1}{m!\Gamma(\Delta+m-d/2+1)} \int_0^{\infty} \mathrm{d}k \\
&\cdot \mathrm{e}^{-(zk)^2/\Lambda^2} \left(\frac{zk}{2}\right)^{2m+\Delta-d/2} \\
&\cdot k^{\Delta+d/2-1}\, {}_0F_1\left(;\frac{d}{2};-\frac{k^2r^2}{4}\right) = \lim_{\Lambda\to\infty} \frac{1}{(2\pi)^d} \\
&\cdot \frac{2\pi^{(d-1)/2}}{\Gamma((d-1)/2)} \frac{\sqrt{\pi}\Gamma((d-1)/2)}{2\Gamma(d/2)} \\
&\cdot \sum_{m=0}^{\infty} \frac{2^{-2m-\Delta+d/2} z^{-\Delta}}{m!\Gamma(\Delta+m-d/2+1)} \Gamma(\Delta+m) \\
&\cdot \Lambda^{2(\Delta+m)}\, {}_1F_1\left(\Delta+m;\frac{d}{2};-\frac{\Lambda^2r^2}{4z^2}\right),
\end{aligned} \tag{A.3}$$

where we have used the fact that the convergence radius of ${}_0F_1$ and ${}_1F_1$ is ∞ and

$$\begin{aligned}
&\int_0^{\pi} \mathrm{d}\theta\, (\sin\theta)^{d-2}\, \mathrm{e}^{ikr\cos\theta} \\
&= \frac{\sqrt{\pi}\Gamma((d-1)/2)}{\Gamma(d/2)}\, {}_0F_1\left(;\frac{d}{2};-\frac{k^2r^2}{4}\right), \\
&\int_0^{\infty} \mathrm{d}k \mathrm{e}^{-k^2/\Lambda^2} k^{2\Delta-1+2n} = \frac{1}{2}\Lambda^{2(\Delta+n)}\Gamma(\Delta+n) \\
&\qquad (\Delta+n>0).
\end{aligned} \tag{A.4}$$

By using the asymptotic expansion of confluent hypergeometric function

$$\begin{aligned}
&{}_1F_1(\alpha;\gamma;z) \\
&= \frac{\Gamma(\gamma)}{\Gamma(\gamma-\alpha)} \mathrm{e}^{i\pi\alpha} z^{-\alpha}\, {}_2F_0\left(\alpha,\alpha-\gamma+1;;-z^{-1}\right) \\
&\quad + \frac{\Gamma(\gamma)}{\Gamma(\alpha)} \mathrm{e}^{z} z^{\alpha-\gamma}\, {}_2F_0\left(\gamma-\alpha,1-\alpha;;z^{-1}\right) \\
&\qquad \text{for } -\frac{\pi}{2} < \arg z < \frac{3\pi}{2}
\end{aligned} \tag{A.5}$$

we find in the regime $(x-x')^2 > z^2$

$$\begin{aligned}
&\lim_{\Lambda\to\infty} \frac{1}{(2\pi)^d} \frac{2\pi^{(d-1)/2}}{\Gamma((d-1)/2)} \frac{\sqrt{\pi}\Gamma((d-1)/2)}{2\Gamma(d/2)} \\
&\cdot \sum_{m=0}^{\infty} \frac{2^{-2m-\Delta+d/2} z^{-\Delta}}{m!\Gamma(\Delta+m-d/2+1)} \Gamma(\Delta+m) \\
&\cdot \Lambda^{2(\Delta+m)}\, {}_1F_1\left(\Delta+m;\frac{d}{2};-\frac{\Lambda^2r^2}{4z^2}\right) \\
&= \frac{2^{\Delta-d/2} z^{-\Delta} \sin(((d-2\Delta)\pi)/2)\,\Gamma(\Delta)}{\pi^{d/2+1}} \\
&\cdot \sum_{m=0}^{\infty} \frac{(-1)^m \Gamma(\Delta+m)}{m!\Gamma(\Delta)} \frac{z^{2(\Delta+m)}}{(x-x')^{2(\Delta+m)}} \\
&= \frac{2^{\Delta-d/2} \sin(((d-2\Delta)\pi)/2)\,\Gamma(\Delta)}{\pi^{d/2+1}} \left(\frac{z}{z^2+(x-x')^2}\right)^{\Delta}.
\end{aligned} \tag{A.6}$$

Thus the $\Phi(z \to 0) \sim z^{\Delta}$ mode reproduces $K(z,x;x')$ for the region $(x-x')^2 > z^2$ as expected.

For $(x-x')^2 < z^2$, we exchange the order of summations and find

$$\begin{aligned}
&\lim_{\Lambda\to\infty} \frac{1}{(2\pi)^d} \frac{2\pi^{(d-1)/2}}{\Gamma((d-1)/2)} \frac{\sqrt{\pi}\Gamma((d-1)/2)}{2\Gamma(d/2)} \\
&\cdot \sum_{m=0}^{\infty} \frac{2^{-2m-\Delta+d/2} z^{-\Delta}}{m!\Gamma(\Delta+m-d/2+1)} \Gamma(\Delta+m) \\
&\cdot \Lambda^{2(\Delta+m)}\, {}_1F_1\left(\Delta+m;\frac{d}{2};\right. \\
&\left. -\frac{\Lambda^2r^2}{4z^2}\right) = \lim_{\Lambda\to\infty} \frac{1}{(2\pi)^d} \frac{2\pi^{(d-1)/2}}{\Gamma((d-1)/2)}
\end{aligned}$$

$$\cdot \frac{\sqrt{\pi}\Gamma\left((d-1)/2\right)}{2\Gamma\left(d/2\right)} \sum_{m=0}^{\infty}\sum_{n=0}^{\infty} \frac{2^{-2m-\Delta+d/2} z^{-\Delta}}{m!\Gamma\left(\Delta+m-d/2+1\right)}$$

$$\cdot \frac{\Gamma\left(\Delta+m+n\right)\Gamma\left(d/2\right)}{n!\Gamma\left(d/2+n\right)} \Lambda^{2(\Delta+m)} \left(-\frac{\Lambda^2 r^2}{4z^2}\right)^n$$

$$= \lim_{\Lambda\to\infty} \frac{1}{(2\pi)^d} \frac{2\pi^{(d-1)/2}}{\Gamma\left((d-1)/2\right)} \frac{\sqrt{\pi}\Gamma\left((d-1)/2\right)}{2\Gamma\left(d/2\right)}$$

$$\cdot \sum_{n=0}^{\infty} \frac{2^{-\Delta+d/2}\Lambda^{2\Delta} z^{-\Delta}}{\Gamma\left(\Delta-d/2+1\right)} \frac{\Gamma\left(\Delta+n\right)\Gamma\left(d/2\right)}{n!\Gamma\left(d/2+n\right)} {}_1F_1\left(\Delta + n; \Delta - \frac{d}{2} + 1; \frac{\Lambda^2}{4}\right)\left(-\frac{\Lambda^2 r^2}{4z^2}\right)^n = \frac{1}{(2\pi)^d}$$

$$\cdot \frac{2\pi^{(d-1)/2}}{\Gamma\left((d-1)/2\right)} \frac{\sqrt{\pi}\Gamma\left((d-1)/2\right)}{2\Gamma\left(d/2\right)}$$

$$\cdot \frac{2^{\Delta+d/2} z^{-\Delta}\Gamma\left(\Delta\right)\sin\left(d\pi/2\right)\Gamma\left(d/2\right)}{\pi} \sum_{n=0}^{\infty} \frac{\Gamma\left(\Delta+n\right)}{n!\Gamma\left(\Delta\right)}$$

$$\cdot \left(-\frac{r^2}{z^2}\right)^n \left[e^{i\pi\Delta} + \lim_{\Lambda\to\infty} (-1)^n \frac{\Gamma\left(1-d/2-n\right)}{\Gamma\left(\Delta+n\right)} \right.$$

$$\cdot e^{\Lambda^2/4} \left(\frac{\Lambda^2}{4}\right)^{\Delta+d/2+2n-1}$$

$$\left. \cdot {}_2F_0\left(1-\frac{d}{2}-n; 1-\Delta-n; \frac{4}{\Lambda^2}\right)\right]$$

$$= \frac{2^{\Delta-d/2}\Gamma\left(\Delta\right)}{\pi^{d/2+1}} e^{i\pi\Delta} \sin\left(\frac{d\pi}{2}\right)\left(\frac{z}{z^2+\left(x-x'\right)^2}\right)^{\Delta}$$

$$+ \frac{2^{\Delta-d/2}}{\pi^{d/2}} \lim_{\Lambda\to\infty} \sum_{n=0}^{\infty} \frac{\left(-r^2/z^2\right)^n}{n!\Gamma\left(d/2+n\right)}$$

$$\cdot e^{\Lambda^2/4} \left(\frac{\Lambda^2}{4}\right)^{\Delta+d/2+2n-1} {}_2F_0\left(1-\frac{d}{2}-n; 1-\Delta - n; \frac{4}{\Lambda^2}\right). \tag{A.7}$$

The result is divergent and the divergent parts are expressed as terms with positive powers of Λ.

A.2. $\Phi(z \to 0) \sim z^{d-\Delta}$ *Modes.* For the $\Phi(z \to 0) \sim z^{\Delta}$ modes, in the regime $(x-x')^2 > z^2$, we have

$$\lim_{\Lambda\to\infty} \frac{z^{d/2}}{(2\pi)^d} \int \mathrm{d}^d k e^{-(zk)^2/\Lambda^2} I_{d/2-\Delta}\left(zk\right) k^{\Delta-d/2} e^{ik(x-x')}$$

$$= \lim_{\Lambda\to\infty} \frac{z^{d/2}}{(2\pi)^d} \frac{2\pi^{(d-1)/2}}{\Gamma\left((d-1)/2\right)} \frac{\sqrt{\pi}\Gamma\left((d-1)/2\right)}{\Gamma\left(d/2\right)}$$

$$\cdot \int_0^{\infty} \mathrm{d}k e^{-(zk)^2/\Lambda^2} I_{d/2-\Delta}\left(zk\right)$$

$$\cdot k^{\Delta+d/2-1} {}_0F_1\left(; \frac{d}{2}; -\frac{k^2 r^2}{4}\right) = \lim_{\Lambda\to\infty} \frac{z^{d/2}}{(2\pi)^d}$$

$$\cdot \frac{2\pi^{(d-1)/2}}{\Gamma\left((d-1)/2\right)} \frac{\sqrt{\pi}\Gamma\left((d-1)/2\right)}{\Gamma\left(d/2\right)}$$

$$\cdot \sum_{m=0}^{\infty} \frac{1}{m!\Gamma\left(-\Delta+m+d/2+1\right)} \int_0^{\infty} \mathrm{d}k e^{-(zk)^2/\Lambda^2}$$

$$\cdot \left(\frac{zk}{2}\right)^{2m-\Delta+d/2} k^{\Delta+d/2-1} {}_0F_1\left(; \frac{d}{2}; -\frac{k^2 r^2}{4}\right)$$

$$= \lim_{\Lambda\to\infty} \frac{1}{(2\pi)^d} \frac{2\pi^{(d-1)/2}}{\Gamma\left((d-1)/2\right)} \frac{\sqrt{\pi}\Gamma\left((d-1)/2\right)}{2\Gamma\left(d/2\right)}$$

$$\cdot \sum_{m=0}^{\infty} \frac{2^{-2m+\Delta-d/2} z^{-\Delta}}{m!\Gamma\left(-\Delta+m+d/2+1\right)} \Gamma\left(\frac{d}{2}+m\right)$$

$$\cdot \Lambda^{d+2m} {}_1F_1\left(\frac{d}{2}+m; \frac{d}{2}; -\frac{\Lambda^2 r^2}{4z^2}\right)$$

$$= \sum_{m=0}^{\infty} \frac{2^{-2m+\Delta-d/2} z^{-\Delta}}{m!\Gamma\left(-\Delta+m+d/2+1\right)} \frac{2^m \Gamma\left(d/2+m\right)}{\pi^{d/2}\Gamma\left(-m\right)}$$

$$\cdot \frac{z^{d+2m}}{\left(x-x'\right)^{d+2m}} = 0, \tag{A.8}$$

where we have also used the asymptotic expansion (A.6) of confluent hypergeometric function ${}_1F_1$. The above result shows that the $\Phi(z \to 0) \sim z^{d-\Delta}$ mode is a quasi-local function which is identically vanishing when $(x-x')^2 > z^2$.

In the $(x-x')^2 < z^2$ regime, we have

$$\frac{z^{d/2}}{(2\pi)^d} \int \mathrm{d}^d k e^{-(zk)^2/\Lambda^2} I_{d/2-\Delta}\left(zk\right) k^{\Delta-d/2} e^{ik(x-x')}$$

$$= \frac{2^{\Delta-d/2} z^{d-\Delta}}{\Gamma\left(d/2-\Delta+1\right)} {}_0F_1\left(; \frac{d}{2}-\Delta+1; -\frac{z^2}{4}\Box\right)$$

$$\cdot \delta^d\left(x-x'\right) = \lim_{\Lambda\to\infty} \frac{2^{\Delta-d/2} z^{d-\Delta}}{\Gamma\left(d/2-\Delta+1\right)} {}_0F_1\left(; \frac{d}{2}\right.$$

$$\left. -\Delta+1; -\frac{z^2}{4}\Box\right) \frac{\Lambda^d}{2^d \pi^{d/2} z^d} e^{-(x-x')^2\Lambda^2/4z^2}$$

$$= \lim_{\Lambda\to\infty} \frac{2^{\Delta-d/2} z^{d-\Delta}}{\Gamma\left(d/2-\Delta+1\right)} \frac{\Lambda^d}{2^d \pi^{d/2} z^d} {}_0F_1\left(; \frac{d}{2}-\Delta\right.$$

$$\left. +1; -\frac{z^2}{4}\Box\right) \sum_{m=0}^{\infty} \frac{1}{m!} \left(\frac{-\left(x-x'\right)^2\Lambda^2}{4z^2}\right)^m$$

$$= \lim_{\Lambda\to\infty} \frac{2^{\Delta-d/2} z^{d-\Delta}}{\Gamma\left(d/2-\Delta+1\right)} \frac{\Lambda^d}{2^d \pi^{d/2} z^d}$$

$$\cdot \sum_{m=0}^{\infty} \sum_{n=0}^{m} \frac{\Gamma(d/2-\Delta+1)}{n!\Gamma(d/2-\Delta+1+n)}$$

$$\cdot \frac{\Gamma(d/2+m)}{\Gamma(m-n+1)\Gamma(d/2+m-n)} \left(\frac{\Lambda^2}{4}\right)^m$$

$$\cdot \left(-\frac{\left(x-x'\right)^2}{z^2}\right)^{(m-n)} = \lim_{\Lambda\to\infty} \frac{2^{\Delta-d/2} z^{d-\Delta}}{\Gamma(d/2-\Delta+1)}$$

$$\cdot \frac{\Lambda^d}{2^d \pi^{d/2} z^d} \sum_{k=0}^{\infty} \frac{1}{k!} {}_1F_1\left(\frac{d}{2}+k; \frac{d}{2}-\Delta+1; \frac{\Lambda^2}{4}\right)$$

$$\cdot \left(-\frac{\Lambda^2\left(x-x'\right)^2}{4z^2}\right)^k = \frac{2^{\Delta-d/2} z^{-\Delta}}{\pi^{d/2}} \sum_{k=0}^{\infty} \left[e^{i(d\pi/2)} \right.$$

$$\cdot \frac{\sin(\pi\Delta)}{\pi} \Gamma(\Delta) \frac{\Gamma(\Delta+k)}{k!\Gamma(\Delta)} \left(-\frac{\left(x-x'\right)^2}{z^2}\right)^k$$

$$+ \lim_{\Lambda\to\infty} \frac{\left(-\left(x-x'\right)^2/z^2\right)^k}{k!\Gamma(d/2+k)} e^{\Lambda^2/4} \left(\frac{\Lambda^2}{4}\right)^{\Delta+d/2+2k-1}$$

$$\left. \cdot {}_2F_0\left(1-\Delta-k, 1-\frac{d}{2}-k; ; \frac{4}{\Lambda^2}\right) \right]$$

$$= \frac{2^{\Delta-d/2}\Gamma(\Delta)}{\pi^{d/2+1}} e^{i(d\pi/2)} \sin(\pi\Delta) \left(\frac{z}{z^2+\left(x-x'\right)^2}\right)^{\Delta}$$

$$+ \lim_{\Lambda\to\infty} \frac{2^{\Delta-d/2} z^{-\Delta}}{\pi^{d/2}} \sum_{k=0}^{\infty} \frac{\left(-\left(x-x'\right)^2/z^2\right)^k}{k!\Gamma(d/2+k)}$$

$$\cdot e^{\Lambda^2/4} \left(\frac{\Lambda^2}{4}\right)^{\Delta+d/2+2k-1} {}_2F_0\left(1-\Delta-k, 1-\frac{d}{2}\right.$$

$$\left. -k; ; \frac{4}{\Lambda^2}\right). \tag{A.9}$$

As in the $\Phi(z\to 0)\sim z^{\Delta}$ case, the result is divergent and the divergent parts are expressed as terms with positive powers of Λ.

Comparing (A.7) and (A.9), we notice that the divergence in the region $(x-x')^2 < z^2$ can only be canceled in the combination

$$I_{\Delta-d/2} - I_{d/2-\Delta} \sim K_{\Delta-d/2}, \tag{A.10}$$

which coincides with the answer obtained in [14] by requiring the $z\to\infty$ regularity of the momentum space solution. We also notice that the remnant finite term gives rise to exactly the analytical continuation of the result in $(x-x')^2 > z^2$ region. Thus one can take the continuity at $|x-x'|^2 = z^2$ as the prescription of the regularization in the coordinate space.

The above derivations are performed under the Euclidean signature. For the Minkowskian signature, the 2-point propagator is not unique due to the existence of the light cone singularity. Depending on which kind of 2-point propagator was considered, the corresponding bulk momentum space formulae are different. These different formulae are related to the different choices of quantum states of the boundary QFT [27, 28]. For example, as pointed in [29–31], the retarded propagator is related to take the ingoing boundary condition at the horizon $z\to\infty$, while the advanced propagator is related to take the outcoming boundary condition at the horizon $z\to\infty$. In these two cases, the relevant bulk momentum space formulae are still linear combinations of the $\Phi(z\to 0)\sim z^{\Delta}$ mode and the $\Phi(z\to 0)\sim z^{d-\Delta}$ mode. It is also possible to have the bulk momentum space formulae with purely normalizable modes where $\Phi(z\to 0)\sim z^{\Delta}$ and $k^2<0$. This case is in fact the one being discussed in [5–7]. In our present consideration, the formula is related to the radial quantization which is initially well established under the Euclidean signature. Therefore, the relevant bulk momentum space formula is taken to be the simple analytical continuation of the Euclidean one [14] which is uniquely fixed by requiring the regularity at $z\to\infty$ since $k^2>0$ for the Euclidean signature.

Conflicts of Interest

The authors declare that there are no conflicts of interest regarding the publication of this paper.

Acknowledgments

The authors are grateful to Piljin Yi for enlightening discussions as well as collaboration at an early stage of this work and also thanks are due to Jiang Long, Hong Lü, Jun-Bao Wu, Xiao Xiao, and Hossein Yavartanoo for useful conversations. This work is supported by National Natural Science Foundation of China with Grant no. 11305125 and no. 11447607 and the Double First-Class University Construction Project of Northwest University.

References

[1] J. Maldacena, "The Large N limit of superconformal field theories and supergravity," *International Journal of Theoretical Physics*, vol. 38, no. 4, pp. 1113–1133, 1999.

[2] J. M. Maldacena, "The Large N Limit of Superconformal Field Theories and Supergravity," *Advances in Theoretical and Mathematical Physics*, vol. 2, no. 2, pp. 231–252, 1998.

[3] S. S. Gubser, I. R. Klebanov, and A. M. Polyakov, "Gauge theory correlators from non-critical string theory," *Physics Letters. B. Particle Physics, Nuclear Physics and Cosmology*, vol. 428, no. 1-2, pp. 105–114, 1998.

[4] E. Witten, "Anti de Sitter space and holography," *Advances in Theoretical and Mathematical Physics*, vol. 2, no. 2, pp. 253–291, 1998.

[5] T. Banks, L. J. Dixon, D. Friedan, and E. Martinec, "Phenomenology and conformal field theory or can string theory predict the weak mixing angle?" *Nuclear Physics B*, vol. 299, no. 3, pp. 613–626, 1988.

[6] V. Balasubramanian, S. B. Giddings, and A. Lawrence, "What do CFTs tell us about Anti-de Sitter space-times?" *The Journal of High Energy Physics*, vol. 9903, 1999.

[7] I. Bena, "On the construction of local fields in the bulk of AdS(5) and other spaces," *Physical Review. D. Third Series*, vol. 62, Article ID 066007, 2000.

[8] A. Hamilton, D. Kabat, G. Lifschytz, and D. A. Lowe, "Holographic representation of local bulk operators," *Physical Review. D. Third Series*, vol. 74, Article ID 066009, 2006.

[9] A. Hamilton, D. Kabat, G. Lifschytz, and D. A. Lowe, "Local bulk operators in AdS/CFT: A Holographic description of the black hole interior," *Physical Review D. Particles, Fields, Gravitation, and Cosmology*, vol. 75, Article ID 106001, 2007.

[10] A. Hamilton, D. Kabat, G. Lifschytz, and D. A. Lowe, "Publisher's Note: Local bulk operators in AdS/CFT correspondence: A holographic description of the black hole interior," *Physical Review D. Particles, Fields, Gravitation, and Cosmology*, vol. 75, Article ID 129902, 2007.

[11] L. Susskind and E. Witten, "The Holographic bound in anti-de Sitter space," *High Energy Physics*, Article ID 9805114, 1998.

[12] I. Heemskerk and J. Polchinski, "Holographic and Wilsonian renormalization groups," *Journal of High Energy Physics*, vol. 1106, 2011.

[13] D. Sarkar, "(A)dS holography with a cutoff," *Physical Review D*, vol. 90, no. 8, Article ID 086005, 2014.

[14] V. Balasubramanian, P. Kraus, and A. Lawrence, "Bulk versus boundary dynamics in anti-de Sitter spacetime," *Physical Review. D. Third Series*, vol. 59, no. 4, 046003, 16 pages, 1999.

[15] D. Z. Freedman, S. D. Mathur, A. Matusis, and L. Rastelli, "Correlation functions in the CFT(d) / AdS(d+1) correspondence," *Nucl. Phys. B*, vol. 546, no. 1-2, pp. 96–118, 1999.

[16] D. Pappadopulo, S. Rychkov, J. Espin, and R. Rattazzi, "Operator product expansion convergence in conformal field theory," *Physical Review D - Particles, Fields, Gravitation and Cosmology*, vol. 86, no. 10, Article ID 105043, 2012.

[17] S. Rychkov, "EPFL Lectures on Conformal Field Theory in D ≥ 3 Dimensions," *High Energy Physics*, 2016.

[18] D. Kabat, G. Lifschytz, and D. A. Lowe, "Constructing local bulk observables in interacting AdS/CFT," *Physical Review D - Particles, Fields, Gravitation and Cosmology*, vol. 83, no. 10, Article ID 106009, 2011.

[19] Z.-L. Wang, "Talk preseneted on KIAS-YITP Joint Workshop 2015: geometry in gauge theories and string theory".

[20] A. A. Belavin, A. M. Polyakov, and A. B. Zamolodchikov, "Infinite conformal symmetry in two-dimensional quantum field theory," *Nuclear Physics. B. Theoretical, Phenomenological, and Experimental High Energy Physics. Quantum Field Theory and Statistical Systems*, vol. 241, no. 2, pp. 333–380, 1984.

[21] E. S. Fradkin and M. Y. Palchik, *Conformal Quantum Field Theory in D-dimensions*, Kluwer Academic Publishers, 1996.

[22] E. S. Fradkin and M. Y. Palchik, "New developments in D-dimensional conformal quantum field theory," *Physics Reports. A Review Section of Physics Letters*, vol. 300, no. 1-2, 111 pages, 1998.

[23] A. Almheiri, D. Marolf, J. Polchinski, and J. Sully, "Black holes: Complementarity or firewalls?" *Journal of High Energy Physics*, vol. 2013, no. 2, pp. 1–19, 2013.

[24] S. L. Braunstein, S. Pirandola, and K. Zyczkowski, "Better late than never: Information retrieval from black holes," *Physical Review Letters*, vol. 110, no. 10, Article ID 101301, 2013.

[25] Y. Nakayama and H. Ooguri, "Bulk locality and boundary creating operators," *Journal of High Energy Physics*, vol. 2015, no. 10, 4 pages, 2015.

[26] M. Miyaji, T. Numasawa, N. Shiba, T. Takayanagi, and K. Watanabe, "cMERA as Surface/State Correspondence in AdS/CFT," *Physical Review Letters*, vol. 115, Article ID 171602, 2015.

[27] V. Balasubramanian, P. Kraus, A. Lawrence, and S. P. Trivedi, "Holographic probes of anti-de Sitter spacetimes," *Physical Review. D. Third Series*, vol. 59, no. 10, Article ID 104021, 14 pages, 1999.

[28] K. Skenderis and B. C. van Rees, "Real-time gauge/gravity duality: prescription, renormalization and examples," *Journal of High Energy Physics. A SISSA Journal*, vol. 0905, 2009.

[29] D. T. Son and A. O. Starinets, "Minkowski space correlators in AdS / CFT correspondence: Recipe and applications," *Journal of High Energy Physics. A SISSA Journal*, vol. 0209, 2002.

[30] D. Marolf, "States and boundary terms: Subtleties of Lorentzian AdS / CFT," *Journal of High Energy Physics. A SISSA Journal*, vol. 0505, 2005.

[31] N. Iqbal and H. Liu, "Real-time response in AdS/CFT with application to spinors," *Fortschritte der Physik. Progress of Physics*, vol. 57, 2009.

Hindawi
Advances in High Energy Physics
Volume 2017, Article ID 6402101, 8 pages
https://doi.org/10.1155/2017/6402101

Research Article

Van der Waals-Like Phase Transition from Holographic Entanglement Entropy in Lorentz Breaking Massive Gravity

Xian-Ming Liu,[1] Hong-Bo Shao,[2] and Xiao-Xiong Zeng[3]

[1]*School of Science, Hubei University for Nationalities, Enshi 445000, China*
[2]*College of Science, Agricultural University of Hebei, Baoding 071000, China*
[3]*School of Material Science and Engineering, Chongqing Jiaotong University, Chongqing 400074, China*

Correspondence should be addressed to Xiao-Xiong Zeng; xxzengphysics@163.com

Received 12 June 2017; Revised 15 August 2017; Accepted 24 August 2017; Published 2 October 2017

Academic Editor: Li Li

Copyright © 2017 Xian-Ming Liu et al. This is an open access article distributed under the Creative Commons Attribution License, which permits unrestricted use, distribution, and reproduction in any medium, provided the original work is properly cited. The publication of this article was funded by SCOAP[3].

Phase transition of AdS black holes in Lorentz breaking massive gravity has been studied in the framework of holography. We find that there is a first-order phase transition (FPT) and second-order phase transition (SPT) both in Bekenstein-Hawking entropy- (BHE-) temperature plane and in holographic entanglement entropy- (HEE-) temperature plane. Furthermore, for the FPT, the equal area law is checked and for the SPT, the critical exponent of the heat capacity is also computed. Our results confirm that the phase structure of HEE is similar to that of BHE in Lorentz breaking massive gravity, which implies that HEE and BHE have some potential underlying relationship.

1. Introduction

The study of HEE and quantum phase transitions of black holes has attracted a lot of interest in recent years. On one hand, HEE can be used as a perfect probe to study quantum information science [1–3], strongly correlated quantum systems [4–13], and Many-Body Systems [14, 15]. On the other hand, investigation on HEE of black holes may shed some light on understanding the nature of BHE [16, 17].

Nearly ten years ago, a holographic derivation of the HEE in conformal quantum field theories was proposed by Ryu and Takayanagi using the famous AdS/CFT correspondence [18, 19]. Recently the HEE has been used as a probe to investigate the phase structure of the Reissner-Nordstrom AdS black hole [20]. The results showed that there is a Van der Waals-like (VDW) phase transition at the same critical temperature in both the fixed charge ensemble and chemical potential ensemble in the HEE-temperature plane. They also found that the SPT occurs for the HEE at the same critical point as the BHE with nearly the same critical exponent. This work was soon generalized to the extended phase space where the cosmological constant is considered as a thermodynamical variable [21]. Very recently, the equal area law of HEE was proved to hold for the FPT in the HEE-temperature plane [22]. Based on [20], VDW phase transition of HEE in various AdS black holes has been studied in [23–32]. All of these works showed that the HEE undergoes the same VDW phase transition as that of the BHE.

Massive gravity theories have attracted considerable interest recently. One of these reasons is that these alternative theories of gravity could explain the accelerated expansion of the universe without dark energy. The graviton behaves like a lattice excitation and exhibits a Drude peak in this theory. Current experimental data from the observation of gravitational waves by advanced LIGO require the graviton mass to be smaller than the inverse period of orbital motion of the binary system; that is, $m_g < 1.2 \times 10^{-22}\,\mathrm{eV}/c^2$ [33]. Another important reason for the interest in massive gravity is that the possibility of the mass graviton could help to understand the quantum gravity effect. The first to introduce a mass to the graviton is in [34]. However this primitive linear massive gravity theory contains the so-called Boulware-Deser ghosts problem [35] that was solved by a nonlinear massive gravity theory [36, 37], where the

mass terms are obtained by introducing a reference metric. Recently Vegh proposed a new reference metric to describe a class of strongly interacting quantum field theories with broken translational symmetry in the holographic framework [38]. The recent progress in massive gravity can be found in [39, 40].

Here, we consider AdS black holes in Lorentz breaking massive gravity. In the massive gravity, the graviton acquires a mass by Lorentz symmetry breaking, which is very similar to the Higgs mechanism. A review of Lorentz-violating massive gravity theory can be found in [41, 42]. In this paper, we focus on the study of the VDW phase transition of AdS black holes in Lorentz breaking massive gravity using the HEE. The main motivation of this paper is to explore whether the BHE phase transition can also be described by HEE in Lorentz breaking massive gravity. Firstly, we would like to extend proposals in [20] to study VDW phase transitions in AdS black hole with a spherical horizon in Lorentz-violating massive gravity with the HEE as a probe. What is more, we also would like to check Maxwell's equal area law and critical exponent of the heat capacity, which are two characteristic quantities in VDW phase transition.

The organization of this paper is as follows. In the next section, we shall provide a brief review of the black hole solution in Lorentz breaking massive gravity firstly. Then we will study the VDW phase transitions and critical phenomena for the AdS black hole in the BHE-temperature plane. In Section 3, we mainly concentrate on the VDW phase transition and critical phenomena in the framework of HEE. The last section is devoted to our discussions and conclusions.

2. Phase Transition and Critical Phenomena of AdS Black Holes in Lorentz Breaking Massive Gravity

2.1. Review of AdS Black Holes in Lorentz Breaking Massive Gravity. The four-dimensional Lorentz breaking massive gravity can be obtained by adding nonderivative coupling scalar fields to the standard Einstein gravity theory. As a matter field is considered, the theory can be described by the following action [41, 42]:

$$S = \int d^4x\sqrt{-g}\left[-M_{\mathrm{Pl}}^2 R + L_m + \ell^4\Psi\left(X, \Pi^{ij}\right)\right]; \quad (1)$$

here the first two terms are the curvature and ordinary matter minimally coupled to gravity, respectively, and the third term Ψ contains two functions X and Π^{ij} which relate to the four scalar fields, Ξ^0 and Ξ^i as

$$X = \frac{\partial^\mu \Xi^0 \partial_\mu \Xi^0}{\ell^4},$$
$$\Pi^{ij} = \frac{\partial^\mu \Xi^i \partial_\mu \Xi^j}{\ell^4} - \frac{\partial^\mu \Xi^i \partial_\mu \Xi^0 \partial^\nu \Xi^j \partial_\nu \Xi^0}{\ell^8 X}. \quad (2)$$

When the four scalar fields get a space-time depending vacuum expectation value, the system will break the Lorentz symmetry. What is more, the action can also be taken as a low-energy effective theory with the ultraviolet cutoff scale ℓ. Here the scale parameter ℓ has the dimension of mass and is in the order of $\sqrt{m_g M_{\mathrm{Pl}}}$, where m_g and M_{Pl} are the graviton mass and the Plank mass, respectively.

The AdS black hole solutions can be obtained from the above theory [43, 44]. The metric corresponding to the AdS black holes is given by

$$ds^2 = -f(r)\,dt^2 + f(r)^{-1}\,dr^2 + r^2\left(d\varphi^2 + \sin^2\varphi d\phi^2\right), \quad (3)$$

with

$$f(r) = 1 - \frac{2M}{r} - \gamma\frac{Q^2}{r^\lambda} - \frac{\Lambda r^2}{3}. \quad (4)$$

Here, the four scalar fields, Ξ^0 and Ξ^i, for this particular solution are given by

$$\Xi^0 = \ell^2\left(t + \eta(r)\right),$$
$$\Xi^i = \ell^2\alpha x^i, \quad (5)$$

in which

$$\eta(r) = \pm\int \frac{dr}{f(r)} \cdot\left[1 - f(r)\left(\frac{\gamma Q^2\lambda(\lambda-1)}{12m_g^2\alpha^6}\frac{1}{r^{\lambda+1}} + 1\right)^{-1}\right]^{1/2}, \quad (6)$$

in which the scalar charge Q is related to massive gravity and the constant α which is determined by the cosmological constant Λ and the graviton mass m_g with the relation $\Lambda = 2m_g^2(1 - \alpha^6)$. In this paper, we will set $\alpha > 1$ such that $\Lambda < 0$ leading to Anti-de Sitter black holes. The constant λ is a positive integration constant. When $\lambda < 1$, the ADM mass of the black hole solution diverges. For $\lambda > 1$, the metric approaches the Schwarzschild-AdS black holes with a finite mass M as $r \to \infty$. Thus we set $\lambda > 1$ in this paper. The constant $\gamma = \pm 1$. When $\gamma = 1$, the black hole only has a single horizon r_h, which is the root of the equation $f(r_h) = 0$. The function $f(r)$ for this case is given in Figure 1, which is similar to the Schwarzschild-AdS black hole. For $\gamma = -1$, the black hole is very similar to the Reissner-Nordstrom-AdS black hole. The function $f(r)$ for this case is given in Figure 2. The black hole event horizon r_h is the largest root of the equation $f(r_h) = 0$.

At the event horizon, the Hawking temperature and BHE can be written as

$$T = \frac{1}{4\pi}f'(r_h) = \frac{1}{4\pi}\left(\frac{1}{r_h} - r_h\Lambda + \frac{\gamma(\lambda-1)Q^2}{r_h^{\lambda+1}}\right), \quad (7)$$

$$S = \pi r_h^2. \quad (8)$$

The chemical potential in this black hole is

$$\Phi = -\gamma\frac{Q}{r_h^{\lambda-1}}. \quad (9)$$

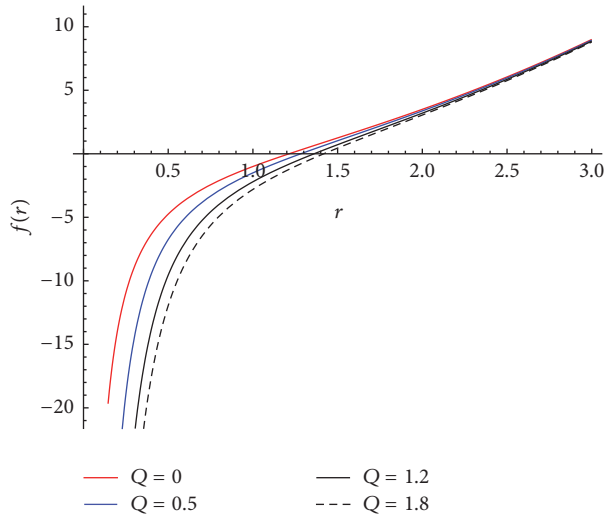

FIGURE 1: The figure shows $f(r)$ versus r for $\gamma = 1$ for varying Q. Here $\lambda = 2.4$, $\Lambda = -3$, and $M = 1.5$.

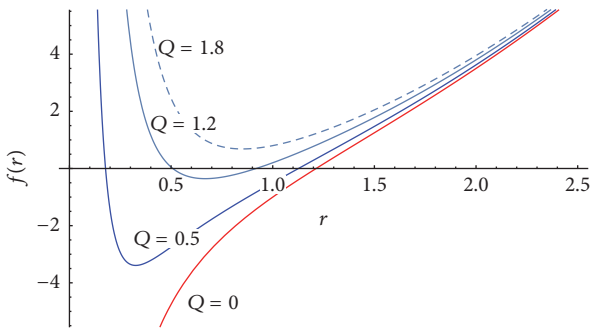

FIGURE 2: The figure shows $f(r)$ versus r for $\gamma = -1$ for varying Q. Here $\lambda = 2.4$, $\Lambda = -3$, and $M = 1.5$.

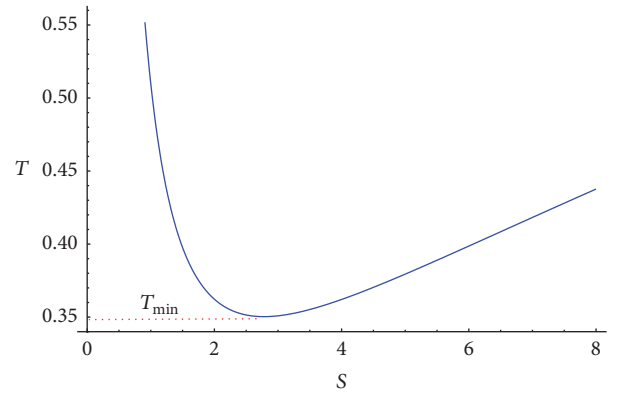

FIGURE 3: The figure shows T versus S for $\gamma = 1$. Here $\lambda = 2.4$, $\Lambda = -3$, and $Q = 0.3$.

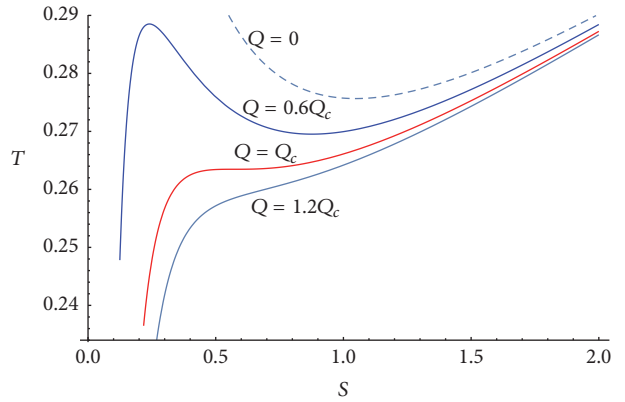

FIGURE 4: The figure shows T versus S for $\gamma = -1$ for varying Q. Here $\lambda = 2.4$, $\Lambda = -3$. The top dashed curve is at $Q = 0$ and the rest have $Q = 0.6Q_c$, Q_c, $1.2Q_c$, where $Q_c = 0.12346$.

We can check the first law of the black hole, which is given by

$$dM = TdS + \Phi dQ. \tag{10}$$

There have been some works to study the thermodynamics and phase transitions of black holes in Lorentz breaking massive gravity [45–48].

2.2. Van der Waals-Like Phase Transition of Bekenstein-Hawking Entropy. In this subsection, we focus on the VDW phase transition of BHE. Substituting (8) into (7) and eliminating the parameter r_h, one can get the relation between the Hawking temperature T and BHE S of the AdS black holes in massive gravity as

$$T = \frac{S^{(1/2)(-\lambda-1)}\left(\gamma\pi^{\lambda/2+1}(\lambda-1)Q - \Lambda S^{\lambda/2+1} + \pi S^{\lambda/2}\right)}{4\pi^{3/2}}. \tag{11}$$

This is the state equation of the AdS black hole thermodynamics system in massive gravity. Using (11), we investigate the phase diagram of the AdS black holes in massive gravity.

The temperature T is plotted as a function of the BHE S in Figures 3 and 4 for $\gamma = 1$ and $\gamma = -1$, respectively. In Figure 3, the temperature is plotted for $\gamma = 1$ where only one event horizon exists. This behavior of temperature is very similar to the behavior in the Schwarzschild-AdS black hole. That is to say, there is a minimum temperature $T_{\min}$ which divides the thermodynamics systems into small and large black holes. It is shown that, above the minimum temperature, small and large black holes coexist. In fact, this behavior will break for there is a first-order transition, which is similar to the Hawking-Page thermodynamic transition in [49].

In Figure 4, the temperature is plotted for $\gamma = -1$ where event horizon and inner horizon exist. Various values of Q are used to plot the relations between the temperature and horizons. The top curve corresponds to $Q = 0$. The system of this case is similar to the case $\gamma = 1$ described above. When the scalar charge Q increases, the temperature has two turning points. Further increasing of the scalar charge Q makes these two turning points merge to one. It is shown that there exists a critical point Q_c. Above the critical point, the curve does not have any turning points. Thus we find that the phase structure is very similar to that of the Van der Waals gas-fluid phase transition. It should be noted that we

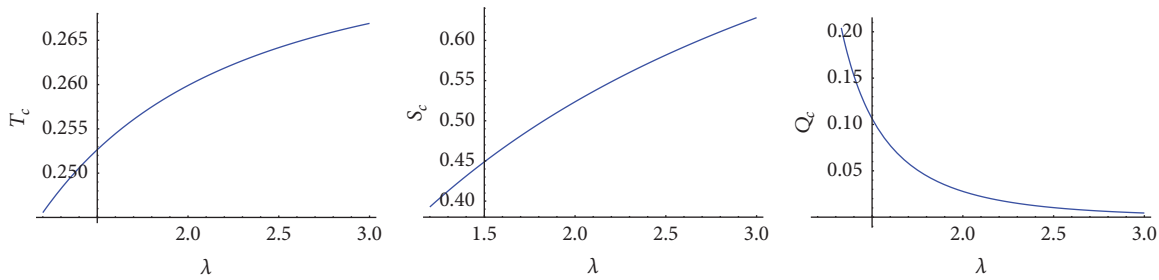

FIGURE 5: The figure shows the critical temperature T_c, the critical entropy S_c, and the critical charge Q_c versus λ for $\gamma = -1$. Here $\Lambda = -3$.

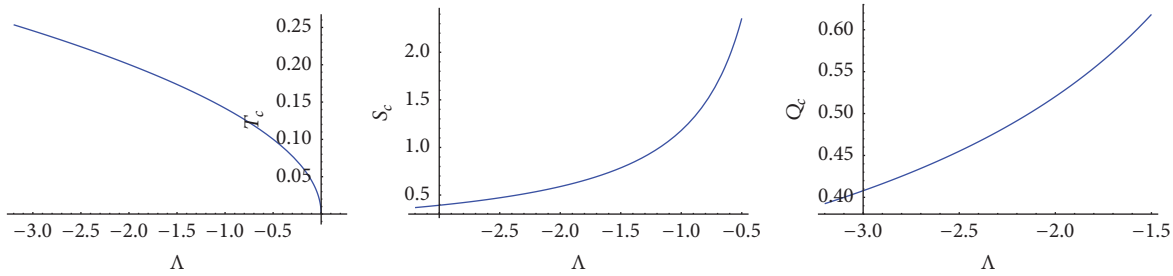

FIGURE 6: The figure shows the critical temperature T_c, the critical entropy S_c, and the critical charge Q_c versus Λ for $\gamma = -1$. Here $\lambda = 1.2$.

mainly concentrate on this type of phase structure in this paper. Furthermore using the definition of the specific heat capacity C_Q, that is,

$$C_Q = T\left(\frac{\partial S}{\partial T}\right)_Q, \tag{12}$$

one can see that the specific heat capacity is divergent at the critical point and it is obvious that this phase transition is a SPT. At this critical point, the critical charge Q_c and critical entropy S_c can be obtained by the following equations:

$$\left(\frac{\partial T}{\partial S}\right)_{Q_c,S_c} = \left(\frac{\partial^2 T}{\partial S^2}\right)_{Q_c,S_c} = 0. \tag{13}$$

After some calculation and using (11), Q_c, S_c, and the corresponding T_c can be also got as

$$Q_c = -\frac{2\left(-\lambda/\left(\lambda+2\right)\Lambda\right)^{\lambda/2}}{\gamma\left(\lambda+2\right)\left(\lambda^2-1\right)}, \tag{14}$$

$$S_c = -\frac{\pi\lambda}{\left(\lambda+2\right)\Lambda}, \tag{15}$$

$$T_c = \frac{\lambda}{2\pi\left(\lambda+1\right)\sqrt{-\lambda/\left(\lambda+2\right)\Lambda}}. \tag{16}$$

Obviously, these critical parameters depend only on the internal parameters of the systems λ and Λ. One can also see that T_c and S_c increase with λ and Q_c decreases with λ as shown in Figure 5; S_c and Q_c increase with Λ and T_c decreases with λ as shown in Figure 6. So the results show that the parameter λ promotes the thermodynamic system to reach the stable state.

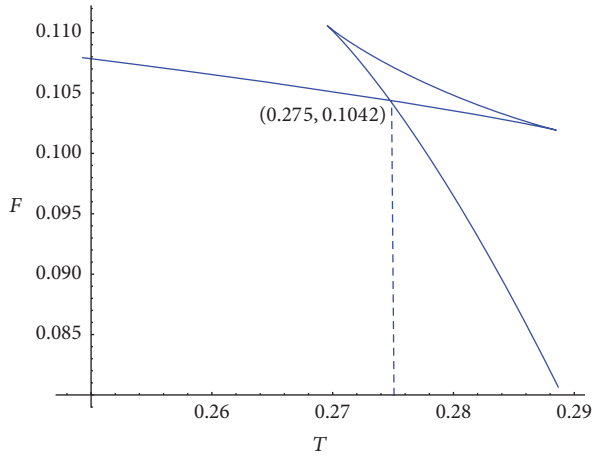

FIGURE 7: The figure shows F versus T for $\gamma = -1$. Here $\lambda = 2.4$, $\Lambda = -3$, and $Q = 0.6Q_c$.

For the FPT, we will also check whether Maxwell's equal area law holds in this thermodynamic system. As is known to all, the first-order transition temperature T^* plays a crucial role for Maxwell's equal area law. Thus in order to get T^*, we first plot the curve about the free energy with respect to the temperature T, where the free energy is defined by $F = M - TS$. The relation between F with T is plotted in Figure 7. One can see that there is a swallowtail structure, which corresponds to the unstable phase in Figure 8. The nonsmoothness of the junction implies that the phase transition is a FPT. The critical temperature T^* is apparently given by the horizontal coordinate of the junction. From Figure 7, we get $T^* = 0.2750$. Substituting this temperature T^* into (11), one can obtain three values of the entropy, $S_1 = 0.1563$,

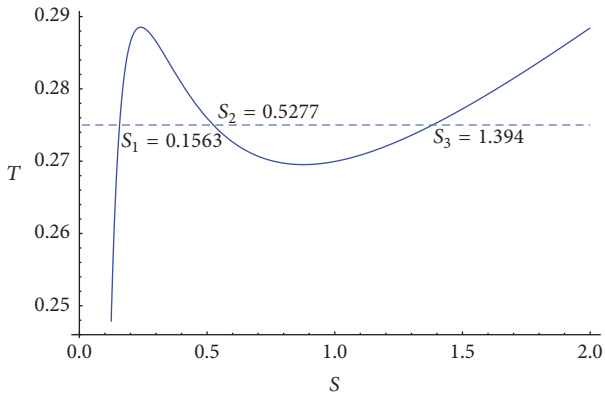

FIGURE 8: The figure shows T versus S for $\gamma = -1$. Here $\lambda = 2.4$, $\Lambda = -3$, and $Q = 0.6Q_c$.

$S_2 = 0.5277$, and $S_3 = 1.394$. With these values, we can now check Maxwell's equal area law

$$T^* (S_3 - S_1) = \int_{S_1}^{S_3} T(S, Q)\, dS. \tag{17}$$

After some calculation, we find that both the left and right sides of (17) are equal to 0.3404 exactly. Thus, our results show that Maxwell's equal area law is satisfied in this background.

For the SPT, we will study the critical exponent associated with the heat capacity definition in (12). Near the critical point, expanding the temperature as the very small amount $S - S_c$, we find

$$T = T_c + \left(\frac{\partial T}{\partial S}\right)_{Q_c, S_c} (S - S_c) + \left(\frac{\partial^2 T}{\partial S^2}\right)_{Q_c, S_c} (S - S_c)^2 + \left(\frac{\partial^3 T}{\partial S^3}\right)_{Q_c, S_c} (S - S_c)^3 + o(S - S_c)^4. \tag{18}$$

Using (13), the second and third terms vanish. Then using (11), (14), and (15), we get

$$T - T_c = \frac{\lambda}{16\pi^4 (-\lambda/(\lambda + 2)\Lambda)^{7/2}} (S - S_c)^3. \tag{19}$$

With the definition of the heat capacity (12), we further get $C_Q \sim (T - T_c)^{-2/3}$. So one can find that the critical exponent of the heat capacity is $-2/3$, which is the same as the one from the mean field theory in Van der Waals gas-fluid system.

3. Van der Waals-Like Phase Transition and Critical Phenomena of Holographic Entanglement Entropy

In this section, our target is to explore whether the HEE has the similar VDW phase structure and critical phenomena as those of the BHE in massive gravity. For simplicity, here we only consider the case $\gamma = -1$. Now we will investigate whether there is VDW phase transition in the HEE-temperature phase plane.

Firstly, we review some basic knowledge about HEE. For detailed introduction of HEE, one can refer to [18, 19]. For a given quantum field theory described by a density matrix ρ, HEE for a region A and its complement B are

$$S_A = -Tr_A (\rho_A \ln \rho_A), \tag{20}$$

where ρ_A is the reduced density matrix. However, it is usually not easy to get this quantity in quantum field theory. Fortunately according to AdS/CFT correspondence, [18, 19] propose a very simple geometric formula for calculating S_A for static states with the area of a bulk minimal surface as ∂A; that is,

$$S_A = \frac{\text{Area}(\gamma_A)}{4}, \tag{21}$$

where γ_A is the codimension-2 minimal surface according to boundary condition $\partial\gamma_A = \partial A$.

Subsequently using definition (21), we will calculate the HEE and study the corresponding phase transition. It is noted that the space on the boundary is spherical in the AdS black hole in massive gravity and the volume of the space is finite. Thus in order to avoid the HEE to be affected by the surface that wraps the event horizon, we will choose a small region as A. More precisely, as done in [23, 25–27], we choose region A to be a spherical cap on the boundary given by $\varphi \le \varphi_0$. Here the area can be written as

$$A = 2\pi \int_0^{\varphi_0} \Theta(r(\varphi), \varphi)\, d\varphi, \qquad \Theta = r \sin\varphi \sqrt{\frac{(r')^2}{f(r)} + r^2}, \tag{22}$$

where $r' = dr/d\varphi$. Then according to the Euler-Lagrange equation, one can get the equation of motion of $r(\varphi)$; that is,

$$0 = r'(\varphi)^2 \left[\sin\varphi r(\varphi)^2 f'(r) - 2\cos\varphi r'(\varphi)\right] - 2r(\varphi) f(r) \left[r(\varphi)\left(\sin\varphi r''(\varphi) + \cos\varphi r'(\varphi)\right) - 3\sin\varphi r'(\varphi)^2\right] + 4\sin\varphi r(\varphi)^3 f(r)^2. \tag{23}$$

After using the boundary conditions $r'(0) = 0$, $r(0) = r_0$, we can get the numeric result of $r(\varphi)$.

It is worth noting that the HEE should be regularized by subtracting off the HEE in pure AdS, because the values of the HEE in (21) are divergent at the boundary. Now let us label the regularized HEE as δS. Here we choose the size of the boundary region to be $\varphi_0 = 0.10, 0.16$ and set the UV cutoff in the dual field theory to be $r(0.099)$ and $r(0.159)$, respectively. The numeric results are shown in Figures 9 and 10. One can see that, for a given scalar charge Q, the relation between the HEE and temperature is similar to that between the BHE and temperature. That is to say, the AdS black holes thermodynamic system with the HEE undergoes the FPT and SPT one after another as the scalar charge Q increases step by step.

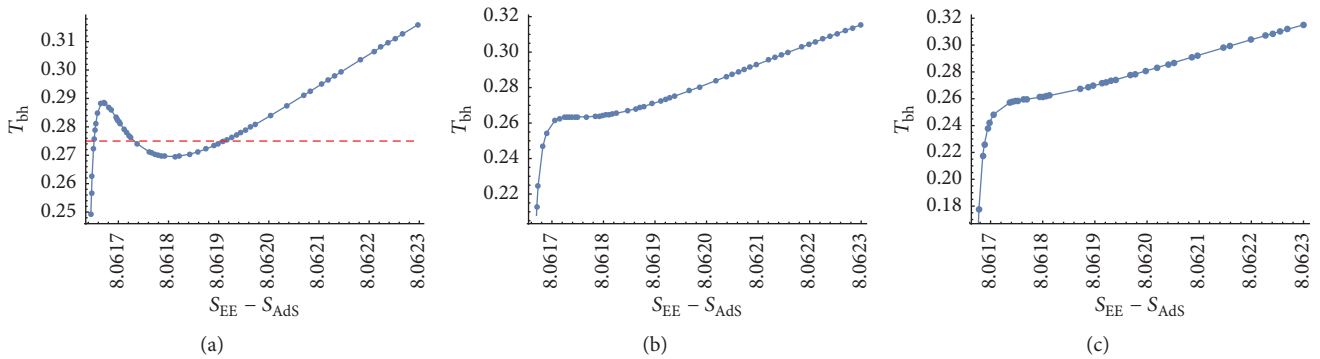

FIGURE 9: The figure shows T versus δS for $\gamma = -1$, $\varphi_0 = 0.10$. Here $\lambda = 2.4$, $Q = 0.6Q_c$, Q_c, $1.2Q_c$ from (a) to (c).

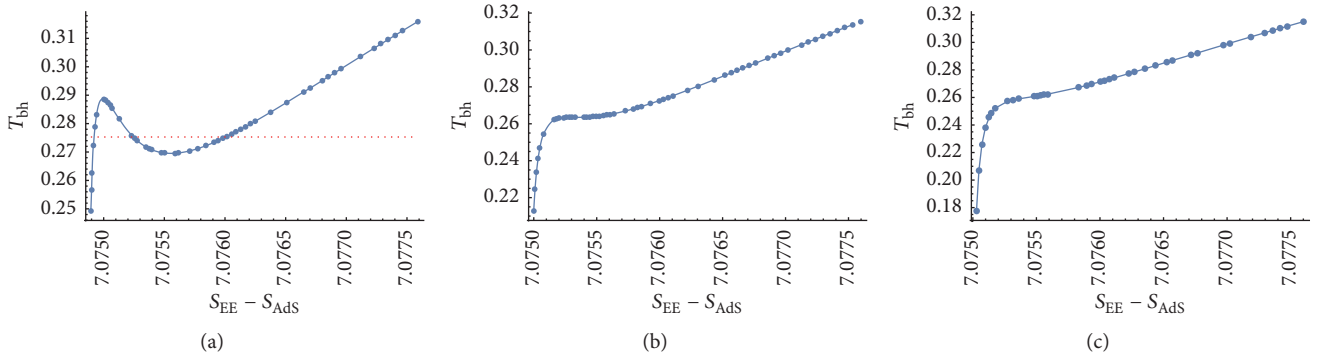

FIGURE 10: The figure shows T versus δS for $\gamma = -1$, $\varphi_0 = 0.16$. Here $\lambda = 2.4$, $Q = 0.6Q_c$, Q_c, $1.2Q_c$ from (a) to (c).

For the FPT of the HEE, we now check whether Maxwell's equal area law is satisfied. Firstly, we get the interpolating function of the temperature $T(\delta S)$ using the data obtained numerically. At the first-order phase transition point, we get the smallest and largest roots for the equation $T(\delta S) = T^*$, which are $\delta S_1 = 8.06165$, $\delta S_3 = 8.06191$ for $\varphi_0 = 0.10$ and $\delta S_1 = 7.07492$, $\delta S_3 = 7.07599$ for $\varphi_0 = 0.16$. Then using these values and the equal area law

$$T^* \left(\delta S_3 - \delta S_1\right) = \int_{\delta S_1}^{\delta S_3} T\left(\delta S\right) d\delta S, \tag{24}$$

we find the left side equals 0.00007137, 0.00029425 and the right side equals 0.00007135, 0.00029446 for $\varphi_0 = 0.10$, 0.16, respectively. Obviously both the left and the right sides are equal within our numerical accuracy and the relative errors are less than 0.022%, 0.071 for $\varphi_0 = 0.10$, 0.16, respectively.

Now let us consider the critical exponent of the SPT in the HEE-temperature phase plane. Here comparing with the definition of specific heat capacity C_Q in (12), one can also define a specific heat capacity for the HEE as

$$C_Q' = T\left(\frac{\partial \delta S}{\partial T}\right)_Q. \tag{25}$$

Then providing a similar relation of the critical points that in (13) is also working and using (25), we can get the critical exponent of SPT of in the HEE-temperature phase. Here we employ the logarithm of the quantities $T - T_c$, $\delta S - \delta S_c$. The relation between $\log|T - T_c|$ and $\log|\delta S - \delta S_c|$ is plotted in Figure 11. The analytical results of these straight lines can also be fitted, which are for $\varphi_0 = 0.10$,

$$\log\left|T - T_c\right| = 23.469 + 3.00654 \log\left|\delta S - \delta S_c\right|, \tag{26}$$

and for $\varphi_0 = 0.16$,

$$\log\left|T - T_c\right| = 19.2089 + 3.00477 \log\left|\delta S - \delta S_c\right|. \tag{27}$$

The results show that the slopes are all around 3 and the relative errors are less than 0.218%, 0.159% for $\varphi_0 = 0.10$, 0.16, respectively, which are consistent with that of the BHE. Then one can find that the critical exponent of the specific heat capacity C_Q' is also approximately $-2/3$. That is to say, the HEE has the same SPT behavior as that of the BHE. Both of them are consistent with the result in the mean field theory of VDW gas-fluid system.

4. Conclusions

In this paper, we have investigated the VDW phase transition with the use of HEE as a probe. Firstly, we investigated the phase diagrams of the BHE in the T-S phase plane and found that the phase structure depends on the scalar charge Q and the parameter γ of the AdS black holes in this massive gravity. For the case that $\gamma = 1$ or $Q = 0$, we found that there always exists the Hawking-Page-like phase transition in this thermodynamic system, while for the case $\gamma = -1$, we found

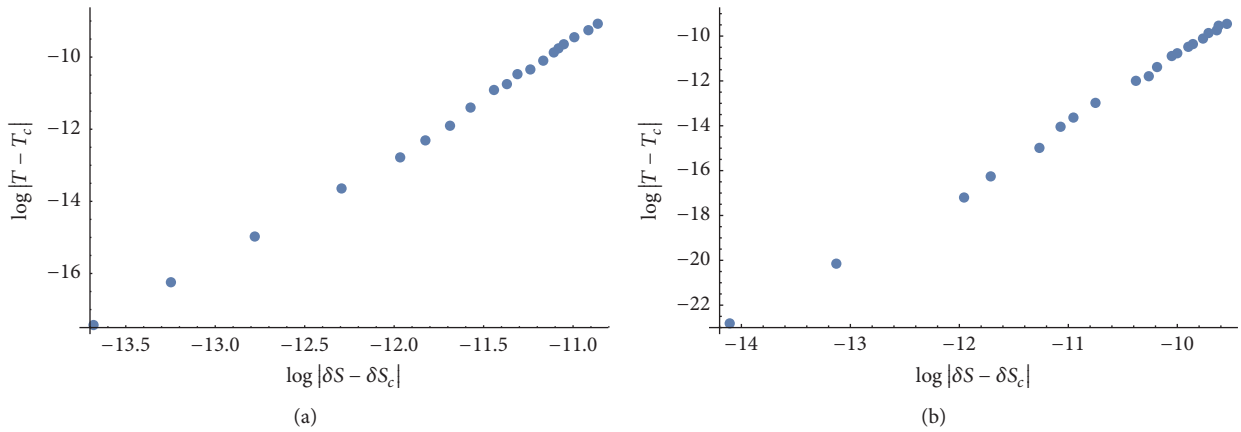

FIGURE 11: The figure shows $\log|T - T_c|$ versus $\log|\delta S - \delta S_c|$ for $\gamma = -1$. Here $\lambda = 2.4$, $Q = Q_c$, where $\varphi_0 = 0.10$ in (a) and $\varphi_0 = 0.16$ in (b).

for the small scalar charge Q, there is always an unstable black hole thermodynamic system interpolating between the small stable black hole system and large stable black hole system. The thermodynamic transition for the small hole to the large hole is a first-order transition and Maxwell's equal area law is valid. As the scalar charge Q increases to the critical value Q_c in this space-time, the unstable black hole merges into an inflection point. We found there is a SPT at the critical point. When the scalar charge is larger than the critical charge, the black hole is stable always. That is to say, we found that there exists the VDW gas-fluid phase transition in the T-S phase plane of the AdS black hole in massive gravity.

The more interesting thing is that we found the HEE also exhibits the VDW phase structure in the T-δS plane when $\gamma = -1$ and the scalar charge $Q \neq 0$. In order to confirm this result, we further showed that Maxwell's equal area law is satisfied and the critical exponent of the specific heat capacity is consistent with that of the mean field theory of the VDW gas-fluid system for the HEE system. These results show that the phase structure of HEE is similar to that of BHE and the HEE is really a good probe to the phase transition of AdS black holes in Lorentz breaking massive gravity. This also implies that HEE and BHE exhibit some potential underlying relationship.

Conflicts of Interest

The authors declare that they have no conflicts of interest.

Acknowledgments

The authors are grateful to De-Fu Hou and Hong-Bao Zhang for their instructive discussions. This work is supported by the National Natural Science Foundation of China (Grant no. 11365008, Grant no. 11465007, and Grant no. 61364030).

References

[1] C. H. Bennett, G. Brassard, C. Crépeau, R. Jozsa, A. Peres, and W. K. Wootters, "Teleporting an unknown quantum state via dual classical and Einstein-Podolsky-Rosen channels," *Physical Review Letters*, vol. 70, no. 13, pp. 1895–1899, 1993.

[2] C. H. Bennett and D. P. Divincenzo, "Quantum information and computation," *Nature*, vol. 404, no. 6775, pp. 247–255, 2000.

[3] M. A. Nielsen and I. L. Chuang, *Quantum Computation and Quantum Information*, Cambridge University Press, Cambridge, UK, 1st edition, 2000.

[4] J. Preskill, "Quantum information and physics: some future directions," *Journal of Modern Optics*, vol. 47, no. 2-3, pp. 127–137, 2000.

[5] T. J. Osborne and M. A. Nielsen, "Entanglement, quantum phase transitions, and density matrix renormalization," *Quantum Information Processing*, vol. 1, no. 1-2, pp. 45–53, 2002.

[6] P. Zanardi and X. Wang, "Fermionic entanglement in itinerant systems," *Journal of Physics. A. Mathematical and General*, vol. 35, no. 37, pp. 7947–7959, 2002.

[7] X.-X. Zeng and W.-B. Liu, "Holographic thermalization in Gauss-Bonnet gravity," *Physics Letters. B. Particle Physics, Nuclear Physics and Cosmology*, vol. 726, no. 1-3, pp. 481–487, 2013.

[8] X.-X. Zeng, X.-M. Liu, and W.-B. Liu, "Holographic thermalization with a chemical potential in Gauss-Bonnet gravity," *Journal of High Energy Physics*, vol. 2014, no. 3, article 031, 2014.

[9] X. X. Zeng, D. Y. Chen, and L. F. Li, "Holographic thermalization and gravitational collapse in a spacetime dominated by quintessence dark energy," *Physical Review D*, vol. 91, no. 4, Article ID 046005, 2015.

[10] X.-X. Zeng, X.-M. Liu, and W.-B. Liu, "Holographic thermalization in noncommutative geometry," *Physics Letters. B. Particle Physics, Nuclear Physics and Cosmology*, vol. 744, pp. 48–54, 2015.

[11] X. X. Zeng, X. Y. Hu, and L. F. Li, "Effect of phantom dark energy on holographic thermalization," *Chinese Physics Letters*, vol. 34, no. 1, Article ID 010401, 2017.

[12] R. Cai, X. Zeng, and H. Zhang, "Influence of inhomogeneities on holographic mutual information and butterfly effect," *Journal of High Energy Physics*, vol. 2017, no. 7, 2017.

[13] R. Cai, L. Li, L. Li, and R. Yang, "Introduction to holographic superconductor models," *Science China Physics, Mechanics & Astronomy*, vol. 58, no. 6, pp. 1–46, 2015.

[14] L. Amico, R. Fazio, A. Osterloh, and V. Vedral, "Entanglement in many-body systems," *Reviews of Modern Physics*, vol. 80, no. 2, pp. 517–576, 2008.

[15] N. Laflorencie, "Quantum entanglement in condensed matter systems," *Physics Reports. A Review Section of Physics Letters*, vol. 646, pp. 1–59, 2016.

[16] L. Susskind and J. Uglum, "Black hole entropy in canonical quantum gravity and superstring theory," *Physical Review. D. Third Series*, vol. 50, no. 4, pp. 2700–2711, 1994.

[17] S. N. Solodukhin, "Entanglement entropy of black holes," *Living Reviews in Relativity*, vol. 14, article 8, 2011.

[18] S. Ryu and T. Takayanagi, "Holographic derivation of entanglement entropy from the anti-de Sitter space/conformal field theory correspondence," *Physical Review Letters*, vol. 96, no. 18, Article ID 181602, 181602, 4 pages, 2006.

[19] S. Ryu and T. Takayanagi, "Aspects of holographic entanglement entropy," *Journal of High Energy Physics. A SISSA Journal*, no. 8, 045, 48 pages, 2006.

[20] C. V. Johnson, "Large N phase transitions, finite volume, and entanglement entropy," *Journal of High Energy Physics*, vol. 2014, article 47, 2014.

[21] E. Caceres, P. H. Nguyen, and J. F. Pedraza, "Holographic entanglement entropy and the extended phase structure of STU black holes," *Journal of High Energy Physics*, vol. 2015, no. 9, article 184, 2015.

[22] P. H. Nguyen, "An equal area law for holographic entanglement entropy of the AdS-RN black hole," *Journal of High Energy Physics*, vol. 15, no. 12, article 139, 2015.

[23] X. X. Zeng, H. Zhang, and L. F. Li, "Phase transition of holographic entanglement entropy in massive gravity," *Physics Letters B*, vol. 756, pp. 170–179, 2016.

[24] A. Dey, S. Mahapatra, and T. Sarkar, "Thermodynamics and entanglement entropy with Weyl corrections," *Physical Review D - Particles, Fields, Gravitation and Cosmology*, vol. 94, no. 2, Article ID 026006, 2016.

[25] X.-X. Zeng, X.-M. Liu, and L.-F. Li, "Phase structure of the Born–Infeld–anti-de Sitter black holes probed by non-local observables," *European Physical Journal C*, vol. 76, no. 11, article 616, 2016.

[26] X.-X. Zeng and L.-F. Li, "Holographic Phase Transition Probed by Nonlocal Observables," *Advances in High Energy Physics*, vol. 2016, Article ID 6153435, 2016.

[27] X. X. Zeng and L. F. Li, "Van der waals phase transition in the framework of holography," *Physics Letters B*, vol. 764, pp. 100–108, 2017.

[28] J.-X. Mo, G.-Q. Li, Z.-T. Lin, and X.-X. Zeng, "Revisiting van der Waals like behavior of *f(R)* AdS black holes via the two point correlation function," *Nuclear Physics B*, vol. 918, pp. 11–22, 2017.

[29] S. He, L. F. Li, and X. X. Zeng, "Holographic van der waals-like phase transition in the Gauss–Bonnet gravity," *Nuclear Physics B*, vol. 915, pp. 243–261, 2017.

[30] X. Zeng and Y. Han, "Holographic van der waals phase transition for a hairy black hole," *Advances in High Energy Physics*, vol. 2017, Article ID 2356174, 8 pages, 2017.

[31] H.-L. Li, S.-Z. Yang, and X.-T. Zu, "Holographic research on phase transitions for a five dimensional AdS black hole with conformally coupled scalar hair," *Physics Letters, Section B: Nuclear, Elementary Particle and High-Energy Physics*, vol. 764, pp. 310–317, 2017.

[32] M. Cadoni, E. Franzin, and M. Tuveri, "Van der Waals-like behaviour of charged black holes and hysteresis in the dual QFTs," *Physics Letters. B. Particle Physics, Nuclear Physics and Cosmology*, vol. 768, pp. 393–396, 2017.

[33] B. P. Abbott et al., "Observation of gravitational waves from a binary black hole merger," *Physical Review Letters*, vol. 116, Article ID 061102, 2016.

[34] M. Fierz and W. Pauli, "On relativistic wave equations for particles of arbitrary spin in an electromagnetic field," *Proceedings of the Royal Society of London Series A: Mathematical and Physical Sciences*, vol. 173, no. 953, pp. 211–232, 1939.

[35] D. G. Boulware and S. Deser, "Can gravitation have a finite range?" *Physical Review D*, vol. 6, no. 12, pp. 3368–3382, 1972.

[36] C. de Rham and G. Gabadadze, "Generalization of the Fierz-Pauli action," *Physical Review D*, vol. 82, Article ID 044020, 2010.

[37] C. De Rham, G. Gabadadze, and A. J. Tolley, "Resummation of massive gravity," *Physical Review Letters*, vol. 106, no. 23, Article ID 231101, 2011.

[38] D. Vegh, "Holography without translational symmetry," 2013, https://arxiv.org/abs/1301.0537.

[39] C. de Rham, "Massive gravity," *Living Reviews in Relativity*, vol. 17, no. 7, 2014.

[40] K. Hinterbichler, "Theoretical aspects of massive gravity," *Reviews of Modern Physics*, vol. 84, no. 2, 2012.

[41] S. L. Dubovsky, "Phases of massive gravity," *Journal of High Energy Physics*, article 076, 2004.

[42] V. A. Rubakov and P. G. Tinyakov, "Infrared-modified gravities and massive gravitons," *Physics-Uspekhi*, vol. 51, no. 8, pp. 759–792, 2008.

[43] M. V. Bebronne and P. G. Tinyakov, "Black hole solutions in massive gravity," *Journal of High Energy Physics*, vol. 09, no. 04, article 100, 2008.

[44] D. Comelli, F. Nesti, and L. Pilo, "Stars and (furry) black holes in Lorentz breaking massive gravity," *Physical Review D - Particles, Fields, Gravitation and Cosmology*, vol. 83, no. 8, Article ID 084042, 2011.

[45] S. Fernando, "Phase transitions of black holes in massive gravity," *Modern Physics Letters A. Particles and Fields, Gravitation, Cosmology, Nuclear Physics*, vol. 31, no. 16, Article ID 1650096, 1650096, 19 pages, 2016.

[46] F. Capela and G. Nardini, "Hairy black holes in massive gravity: thermodynamics and phase structure," *Physical Review D*, vol. 86, no. 2, Article ID 024030, 12 pages, 2012.

[47] B. Mirza and Z. Sherkatghanad, "Phase transitions of hairy black holes in massive gravity and thermodynamic behavior of charged AdS black holes in an extended phase space," *Physical Review D*, vol. 90, no. 8, Article ID 084006, 2014.

[48] S. Fernando, "P-V criticality in AdS black holes of massive gravity," *Physical Review D*, vol. 94, no. 12, Article ID 124049, 2016.

[49] S. W. Hawking and D. N. Page, "Thermodynamics of black holes in anti-de Sitter space," *Communications in Mathematical Physics*, vol. 87, no. 4, pp. 577–588, 1982/83.

Hindawi
Advances in High Energy Physics
Volume 2017, Article ID 2356174, 8 pages
https://doi.org/10.1155/2017/2356174

Research Article

Holographic van der Waals Phase Transition for a Hairy Black Hole

Xiao-Xiong Zeng[1,2] and Yi-Wen Han[3]

[1]*School of Material Science and Engineering, Chongqing Jiaotong University, Chongqing 400074, China*
[2]*State Key Laboratory of Theoretical Physics, Institute of Theoretical Physics, Chinese Academy of Sciences, Beijing 100190, China*
[3]*School of Computer Science and Information Engineering, Chongqing Technology and Business University, Chongqing 400070, China*

Correspondence should be addressed to Xiao-Xiong Zeng; xxzengphysics@163.com

Received 2 March 2017; Accepted 29 May 2017; Published 12 July 2017

Academic Editor: Bum-Hoon Lee

Copyright © 2017 Xiao-Xiong Zeng and Yi-Wen Han. This is an open access article distributed under the Creative Commons Attribution License, which permits unrestricted use, distribution, and reproduction in any medium, provided the original work is properly cited. The publication of this article was funded by SCOAP[3].

The van der Waals (VdW) phase transition in a hairy black hole is investigated by analogizing its charge, temperature, and entropy as the temperature, pressure, and volume in the fluid, respectively. The two-point correlation function (TCF), which is dual to the geodesic length, is employed to probe this phase transition. We find the phase structure in the temperature-thermal entropy plane besides the scale of the horizontal coordinate (geodesic length plane resembles that in the temperature). In addition, we find the equal area law (EAL) for the first-order phase transition and critical exponent of the heat capacity for the second-order phase transition in the temperature-thermal entropy plane (geodesic length plane is consistent with that in temperature), which implies that the TCF is a good probe to probe the phase structure of the back hole.

1. Introduction

Phase transition of the black holes is always a hot topic in theoretical physics for it provides a platform to relate the gravity, thermodynamics, and quantum theory. Phase transition in AdS space is more fascinated owing to the AdS/CFT correspondence. The Hawking-Page phase transition [1], which portrays the transition of thermal gas to the Schwarzschild black hole, can be used to describe the confinement to deconfinement transition of the quark-gluon plasma in Yang-Mills theory [2]. The phase transition of a scalar field condensation around charged AdS black holes can be used to describe the superconductor transition [3–5]. In particular, one often can use the nonlocal observables such as holographic entanglement entropy, Wilson loop, and TCF to probe these phase transitions [6, 7].

VdW phase transition is another important property of the charged AdS black hole. It was observed that a charged black hole will undergo a first-order phase transition and a second-order phase transition successively as the charge of the black hole increases from small to large, which is analogous to the van der Waals liquid-gas phase transition [8]. This phase transition was perfected recently by regarding the cosmological constant as the pressure for in this case we need not any analogy [9, 10].

Whether the VdW phase transition of the charged black hole can be probed by the nonlocal observables thus is worth exploring. Recently, Chamblin et al. [11] investigated the VdW phase transition of the Reissner-Nordström AdS black hole from the viewpoint of holography and found that the phase structure in the temperature-entanglement entropy plane resembles that in temperature-thermal entropy plane. Thereafter Nguyen [12] investigated exclusively the EAL in the temperature-entanglement entropy plane and found that the EAL holds regardless of the size of the entangling region. Now there have been some extensive studies [13–19] and all the results show that, in the case of thermal entropy, the entanglement entropy exhibits the similar VdW phase transition.

In this paper, we are going to use the equal time TCF to probe the phase structure of the hairy black holes. It has been shown that the TCF has the same effect as that of the holographic entanglement entropy as it was used to probe the thermalization behavior [20–33]; thus, it will be interesting to explore whether this observable can probe the phase structures of the black holes. The hairy AdS black hole is a solution of Einstein-Maxwell-Λ theory conformally coupled to a scalar field [34]. This model has at least two advantages. One is that it is an ordinary and tractable model for studying superconducting phase transition with consideration of the back-reaction of the scalar field. Another is that it exhibits more fruitful phase transition behavior, namely, not only the VdW behavior in both the charged and uncharged cases, but also reentrant phase transition in the charged case [35]. In this paper, we mainly concentrate on the VdW phase transition behavior. Beside the thermal entropy-temperature plane, we will also study the EAL and critical exponent of the heat capacity in the geodesic length-temperature plane. We find that the results obtained in both frameworks are consistent.

Our paper is outlined as follows. In Section 1, we present the hairy AdS black hole solution and study the VdW phase transition in the thermal entropy-temperature plane. In Section 2, we employ the TCF to probe the VdW phase transition. In particular, we study the EAL and critical exponent of the heat capacity in the framework of holography and find that the result is similar as that obtained in the thermal entropy-temperature plane. The conclusion and discussion are presented in Section 3. Hereafter in this paper we use natural units ($G = c = \hbar = 1$) for simplicity.

2. Thermodynamic Phase Transition of the Hairy Black Hole

The five-dimensional hairy black hole solution can be written as [34]

$$ds^2 = -f(r)\,dt^2 + \frac{dr^2}{f(r)} + r^2\left[d\theta^2 + \sin^2\theta\left(d\phi^2 + \sin^2\theta d\psi^2\right)\right], \tag{1}$$

in which

$$f(r) = \frac{e^2}{r^4} + \frac{r^2}{l^2} - \frac{m}{r^2} - \frac{q}{r^3} + 1, \tag{2}$$

where e is the electric charge, m is the mass parameter, l is the AdS radius that relates to the cosmology constant Λ, and q is related to the coupling constants of the conformal field b_0, b_1, and b_2. For the planar solution, $q = 0$, while for the spherical symmetric black hole, q can be expressed as

$$q = \frac{64\pi}{5}\varepsilon b_1\left(\frac{-18b_1}{5b_0}\right)^{3/2}, \tag{3}$$

in which ε takes the values -1, 0, and 1. In addition, to satisfy the field equations, the scalar coupling constants should obey the constraint

$$100 b_0 b_2 = 9 b_1^2. \tag{4}$$

As stressed in [34, 35], the hair parameter q is not a conserved charge corresponding to some symmetry; it is a variable provided that the scalar field coupling constants are dynamic. In this paper, we will fix q to investigate the phase structure of this black hole for q has little effect on the phase structure.

The black hole event horizon r_h is the largest root of the equation $f(r_h) = 0$. At the event horizon, the Hawking temperature can be expressed as

$$T = \frac{-2e^2l^2 + l^2 r_h\left(q + 2r_h^3\right) + 4r_h^6}{4\pi l^2 r_h^5}, \tag{5}$$

in which we have used the relation

$$m = \frac{e^2l^2 - l^2 q r_h + l^2 r_h^4 + r_h^6}{l^2 r_h^2}. \tag{6}$$

In terms of the AdS/CFT correspondence, the temperature in (5) can be treated as the temperature of the dual conformal field theory. The Maxwell potential in this background is given by

$$A_t = \frac{\sqrt{3e}}{r_h^2}. \tag{7}$$

The entropy of the black hole is

$$S = \frac{\pi^2 r_h^3}{2} - \frac{5\pi^2 q}{4}. \tag{8}$$

Substituting (8) into (5), we can get the following relation:

$$T = \frac{-2\pi^4e^2l^2 + 3\ 2^{2/3}\pi^{10/3}l^2q\sqrt[3]{5\pi^2q + 4S} + 2\ 2^{2/3}\pi^{4/3}l^2S\sqrt[3]{5\pi^2q + 4S} + 25\pi^4q^2 + 40\pi^2qS + 16S^2}{\sqrt[3]{2}l^2\left(5\pi^3q + 4\pi S\right)^{5/3}}. \tag{9}$$

Next, we will employ this equation to study the phase structure of the hairy black hole. The Helmholtz free energy of this system is given by [34]

$$F = M - TS$$

$$= -\frac{5\pi e^2 q}{8r_h^5} + \frac{5\pi e^2}{8r_h^2} + \frac{5\pi q r_h}{4l^2} - \frac{\pi r_h^4}{8l^2} + \frac{5\pi q^2}{16r_h^4} + \frac{\pi q}{8r_h} + \frac{\pi r_h^2}{8}, \tag{10}$$

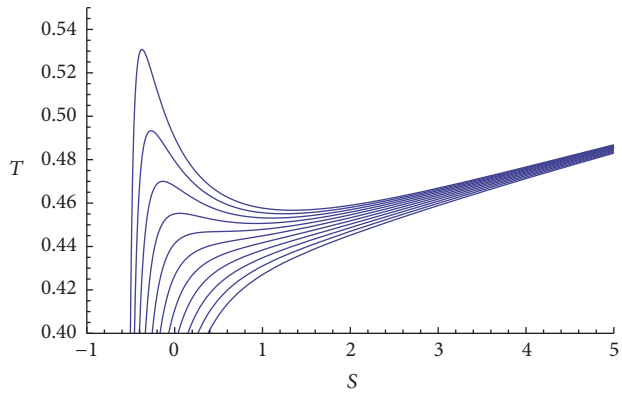

Figure 1: Relations between temperature and thermal entropy for different e with $q = 0.05$; curves from top to down correspond to cases e varying from 0.1 to 0.2 with step 0.01.

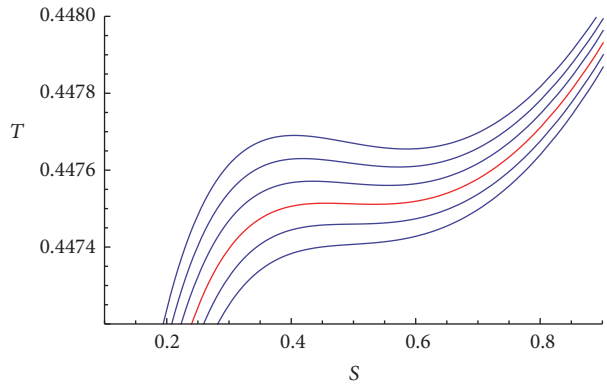

Figure 2: Relations between temperature and thermal entropy for different e with $q = 0.05$; curves from top to down correspond to cases e varying from 0.1385 to 0.139 with step 0.0001.

in which $M = 3\pi m/8G$, where G is the gravitational constant.

Now we concentrate on studying the phase structure of the hairy AdS black holes. In fluid, the VdW phase transition is depicted in the P-V plane, where P, V correspond to pressure and volume of fluid. In black holes, there are two schemes to produce the VdW phase transition. One is presented in [9, 10] where the cosmology constant and curvature are treated as pressure and volume. The other is presented in [8] in which one should adopt analogy shown in Table 1.

In this paper, we will follow the later scheme. In this case, the phase structure depends on the charge of the black hole, and we know that there is a critical charge, for which the temperature satisfies the following relation:

$$\left(\frac{\partial T}{\partial S}\right)_e = \left(\frac{\partial^2 T}{\partial S^2}\right)_e = 0. \tag{11}$$

In this paper, we will get the critical charge numerically. We will set $l = 1$. We first plot a bunch of curves by taking different values of e in the T-S plane in Figure 1. From this figure, we can read off the rough critical value of the charge which satisfies the condition $(\partial T/\partial S)_e = 0$. Having obtained this rough value, we plot several curves in the T-S plane further with smaller step so that we can get the probable critical value of e. From Figure 2, we find that the probable critical value is 0.1388, which is labeled by the red solid line. Finally, we adjust the value of e by hand to find the exact value of e that satisfies $(\partial T/\partial S)_e = 0$, which produces $e_c = 0.13888$. With this critical value and (11), we can get the critical entropy $S_c = 0.533926$. Having obtained the critical charge and critical entropy, the critical temperature and critical free energy also can be produced by relations (9) and (10) directly.

Table 1

Analogy	
Fluid	AdS black hole
Temperature, T	Charge, e
Pressure, P	Temperature, $T(S, e)$
Volume, V	Entropy, S

As the critical charge e is given, we can set different charges to show the VdW phase transition in the T-S plane, which is shown in Figure 3. From this figure, we know that as the value of the charge is smaller than the critical charge, a small black hole, large black hole, and an intermediate black hole coexist. There is a critical temperature, labeled as T_1. For

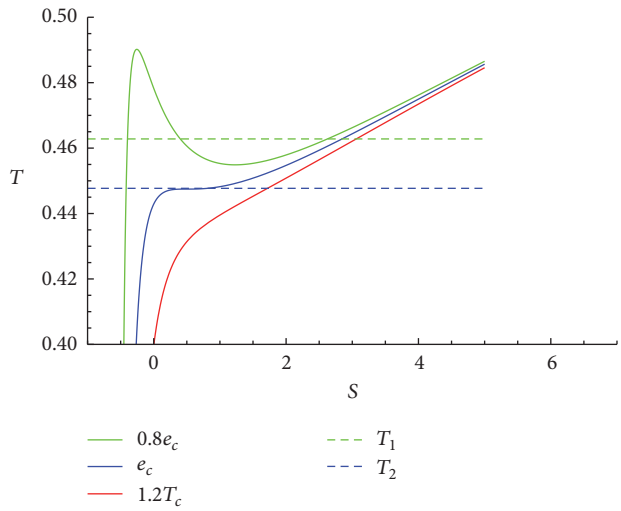

FIGURE 3: Relations between temperature and thermal entropy for different e with $q = 0.05$.

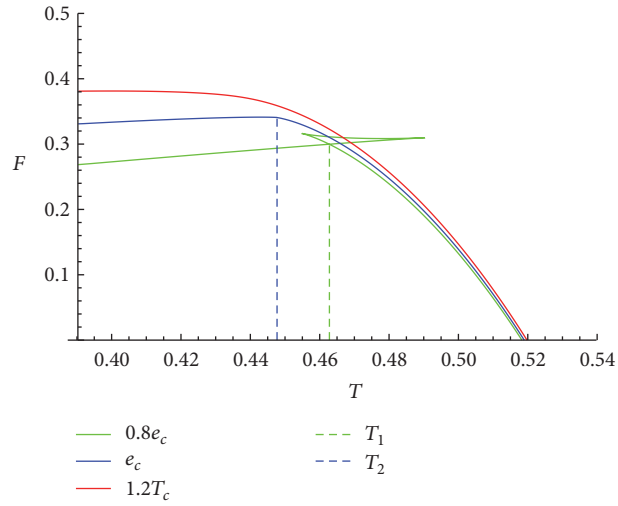

FIGURE 4: The F-T relation for different e with $q = 0.05$.

the case $T < T_1$, the small black hole dominates while for the case $T > T_1$, the large black hole dominates. The phase transition for the small black hole to the large black hole is first order. For the case $e = e_c$, we find that the unstable region vanishes and an inflection point emerges. The heat capacity in this case is divergent, which implies that the phase transition is second order, and the corresponding phase transition temperature is labeled as T_2. For the case $e > e_c$, the black hole is stable always.

The phase structures can also be observed in the F-T plane. From the green curve of Figure 4, we know that the swallowtail structure corresponds to the unstable phase in the top curve of Figure 3. The value of the first-order phase transition temperature, $T_1 = 0.4628$, can be read off from the horizontal coordinate of the junction. From the blue curve of Figure 4, we also can read off the second-order phase transition temperature $T_2 = 0.4477$.

The first-order phase transition temperature T_1 also can be obtained from the EAL:

$$A_L \equiv \int_{S_1}^{S_3} T(S, e)\, dS = T_1 (S_3 - S_1) \equiv A_R, \tag{12}$$

in which $T(S, e)$ is the analytical function in (9) and S_1 and S_3 are the smallest and largest roots of the equation $T(S, e) = T_1$. On the contrary, as T_1 is given, we can use it to check the EAL numerically. In fact, this relation holds always in thermodynamics. We give the numerical check here in order to compare with the result which will be produced in the framework of holography in the next section.

For the case $q = 0.05$, we know that $T_1 = 0.4628$, $S_1 = 0.40247$, and $S_3 = 2.62429$. Substituting these values into (12), we find $A_L = 1.01677$, $A_R = 1.02826$. It is obvious that A_L and A_R are equal nearly, which implies that the EAL holds in the T-S plane within our numerical accuracy.

For the second-order phase transition, we know that near the critical temperature T_2, there is always a relation [11]

$$\log|T - T_2| = 3\log|S - S_c| + \text{constant}, \tag{13}$$

in which S_c is the critical entropy corresponding to the critical temperature T_2. With the definition of the heat capacity,

$$C_e = T\left.\frac{\partial S}{\partial T}\right|_e. \tag{14}$$

One can get further that $C_e \sim (T-T_2)^{-2/3}$; namely, the critical exponent is $-2/3$ [11]. Next, we will check whether there is a similar linear relation and critical exponent in the framework of holography.

3. Probe the Phase Transition with Two-Point Correlation Function

Having obtained the thermodynamic phase structure of the hairy black hole, we will check whether this property can be probed by the TCF. In terms of the AdS/CFT correspondence, we know that, for the case that the conformal weight Δ is large, the equal time two-point function of operators $\mathcal{O}$ can be computed by the length of space-like geodesics in the bulk geometry; that is [36],

$$\left\langle \mathcal{O}(t, x_i)\, \mathcal{O}\left(t, x_j\right)\right\rangle \approx e^{-\Delta \mathrm{L}}, \tag{15}$$

in which L is the length of the bulk geodesic connecting two points (t, x_i) and (t, x_j) on the AdS boundary. For the spherically symmetric black hole, we will choose $(\phi = \pi/2, \theta = 0, \psi = 0)$ and $(\phi = \pi/2, \theta = \theta_0, \psi = \pi)$ as the two boundary points. Then with θ to parameterize the trajectory, the proper length can be written as

$$\mathrm{L} = \int_0^{\theta_0} \sqrt{\frac{r'^2}{f(r)} + r^2}\, d\theta, \tag{16}$$

in which $r' = dr/d\theta$. Treating the integral as a Lagrangian, we can get the motion equation of r; namely,

$$\begin{aligned}&\frac{1}{2} r(\theta)\, r'(\theta)^2\, g'(r(\theta)) - r(\theta)\, g(r(\theta))\, r''(\theta)\\ &\quad + 2g(r(\theta))\, r'(\theta)^2 + r(\theta)^2\, g(r(\theta))^2 = 0.\end{aligned} \tag{17}$$

With the boundary conditions

$$\begin{aligned} r'(0) &= 0,\\ r(0) &= r_0,\end{aligned} \tag{18}$$

we can get the numeric result of $r(\theta)$ and further get L by substituting $r(\theta)$ into (16). As in [11], we are interested in the regularized geodesic length as $\delta L \equiv \mathrm{L} - \mathrm{L}_0$, in which L_0 is the geodesic length in pure AdS. As the value of δL is given, we can get the relation between δL and T for different charge e. In this paper, we will also explore whether this relation is θ_0 independent. Without loss of the generality, we choose $\theta_0 = 0.1, 0.2$ and set the corresponding UV cutoff in the dual field theory to be $r(0.099)$, $r(0.199)$, respectively. The corresponding pictures are shown in Figure 3. It is obvious that both Figures 5 and 6 resemble Figure 3 besides the scale of horizontal coordinate, which implies that the geodesic length owns the same phase structure as that of the thermal entropy. To confirm this conclusion, we will check the EAL for the first-order phase transition and critical exponent for the second-order phase transition in the T-δL plane.

The EAL in the T-δL plane can be defined as

$$\begin{aligned} A_L &\equiv \int_{\delta L_{\min}}^{\delta L_{\max}} T(\delta L, e)\, d\delta L = T_1\left(\delta L_{\max} - \delta L_{\min}\right)\\ &\equiv A_R,\end{aligned} \tag{19}$$

in which $(\delta L, e)$ is an interpolating function obtained from the numeric data, and $\delta L_{\min}, \delta L_{\max}$ are the smallest and largest values of the equation $T(\delta L, e) = T_1$. For different θ_0, the calculated results are listed in Table 2. From this table, we can see that, for the unstable region of the first-order phase transition in the T-δL plane, the EAL holds within our numeric accuracy. This conclusion is independent of the boundary separation θ_0.

We also can investigate the critical exponent of the heat capacity for the second-order phase transition in the T-δL plane by defining an analogous heat capacity

$$C = T\frac{\partial \delta L}{\partial T}. \tag{20}$$

Provided a similar relation as shown in (13) is satisfied, one can get the critical exponent of the analogous heat capacity immediately.

So next, we are interested in the relation between $\log|T - T_2|$ and $\log|\delta L - \delta L_c|$, in which δL_c is the solution that satisfies the relation $T(\delta L, e) = T_2$. For different θ_0, the numeric results are shown in Figure 7. By data fitting, the straight lines in Figure 7 can be fitted as

$$\log|T - T_2| = \begin{cases} 28.2901 + 3.05999\log|\delta L - \delta L_c|, & \text{for } q = 0.05, e = e_c, \theta_0 = 0.1,\\ 19.3767 + 3.07505\log|\delta L - \delta L_c|, & \text{for } q = 0.05, e = e_c, \theta_0 = 0.2.\end{cases} \tag{21}$$

Obviously, for all the lines, the slope is about 3, which resembles that in (13). That is, the critical exponent of the analogous heat capacity in T-δL plane is the same as that in the T-S plane, which confirms the conclusion that

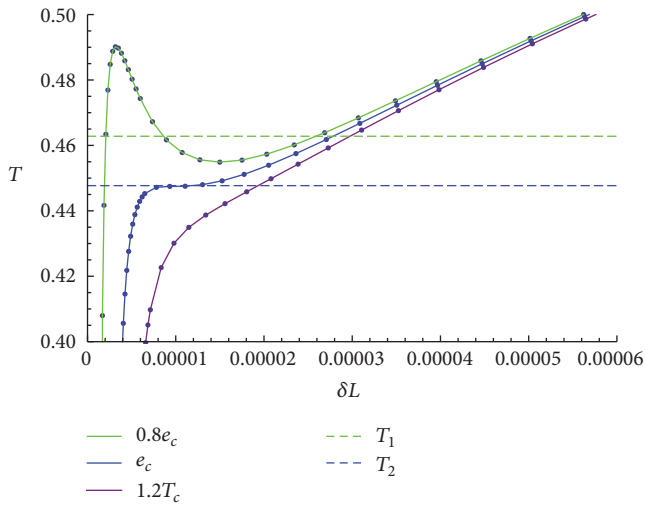

Figure 5: Relations between geodesic length and temperature for different e with $q = 0.05$, $\theta_0 = 0.1$.

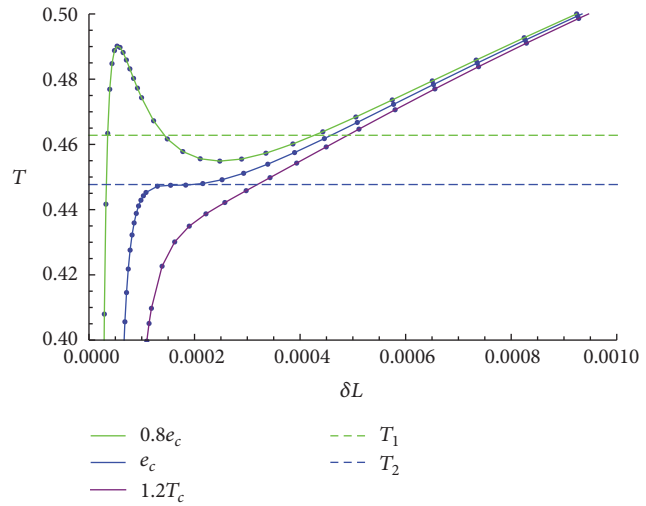

Figure 6: Relations between geodesic length and temperature for different e with $q = 0.05$, $\theta_0 = 0.2$.

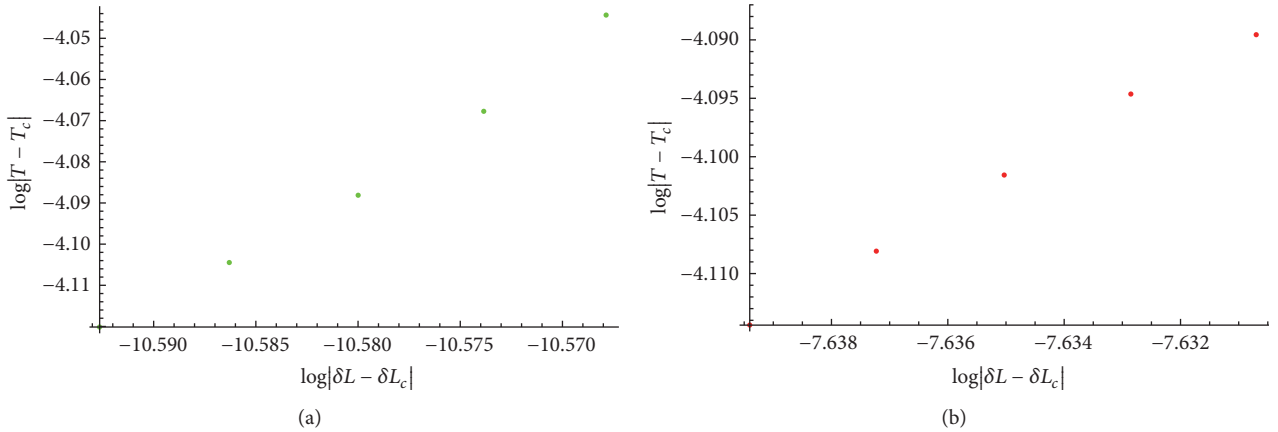

Figure 7: Relations between $\log|T - T_2|$ and $\log|\delta L - \delta L_c|$ for the case $q = 0.05, e = e_c$. (a) corresponds to the case $\theta_0 = 0.1$ while (b) corresponds to $\theta_0 = 0.2$.

Table 2: EAL in the T-δL plane; here relative error = $(A_L - A_R)/A_R$.

Boundary size	T_1	$\delta L_{\min}$	$\delta L_{\max}$	A_L	A_R	Relative error
$\theta_0 = 0.1$	0.4628	0.0000014	0.0000259	0.0000111	0.0000113	1.8869%
$\theta_0 = 0.2$	0.4628	0.0000354	0.0004267	0.0001812	0.0001811	0.4549%

the TCF can probe the phase structure of the hairy black hole.

4. Conclusion and Discussion

As the usual charged black hole, we find that the hairy black hole also exhibits the VdW phase transition. That is, the phase structure of the hairy black hole depends on the charge of the spacetime. For the case where the charge is smaller than the critical charge, the small black hole, immediate black hole, and large black hole coexist. The small black hole will transit to the large black hole as the temperature reaches the critical temperature T_1. The order of this phase transition is first for the nonsmoothness of the free energy in the F-T plane. As the charge equals the critical charge, the immediate black hole vanishes and the order for the small black hole transit to the large black hole is second for the heat capacity is divergent in this case. We also check the EAL numerically for the first-order phase transition and get the critical exponent of the heat capacity for the second-order phase transition.

With the TCF, we also probe the phase structure of the black hole. For the TCF in the field theory is dual to the geodesic length in the bulk, we thus employ the geodesic length to probe the phase structure of the hairy black hole. We find that the phase structure in the T-δL plane resembles that in the T-S plane, regardless of the size of the boundary separation. In addition, we find in the framework of holography that the EAL still holds and the critical exponent of the analogous heat capacity is the same as that in the usual thermodynamic system.

In this paper, we fix the parameter $q = 0.05$ to investigate the phase structure of the black hole. For other values of q, we find that the phase structure is similar as the case $q = 0.05$. To avoid encumbrance, we will not list these values. In addition, we employ the analogy in Table 1 to study the VdW phase transition. In fact, as the cosmological constant is treated as a thermodynamic pressure, P, and its conjugate quantity as a thermodynamic volume, V, the VdW phase transition also can be constructed in the P-V plane [13]. In [35], the holography entanglement entropy has been used to probe the phase structure in this case. For the hairy black hole, the TCF also can be used to probe its phase structure in the P-V plane.

Conflicts of Interest

The authors declare that they have no conflicts of interest.

Acknowledgments

This work is supported by the National Natural Science Foundation of China (Grant no. 11405016), China Postdoctoral Science Foundation (Grant no. 2016M590138), Natural Science Foundation of Education Committee of Chongqing (Grant no. KJ1500530), and Basic Research Project of Science and Technology Committee of Chongqing (Grant no. cstc2016jcyja0364).

References

[1] S. W. Hawking and D. N. Page, "Thermodynamics of black holes in anti-de Sitter space," *Communications in Mathematical Physics*, vol. 87, no. 4, pp. 577–588, 1982/83.

[2] E. Witten, "Anti-de Sitter space, thermal phase transition and confinement in gauge theories," *International Journal of Modern Physics A. Particles and Fields. Gravitation. Cosmology*, vol. 16, no. 16, pp. 2747–2769, 2001.

[3] S. A. Hartnoll, C. P. Herzog, and G. T. Horowitz, "Building a holographic superconductor," *Physical Review Letters*, vol. 101, no. 3, Article ID 031601, 2008.

[4] X. X. Zeng, M. X. Liu, and W. B. Liu, "Analytic treatment on stimulated holographic superconductors," *Int J Mod Phys A*, vol. 27, Article ID 1250010, 2012.

[5] R. Cai, L. Li, L. Li, and R. Yang, "Introduction to holographic superconductor models," *Science China Physics, Mechanics & Astronomy*, vol. 58, no. 6, pp. 1–46, 2015.

[6] R.-G. Cai, S. He, L. Li, and Y.-L. Zhang, "Holographic entanglement entropy in P-wave superconductor phase transition," *Journal of High Energy Physics*, vol. 2012, no. 7, article no. 027, 2012.

[7] S. N. Solodukhin, "Entanglement entropy of black holes," *Living Reviews in Relativity*, vol. 14, article 8, 2011.

[8] C. V. Johnson, "Large N phase transitions, finite volume, and entanglement entropy," *Journal of High Energy Physics*, vol. 2014, article 47, 2014.

[9] D. Kastor, S. Ray, and J. Traschen, "Enthalpy and the mechanics of AdS black holes," *Classical and Quantum Gravity*, vol. 26, no. 19, Article ID 195011, 195011, 16 pages, 2009.

[10] D. Kubiznak and R. B. Mann, "$P - V$ criticality of charged AdS black holes," *Journal of High Energy Physics*, vol. 1207, article 33, 2012.

[11] A. Chamblin, R. Emparan, C. V. Johnson, and R. C. Myers, "Charged AdS black holes and catastrophic holography," *Physical Review. D. Third Series*, vol. 60, no. 6, 064018, 17 pages, 1999.

[12] P. H. Nguyen, "An equal area law for the van der Waals transition of holographic entanglement entropy," *Journal of High Energy Physics*, vol. 12, article 139, 2015.

[13] E. Caceres, P. H. Nguyen, and J. F. Pedraza, "Holographic entanglement entropy and the extended phase structure of STU black holes," *Journal of High Energy Physics*, vol. 2015, no. 9, article no. 184, 2015.

[14] X.-X. Zeng, H. Zhang, and L.-F. Li, "Phase transition of holographic entanglement entropy in massive gravity," *Physics Letters, Section B: Nuclear, Elementary Particle and High-Energy Physics*, vol. 756, pp. 170–179, 2016.

[15] X.-X. Zeng and L.-F. Li, "Holographic Phase Transition Probed by Nonlocal Observables," *Advances in High Energy Physics*, vol. 2016, Article ID 6153435, 2016.

[16] S. He, L. F. Li, and X. X. Zeng, "Holographic van der waals-like phase transition in the Gauss–Bonnet gravity," *Nuclear Physics B*, vol. 915, pp. 243–261, 2017.

[17] A. Dey, S. Mahapatra, and T. Sarkar, "Thermodynamics and entanglement entropy with Weyl corrections," *Physical Review D - Particles, Fields, Gravitation and Cosmology*, vol. 94, no. 2, Article ID 026006, 2016.

[18] X. X. Zeng and L. F. Li, "Van der waals phase transition in the framework of holography," *Physics Letters B*, vol. 764, pp. 100–108, 2017.

[19] J.-X. Mo, G.-Q. Li, Z.-T. Lin, and X.-X. Zeng, "Revisiting van der Waals like behavior of $f(R)$ AdS black holes via the two point correlation function," *Nuclear Physics. B. Theoretical, Phenomenological, and Experimental High Energy Physics. Quantum Field Theory and Statistical Systems*, vol. 918, pp. 11–22, 2017.

[20] V. Balasubramanian, A. Bernamonti, J. de Boer et al., "Inhomogeneous thermalization in strongly coupled field theories," *Physical Review Letters*, vol. 106, article 191601, 2011.

[21] V. Balasubramanian, A. Bernamonti, and J. de Boer, "Holographic thermalization," *Physical Review D*, vol. 84, article 026010, no. 2, Article ID 026010, 2011.

[22] D. Galante and M. Schvellinger, "Thermalization with a chemical potential from AdS spaces," *Journal of High Energy Physics*, vol. 2012, no. 7, article no. 096, 2012.

[23] E. Caceres and A. Kundu, "Holographic thermalization with chemical potential," *Journal of High Energy Physics*, vol. 2012, article 55, 2012.

[24] X.-X. Zeng and W.-B. Liu, "Holographic thermalization in Gauss-Bonnet gravity," *Physics Letters. B. Particle Physics, Nuclear Physics and Cosmology*, vol. 726, no. 1-3, pp. 481–487, 2013.

[25] X.-X. Zeng, X.-M. Liu, and W.-B. Liu, "Holographic thermalization with a chemical potential in Gauss-Bonnet gravity," *Journal of High Energy Physics*, vol. 2014, no. 3, article no. 031, 2014.

[26] X. X. Zeng, D. Y. Chen, and L. F. Li, "Holographic thermalization and gravitational collapse in a spacetime dominated by quintessence dark energy," *Physical Review D*, vol. 91, no. 4, Article ID 046005, 2015.

[27] X.-X. Zeng, X.-M. Liu, and W.-B. Liu, "Holographic thermalization in noncommutative geometry," *Physics Letters. B. Particle Physics, Nuclear Physics and Cosmology*, vol. 744, pp. 48–54, 2015.

[28] X. X. Zeng, X. Y. Hu, and L. F. Li, "Effect of phantom dark energy on holographic thermalization," *Chinese Physics Letters*, vol. 34, article 010401, no. 1, 2017.

[29] Y. P. Hu, X. X. Zeng, and H. Q. Zhang, "Holographic thermalization and generalized vaidya-ads solutions in massive gravity," *Physics Letters B*, vol. 765, pp. 120–126, 2017.

[30] H. Liu and S. J. Suh, "Entanglement tsunami: Universal scaling in holographic thermalization," *Physical Review Letters*, vol. 112, no. 1, Article ID 011601, 2014.

[31] S.-J. Zhang and E. Abdalla, "Holographic thermalization in charged dilaton anti–de Sitter spacetime," *Nuclear Physics. B. Theoretical, Phenomenological, and Experimental High Energy Physics. Quantum Field Theory and Statistical Systems*, vol. 896, pp. 569–586, 2015.

[32] A. Buchel, Myers R. C., and Niekerk A. v., "Nonlocal probes of thermalization in holographic quenches with spectral methods," *Journal of High Energy Physics*, vol. 02, article 017, 2015.

[33] B. Craps, E. Kiritsis, C. Rosen, A. Taliotis, J. Vanhoof, and H. Zhang, "Gravitational collapse and thermalization in the hard wall model," *Journal of High Energy Physics*, vol. 2014, no. 2, article no. 120, 2014.

[34] M. Galante, G. Giribet, A. Goya, and J. Oliva, "Chemical potential driven phase transition of black holes in anti-de Sitter space," *Physical Review D - Particles, Fields, Gravitation and Cosmology*, vol. 92, no. 10, Article ID 104039, 2015.

[35] R. A. Hennigar and R. B. Mann, "Reentrant phase transitions and van derwaals behaviour for hairy black holes," *Entropy*, vol. 17, no. 12, pp. 8056–8072, 2015.

[36] V. Balasubramanian and S. F. Ross, "Holographic particle detection," *Physical Review D*, vol. 61, no. 4, Article ID 044007, 2000.

Hindawi
Advances in High Energy Physics
Volume 2017, Article ID 8910210, 6 pages
https://doi.org/10.1155/2017/8910210

Research Article

Entropic Destruction of Heavy Quarkonium from a Deformed AdS_5 Model

Zi-qiang Zhang,[1] Zhong-jie Luo,[1] De-fu Hou,[2] and Gang Chen[1]

[1]*School of Mathematics and Physics, China University of Geosciences, Wuhan 430074, China*
[2]*Key Laboratory of Quark and Lepton Physics (MOE), Central China Normal University, Wuhan 430079, China*

Correspondence should be addressed to Zi-qiang Zhang; zhangzq@cug.edu.cn

Received 11 February 2017; Accepted 9 April 2017; Published 30 April 2017

Academic Editor: Song He

Copyright © 2017 Zi-qiang Zhang et al. This is an open access article distributed under the Creative Commons Attribution License, which permits unrestricted use, distribution, and reproduction in any medium, provided the original work is properly cited. The publication of this article was funded by SCOAP[3].

We study the destruction of heavy quarkonium due to the entropic force in a deformed AdS_5 model. The effects of the deformation parameter on the interdistance and the entropic force are investigated. The influence of the deformation parameter on the quarkonium dissociation is analyzed. It is shown that the interdistance increases in the presence of the deformation parameter. In addition, the deformation parameter has the effect of decreasing the entropic force. These results imply that the quarkonium dissociates harder in a deformed AdS background than in a usual AdS background, in agreement with earlier findings.

1. Introduction

It is well-known that the dissociation of heavy quarkonium can be regarded as an important experimental signal of the formation of strongly coupled quark-gluon plasma (QGP) [1]. It was argued earlier that the quarkonium suppression is due to the Debye screening effects induced by the high density of color charges in QGP. But the recent experimental research showed a puzzle: the charmonium suppression at RHIC (lower energy density) is stronger than that at LHC (larger energy density) [2, 3]. Obviously, this is in contradiction to the Debye screening scenario [1] as well as the thermal activation through the impact of gluons [4, 5]. To explain this puzzle, some authors suggested that the recombination of the produced charm quarks into charmonia may be a solution. This argument was based on the results [6, 7] that if a region of deconfined quarks and gluons is formed, the quarkonia (or bound states) can be formed from a quark and an antiquark which were originally produced in separate incoherent interactions. Recently, Kharzeev [8] argued that this puzzle may be related to the nature of deconfinement and the entropic force would be responsible for melting the quarkonium. This argument originated from the Lattice results that a large amount of entropy associated with the heavy quarkonium placed in QGP [9–11].

AdS/CFT, which maps a d-dimensional quantum field theory to its dual gravitational theory, living in $d + 1$-dimensional, has yielded many important insights into the dynamics of strongly coupled gauge theories [12–14]. In this approach, Hashimoto and Kharzeev have studied the entropic destruction of static heavy quarkonium in $\mathcal{N} = 4$ SYM theory and a confining YM theory firstly. They found that in both cases the entropy grows as a function of the interquark distance giving rise to the entropic force [15]. Recently, these studies have been extended to the case of moving quarkonium [16]. It was shown that the velocity has the effect of increasing the entropic force, thus making the quarkonium melt easier. In a more recent work, we have analyzed the effect of chemical potential on the entropic force and observed that the moving quarkonium dissociates easier at finite density [17].

Now, we would like to give such analyses from AdS/QCD. The motivation is that AdS/QCD models can provide a nice phenomenological description of hadronic properties as well as quark-antiquark interaction; see [18–26] and references therein. In this paper, we will study the entropic force in the Andreev-Zakharov model [21], one of "soft wall" models. The Andreev-Zakharov model has some properties: (1) the positive quadratic term modification in the deformed warp factor $h(z) = e^{(1/2)cz^2}$ produces linear behavior of heavy

flavor potential; namely, it can provide confinement at low temperature. (2) The value of c can be fixed from the ρ meson trajectory, so that the metric contains no free parameter. Actually, this model has been used to investigate some quantities, such as thermal phase transition [27], thermal width [28, 29], and heavy quark potential [30]. Likewise, it is of interest to study the entropic force in this model. Besides that, we have several other reasons: first, we want to know what will happen if we have meson in a deformed AdS background or how the deformation parameter affects the quarkonium dissociation? Moreover, evaluation of the entropic force helps us to understand the "usual" or "unusual" behavior of meson, because one can compare the results of $c \neq 0$ with $c = 0$, while the "usual" behavior of meson can be recovered in the limit $c \to 0$. On the other hand, such an investigation can be regarded as a good test of AdS/QCD.

The paper is organized as follows. In the next section, we briefly review the action of holographic models and then introduce the Andreev-Zakharov model. In Section 3, we study the effects of the deformation parameter on the inter-distance as well as the entropic force and then analyze how the deformation parameter affects the quarkonium dissociation. The last part is devoted to discussion and conclusion.

2. The Andreev-Zakharov Model

Before reviewing the Andreev-Zakharov model, let us briefly introduce the holographic models in terms of the action [26]:

$$S = \frac{1}{16\pi G_5}\int d^5x\sqrt{g}\left(\mathscr{R} - \frac{1}{2}\left(\partial\phi\right)^2 - V\left(\phi\right) - \frac{f\left(\phi\right)}{4}F_{MN}F^{MN}\right), \tag{1}$$

where G_5 is the five-dimensional Newton constant. g denotes the determinant of the metric g_{MN}. $\mathscr{R}$ refers to the Ricci scalar. ϕ is called the scalar and induces the deformation away from conformality. $f(\phi)$ represents the gauge kinetic function. F_{MN} stands for the field strength associated with an Abelian gauge connection A_M. $V(\phi)$ is the potential which contains the cosmological constant term 2Λ and some other terms.

To obtain an AdS-black hole space-time, one considers a constant scalar field ϕ (or called dilaton) and assumes that $V(\phi) = 2\Lambda$ as well as $f(\phi) = 1$. Then the action of (1) can be simplified as

$$S = \frac{1}{16\pi G_5}\cdot\int d^5x\sqrt{g}\left(\mathscr{R} - 2\Lambda - \frac{1}{4}F_{MN}F^{MN}\right), \tag{2}$$

with the equations of motion

$$\mathscr{R}_{MN} - \frac{1}{2}\mathscr{R}g_{MN} + \Lambda g_{MN} = \frac{1}{2}\left(F_{MA}F_N^A - \frac{1}{4}g_{MN}F_{AB}F^{AB}\right), \tag{3}$$

$$\nabla_M F^{MN} = 0, \tag{4}$$

where ∇_M is the Levi-Civita covariant derivative with respect to the metric g_{MN}.

Supposing that the horizon function $f(z)$ vanishes at the point $z = z_h$, then the solution of (3) (with vanishing right-hand side) becomes the AdS_5-Schwarzschild metric:

$$ds^2 = \frac{R^2}{z^2}\left(-f\left(z\right)dt^2 + d\vec{x}^2 + \frac{1}{f\left(z\right)}dz^2\right), \tag{5}$$

with

$$f\left(z\right) = 1 - \frac{z^4}{z_h^4}, \tag{6}$$

where z_h can be related to the temperature as $T = 1/(\pi z_h)$. Notice that, in the limit $z_h \to \infty$ (correspond to zero temperature), the metric of (5) reduces to the AdS_5 metric, as expected.

To emulate confinement in the boundary theory, one can introduce a quadratic dilaton, $\phi \propto z^2$, similar to the manipulation mentioned in [20]. To this end, the Andreev-Zakharov model can be defined by the metric of (5) multiplied by a warp factor, $h(z) = e^{\phi} = e^{(1/2)cz^2}$, where c is the deformation parameter whose value can be fixed from the ρ meson trajectory as $c \sim 0.9\,\mathrm{GeV}^2$ [27]. Then the metric of the Andreev-Zakharov model is given by [21]

$$ds^2 = \frac{R^2h\left(z\right)}{z^2}\left(-f\left(z\right)dt^2 + d\vec{x}^2 + \frac{1}{f\left(z\right)}dz^2\right). \tag{7}$$

If one works with $r = R^2/z$ as the radial coordinate, the metric of (7) turns into

$$ds^2 = \frac{r^2h\left(r\right)}{R^2}\left(-f\left(r\right)dt^2 + d\vec{x}^2\right) + \frac{R^2h\left(r\right)}{r^2f\left(r\right)}dr^2, \tag{8}$$

with

$$f\left(r\right) = 1 - \frac{r_h^4}{r^4}. \tag{9}$$

Now, the wrap factor becomes $h(r) = e^{cR^4/2r^2}$ and the temperature is $T = r_h/(\pi R^2)$ with $r = r_h$ as the horizon. Note that the two metrics (7) and (8) are equal but only with different coordinate systems.

3. The Entropic Force

The entropic force is an emergent force. According to the second law of thermodynamics, it stems from multiple interactions which drive the system toward the state with a larger entropy. This force was originally introduced in [31] many years ago and proposed to responsible for the gravity [32] recently. In a more recent work, Kharzeev [8] argued that it would be responsible for dissociating the quarkonium.

In [8], the entropic force is expressed as

$$\mathcal{F} = T\frac{\partial S}{\partial L}, \tag{10}$$

where T is the temperature of the plasma, L represents the interdistance of $Q\overline{Q}$, and S stands for the entropy.

On the other hand, the entropy is given by

$$S = -\frac{\partial F}{\partial T}, \tag{11}$$

where F is the free energy of $Q\overline{Q}$, which is equal to the on-shell action of the fundamental string in the dual geometry from the holographic point of view. In fact, the free energy has been studied, for example, in [33–35].

We now follow the calculations of [15] to analyze the entropic force with the metric (8). The Nambu-Goto action is

$$S = T_F \int d\tau\, d\sigma \mathcal{L} = T_F \int d\tau\, d\sigma \sqrt{g}, \tag{12}$$

where $T_F = 1/2\pi\alpha'$ is the fundamental string tension and α' can be related to the 't Hooft coupling constant by $\alpha' = R^2/\sqrt{\lambda}$. g denotes the determinant of the induced metric with

$$g_{\alpha\beta} = g_{\mu\nu}\frac{\partial X^\mu}{\partial\sigma^\alpha}\frac{\partial X^\nu}{\partial\sigma^\beta}, \tag{13}$$

where X^μ is the target space coordinates and $g_{\mu\nu}$ is the metric.

Parameterizing the static string coordinates by

$$X^\mu = \left(\tau, \sigma, 0, 0, r(\sigma)\right), \tag{14}$$

one finds the induced metric as

$$\begin{aligned} g_{00} &= \frac{r^2}{R^2}h(r)\, f(r), \\ g_{01} &= g_{10} = 0, \\ g_{11} &= \frac{r^2}{R^2}h(r) + \frac{R^2}{r^2}h(r)\, f(r)^{-1}\dot{r}^2, \end{aligned} \tag{15}$$

with $\dot{r} = \partial r/\partial\sigma$.

Then the Lagrangian density is found to be

$$\mathcal{L} = \sqrt{a(r) + b(r)\dot{r}^2}, \tag{16}$$

with

$$\begin{aligned} a(r) &= \frac{h^2(r)\, f(r)\, r^4}{R^4}, \\ b(r) &= h^2(r). \end{aligned} \tag{17}$$

Note that $\mathcal{L}$ does not depend on σ explicitly, so the Hamiltonian density is a constant:

$$\mathcal{H} = \mathcal{L} - \frac{\partial\mathcal{L}}{\partial\dot{r}}\dot{r} = \text{constant}. \tag{18}$$

Applying the boundary condition at $\sigma = 0$,

$$\begin{aligned} \dot{r} &= 0, \\ r &= r_c, \end{aligned} \tag{19}$$

one finds

$$\mathcal{H} = \sqrt{\frac{h^2(r_c)\, f(r_c)\, r_c^4}{R^4}}, \tag{20}$$

with

$$\begin{aligned} f(r_c) &= 1 - \frac{r_h^4}{r_c^4}, \\ h(r_c) &= e^{cR^4/2r_c^2}, \end{aligned} \tag{21}$$

where r_c is the lowest position of the string in the bulk.

From (16), (18), and (20), one gets

$$\dot{r} = \frac{dr}{d\sigma} = \sqrt{\frac{a^2(r) - a(r)\, a(r_c)}{a(r_c)\, b(r)}}. \tag{22}$$

By integrating (22), the interquark distance is obtained:

$$L = 2\int_{r_c}^{\infty} dr \sqrt{\frac{a(r_c)\, b(r)}{a^2(r) - a(r)\, a(r_c)}}, \tag{23}$$

with

$$a(r_c) = \frac{h^2(r_c)\, f(r_c)\, r_c^4}{R^4}. \tag{24}$$

To analyze the effect of the deformation parameter on the interdistance, we plot LT as a function of ε with $\varepsilon \equiv r_h/r_c$ for $c = 0$ and $c = 0.9\,\text{GeV}^2$ in Figure 1. From the figures, one can see that LT increases in the presence of c. Namely, the deformation parameter has the effect of increasing the interdistance.

Moreover, one finds that for each plot LT is an increasing function for $\varepsilon < \varepsilon_{\max}$ but a decreasing one for $\varepsilon > \varepsilon_{\max}$. In fact, in the latter case, some new configurations [36] should be taken into account. However, these configurations are not solutions of the Nambu-Goto action so that the range of $LT > LT_{\max}$ is not trusted. In other words, we have more interest in the range of $LT < LT_{\max}$. For convenience, we write $b = LT_{\max}$. With numerical methods, we find $b \simeq 0.31$ for $c = 0.9\,\text{GeV}^2$ and $b \simeq 0.27$ for $c = 0$.

Next, we discuss the free energy. There are two cases.

(1) If $L > b/T$, the fundamental string will break in two pieces implying that the quarks are completely screened. For this case, the choice of the free energy $F^{(2)}$ is not unique [37],

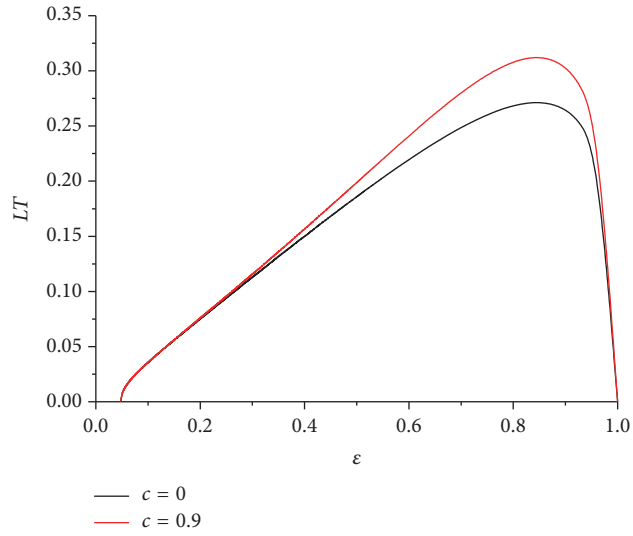

FIGURE 1: LT versus ε with $\varepsilon \equiv r_h/r_c$. From top to bottom, $c = 0.9\,\mathrm{GeV}^2$ and $c = 0$, respectively. Here, we take $R = 1$.

and we here choose a configuration of two disconnected trailing drag strings [38]; that is,

$$F^{(2)} = 2T_F \int_{r_h}^{\infty} h(r)\, dr. \tag{25}$$

In terms of (11), one finds

$$S^{(2)} \simeq e^{c/2r_h^2} \left(1 - \frac{c}{r_h^2}\right) \sqrt{\lambda}\theta \left(L - \frac{b}{T}\right). \tag{26}$$

Notice that the results of [15] can be reproduced if one neglects the effect of the reformation parameter by plugging $c = 0$ in (26).

(2) If $L < b/T$, the fundamental string is connected. The free energy of the quark-antiquark pair can be obtained by substituting (22) into (12); that is,

$$F^{(1)} = \frac{1}{\pi\alpha'} \int_{r_c}^{\infty} dr \sqrt{\frac{a(r)\, b(r)}{a(r) - a(r_c)}}. \tag{27}$$

Likewise, using (11), one finds

$$S^{(1)} = -\frac{\sqrt{\lambda}}{2\pi} \int_{r_c}^{\infty} dr \frac{\left[a'(r)\, b(r) + a(r)\, b'(r)\right]\left[a(r) - a(r_c)\right] - a(r)\, b(r)\left[a'(r) - a'(r_c)\right]}{\sqrt{a(r)\, b(r)\left[a(r) - a(r_c)\right]^3}}, \tag{28}$$

where the derivatives are with respect to r_h and we have used the relation $\alpha' = R^2/\sqrt{\lambda}$.

To analyze the effect of the deformation parameter on the entropic force, we plot $S^{(1)}/\sqrt{\lambda}$ as a function of LT for $c = 0$ and $c = 0.9\,\mathrm{GeV}^2$ in Figure 2, respectively. One can see that increasing c leads to smaller entropy at small distances. In addition, from (10), one knows that the entropic force is related to the growth of the entropy with the distance, so one finds that increasing c leads to decreasing the entropic force. On the other hand, the entropic force is responsible for melting the quarkonium. Thus, one concludes that the presence of the deformation parameter tends to decrease the entropic force, thus making the heavy quarkonium dissociates harder. These results can be understood as follows. Increase of the interdistance can be regarded as decrease of r_h or decrease of the system temperature. Since the deformation parameter has the effect of increasing the interdistance, it will cool the system temperature, thus making the quarkonium dissociates harder. Interestingly, it was argued [29] that the deformation parameter has the effect of increasing the thermal width, thus increasing the dissociation length, in agreement with our findings.

4. Summary and Discussions

In heavy ion collisions, the dissociation of heavy quarkonium is an important experimental signal for QGP formation. Recently, the destruction of heavy quarkonium due to the entropic force has been discussed in the context of AdS/CFT [15]. It was shown that a sharp peak of the entropy exists near the deconfinement transition and the growth of the entropy with the distance is responsible for the entropic force.

In this paper, we have investigated the destruction of heavy quarkonium in a deformed AdS_5 model. The effect of the deformation parameter on the interdistance was analyzed. The influence of the deformation parameter on

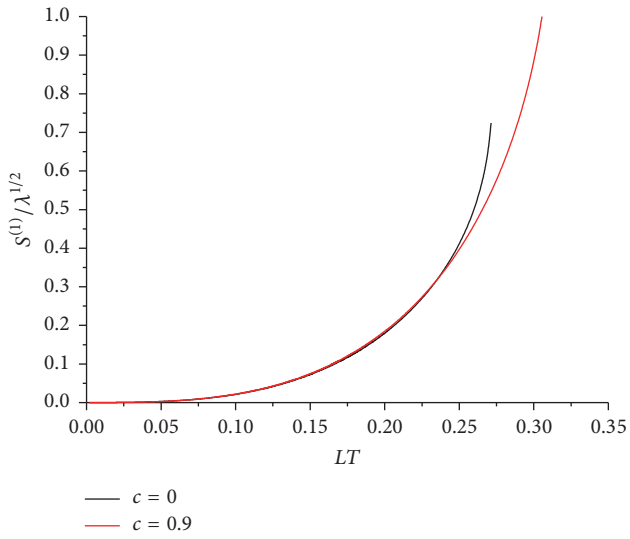

FIGURE 2: $S^{(1)}/\sqrt{\lambda}$ against LT. Here, we take $R = 1$.

the entropic force was also studied. It is shown that the interquark distance increases in the presence of the deformation parameter. Moreover, the deformation parameter has the effect of decreasing the entropic force. Since the entropic force is responsible for destroying the bound quarkonium states, we conclude that the presence of the deformation parameter tends to decrease the entropic force, thus making the quarkonium melt harder, consistent with the findings of [29]. Also, we have presented a possible understanding to this result: increase of the interdistance is equivalent to decrease of r_h or decrease of the system temperature. As the deformation parameter can increase the interdistance, it will cool the system temperature, thus making the quarkonium dissociate harder.

In addition, to understand the "usual" or "unusual" behavior of meson, we have compared the results between $c \neq 0$ and $c = 0$. It is found that the quarkonium dissociates harder in a deformed AdS background than in a usual AdS background.

Finally, it would be interesting to study the entropic force in some other holographic QCD models, such as the Sakai-Sugimoto model [18] and the Pirner-Galow model [24]. This will be left as a further investigation.

Conflicts of Interest

The authors declare that they have no conflicts of interest.

Acknowledgments

This research is partly supported by the Ministry of Science and Technology of China (MSTC) under 973 Project no. 2015CB856904(4). Zi-qiang Zhang and Gang Chen are supported by the NSFC under Grant no. 11475149. De-fu Hou is supported by the NSFC under Grants nos. 11375070 and 11521064.

References

[1] T. Matsui and H. Satz, "J/ψ suppression by quark-gluon plasma formation," *Physics Letters B*, vol. 178, no. 4, pp. 416–422, 1986.

[2] A. Adare and et al., "J/ψ production versus centrality, transverse momentum, and rapidity in Au + Au collisions a $\sqrt{S_{NN}}$ = 200 GeV," *Physical Review Letters*, vol. 98, no. 24, p. 8, 2007.

[3] B. B. Abelev and et al., "Centrality, rapidity and transverse momentum dependence of J/ψ suppression in Pb–Pb collisions at $\sqrt{S_{NN}}$ = 2.76 TeV," *Physics Letters B*, vol. 734, pp. 314–327, 2014.

[4] D. Kharzeev and H. Satz, "Quarkonium interactions in hadronic matter," *Physics Letters B*, vol. 334, no. 1-2, pp. 155–162, 1994.

[5] E. V. Shuryak, "Quark-gluon plasma and hadronic production of leptons, photons and psions," *Physics Letters B*, vol. 78, no. 1, pp. 150–153, 1978.

[6] P. Braun-Munzinger and J. Stachel, "(Non)thermal aspects of charmonium production and a new look at J/ψ suppression," *Physics Letters B*, vol. 490, no. 3-4, pp. 196–202, 2000.

[7] R. L. Thews, M. Schroedter, and J. Rafelski, "Enhanced J/ψ production in deconfined quark matter," *Physical Review C—Nuclear Physics*, vol. 63, no. 5, pp. 549051–549055, 2001.

[8] D. E. Kharzeev, "Deconfinement as an entropic self-destruction: a solution for the quarkonium suppression puzzle?" *Physical Review D*, vol. 90, no. 7, Article ID 074007, 2014.

[9] O. Kaczmarek, F. Karsch, P. Petreczky, and F. Zantow, "Heavy quark-antiquark free energy and the renormalized Polyakov loop," *Physics Letters, Section B: Nuclear, Elementary Particle and High-Energy Physics*, vol. 543, no. 1-2, pp. 41–47, 2002.

[10] O. Kaczmarek and F. Zantow, "Static quark anti-quark interactions at zero and finite temperature QCD. II. Quark anti-quark internal energy and entropy," https://arxiv.org/abs/hep-lat/0506019.

[11] P. Petreczky and K. Petrov, "Free energy of a static quark-antiquark pair and the renormalized Polyakov loop in three flavor QCD," *Physical Review D*, vol. 70, no. 5, Article ID 054503, 2004.

[12] J. Maldacena, "The large N limit of superconformal field theories and supergravity," *Advances in Theoretical and Mathematical Physics*, vol. 2, no. 2, pp. 231–252, 1998.

[13] S. S. Gubser, I. R. Klebanov, and A. M. Polyakov, "Gauge theory correlators from non-critical string theory," *Physics Letters B*, vol. 428, no. 1-2, pp. 105–114, 1998.

[14] O. Aharony, S. S. Gubser, J. Maldacena, H. Ooguri, and Y. Oz, "Large N field theories, string theory and gravity," *Physics Reports*, vol. 323, no. 3-4, pp. 183–386, 2000.

[15] K. Hashimoto and D. E. Kharzeev, "Entropic destruction of heavy quarkonium in non-Abelian plasma from holography," *Physical Review D*, vol. 90, no. 12, Article ID 125012, 2014.

[16] K. B. Fadafan and S. K. Tabatabaei, "Entropic destruction of a moving heavy quarkonium," *Physical Review D*, vol. 94, no. 2, Article ID 026007, 2016.

[17] Z.-q. Zhang, D.-f. Hou, and G. Chen, "The effect of chemical potential on imaginary potential and entropic force," *Physics Letters B*, vol. 768, pp. 180–186, 2017.

[18] T. Sakai and S. Sugimoto, "Low energy hadron physics in holographic QCD," *Progress of Theoretical Physics*, vol. 113, no. 4, pp. 843–882, 2005.

[19] J. Erlich, E. Katz, D. T. Son, and M. A. Stephanov, "QCD and a holographic model of hadrons," *Physical Review Letters*, vol. 95, no. 26, Article ID 261602, 2005.

[20] A. Karch, E. Katz, D. T. Son, and M. A. Stephanov, "Linear confinement and AdS/QCD," *Physical Review D*, vol. 74, no. 1, Article ID 015005, 2006.

[21] O. Andreev and V. I. Zakharov, "The spatial string tension, thermal phase transition, and AdS/QCD," *Physics Letters B*, vol. 645, no. 5-6, pp. 437–441, 2007.

[22] S. He, M. Huang, and Q.-S. Yan, "Logarithmic correction in the deformed AdS_5 model to produce the heavy quark potential and QCD beta function," *Physical Review D*, vol. 83, no. 4, Article ID 045034, 2011.

[23] U. Gürsoy and E. Kiritsis, "Exploring improved holographic theories for QCD: part I," *Journal of High Energy Physics*, vol. 2008, no. 2, Article ID 032, 2008.

[24] H. J. Pirner and B. Galow, "Equivalence of the AdS-metric and the QCD running coupling," *Physics Letters, Section B: Nuclear, Elementary Particle and High-Energy Physics*, vol. 679, no. 1, pp. 51–55, 2009.

[25] D. Li, S. He, M. Huang, and Q.-S. Yan, "Thermodynamics of deformed AdS_5 model with a positive/negative quadratic correction in graviton-dilaton system," *Journal of High Energy Physics*, vol. 2011, no. 9, Article ID 041, 2011.

[26] O. Dewolfe, S. S. Gubser, and C. Rosen, "A holographic critical point," *Physical Review D*, vol. 83, no. 8, Article ID 086005, 2011.

[27] O. Andreev, "$1/q^2$ corrections and gauge/string duality," *Physical Review D*, vol. 73, no. 10, Article ID 107901, 2006.

[28] N. R. F. Braga and L. F. Ferreira, "Thermal width of heavy quarkonia from an AdS/QCD model," *Physical Review D*, vol. 94, no. 9, Article ID 094019, 2016.

[29] J. Sadeghi and S. Tahery, "The effects of deformation parameter on thermal width of moving quarkonia in plasma," *Journal of High Energy Physics*, vol. 2015, no. 6, Article ID 204, pp. 1–20, 2015.

[30] Z.-q. Zhang, D.-f. Hou, and G. Chen, "Heavy quark potential from deformed AdS_5 models," *Nuclear Physics A*, vol. 960, pp. 1–10, 2017.

[31] K. H. Meyer, G. V. Susich, and E. Valkó, "Die elastischen Eigenschaften der organischen Hochpolymeren und ihre kinetische Deutung," *Kolloid-Zeitschrift*, vol. 59, no. 2, pp. 208–216, 1932.

[32] E. Verlinde, "On the origin of gravity and the laws of Newton," *Journal of High Energy Physics*, vol. 2011, no. 4, Article ID 029, 2011.

[33] J. Maldacena, "Wilson loops in large N field theories," *Physical Review Letters*, vol. 80, no. 22, pp. 4859–4862, 1998.

[34] A. Brandhuber, N. Itzhaki, J. Sonnenschein, and S. Yankielowicz, "Wilson loops in the large N limit at finite temperature," *Physics Letters B*, vol. 434, no. 1-2, pp. 36–40, 1998.

[35] S. Rey, S. Theisen, and J. Yee, "Wilson-Polyakov loop at finite temperature in large-N gauge theory and anti-de Sitter supergravity," *Nuclear Physics B*, vol. 527, no. 1-2, pp. 171–186, 1998.

[36] D. Bak, A. Karch, and L. G. Yaffe, "Debye screening in strongly coupled $\mathcal{N} = 4$ supersymmetric Yang-Mills plasma," *Journal of High Energy Physics*, vol. 2007, no. 8, Article ID 049, 2007.

[37] M. Chernicoff, J. A. García, and A. Güijosa, "The energy of a moving quark-antiquark pair in an $\mathcal{N} = 4$ SYM plasma," *Journal of High Energy Physics*, vol. 2006, no. 9, Article ID 068, 2006.

[38] C. P. Herzog, A. Karch, P. Kovtun, C. Kozcaz, and L. G. Yaffe, "Energy loss of a heavy quark moving through $\mathcal{N} = 4$ supersymmetric Yang-Mills plasma," *Journal of High Energy Physics*, vol. 2006, no. 7, Article ID 013, 2006.

Hindawi
Advances in High Energy Physics
Volume 2017, Article ID 8276534, 7 pages
https://doi.org/10.1155/2017/8276534

Research Article

Heavy Quark Potential with Hyperscaling Violation

Zi-qiang Zhang,[1] Chong Ma,[1] De-fu Hou,[2] and Gang Chen[1]

[1]*School of Mathematics and Physics, China University of Geosciences, Wuhan 430074, China*
[2]*Institute of Particle Physics and Key Laboratory of Quark and Lepton Physics (MOE), Central China Normal University, Wuhan 430079, China*

Correspondence should be addressed to Zi-qiang Zhang; zhangzq@cug.edu.cn

Received 19 December 2016; Accepted 23 January 2017; Published 6 March 2017

Academic Editor: Song He

Copyright © 2017 Zi-qiang Zhang et al. This is an open access article distributed under the Creative Commons Attribution License, which permits unrestricted use, distribution, and reproduction in any medium, provided the original work is properly cited. The publication of this article was funded by SCOAP[3].

We investigate the behavior of the heavy quark potential in the backgrounds with hyperscaling violation. The metrics are covariant under a generalized Lifshitz scaling symmetry with the dynamical Lifshitz parameter z and hyperscaling violation exponent θ. We calculate the potential for a certain range of z and θ and discuss how it changes in the presence of the two parameters. Moreover, we add a constant electric field to the backgrounds and study its effects on the potential. It is shown that the heavy quark potential depends on the nonrelativistic parameters. Also, the presence of the constant electric field tends to increase the potential.

1. Introduction

AdS/CFT [1–3], which relates a d-dimensional quantum field theory with its dual gravitational theory, living in $(d + 1)$ dimensions, has yielded many important insights into the dynamics of strongly coupled gauge theories. For reviews, see [4–15] and references therein.

Due to the broad application of this characteristic, many authors have considered the generalizations of the metrics dual to field theories. One of such generalizations is to use metric with hyperscaling violation. Usually, the metric is considered to be an extension of the Lifshitz metric and has a generic Lorentz violating form [16–20]. As we know, Lorentz symmetry represents a foundation of both general relativity and the standard model, so one may expect new physics from Lorentz invariance violation. For that reason, the metrics with hyperscaling violation have been used to describe the string theory [21–25] and holographic superconductors [26–29] as well as QCD [30–32].

The heavy quark potential of QCD is an important quantity that can probe the confinement mechanism in the hadronic phase and the meson melting in the plasma phase. In addition, it has been measured in great detail in lattice simulations. The heavy quark potential for $\mathcal{N} = 4$ SYM theory was first obtained by Maldacena in his seminal work [33]. Interestingly, it is shown that for the AdS_5 space the energy shows a purely Coulombian behavior which agrees with a conformal gauge theory. This proposal has attracted lots of interest. After [33], there are many attempts to address the heavy quark potential from the holography. For example, the potential at finite temperature has been studied in [34, 35]. The subleading order correction to this quantity is discussed in [36, 37]. The potential has also been investigated in some AdS/QCD models [38, 39]. Other important results can be found, for example, in [40–44].

Although the theories with hyperscaling violation are intrinsically nonrelativistic, we can use them as toy models for quarks from the holography point of view. In addition, one can expect that the results obtained from these theories provide qualitative insights into analogous questions in QCD. In this paper, we will investigate the heavy quark potential in the Lifshitz backgrounds with hyperscaling violation. We want to know what will happen to the potential if we have the quark-antiquark pair in such backgrounds? More specifically, we would like to see how the potential changes in the presence of the nonrelativistic parameters. In addition, we will add a

constant electric field to the backgrounds and study how it affects the potential. These are the main motivations of the present work.

We organize the paper as follows. In the next section, the backgrounds of the hyperscaling violation theories in [25] are briefly reviewed. In Section 3, we study the heavy quark potential in these backgrounds in terms of the z and θ parameters. In Section 4, we investigate a constant electric field effect on the heavy quark potential. The last part is devoted to conclusion and discussion.

2. Hyperscaling Violation Theories

Let us begin with a brief review of the background in [25]. It has been argued that the Lorentz invariance is broken in this background metric. Although charge densities induce a trivial (gapped) behavior at low energy/temperature, there still exist special cases where there are nontrivial IR fixed points (quantum critical points) where the theory is scale invariant. Usually, the metric is expressed as [21]

$$ds^2 = u^\theta \left[-\frac{dt^2}{u^{2z}} + \frac{b_0 du^2 + dx^i dx^i}{u^2} \right], \tag{1}$$

where $b_0 = \ell^2$ with ℓ being the IR scale. The above metric is covariant under a generalized Lifshitz scaling symmetry; that is,

$$\begin{aligned} t &\longrightarrow \lambda^z t, \\ u &\longrightarrow \lambda u, \\ x^i &\longrightarrow \lambda x^i, \\ ds^2 &\longrightarrow \lambda^{-\theta} ds^2, \end{aligned} \tag{2}$$

where z is called the dynamical Lifshitz parameter or the dynamical critical exponent which characterizes the behavior of system near the phase transition. θ stands for the hyperscaling violation exponent which is responsible for the nonstand scaling of physical quantities and controls the transformation of the metric. The scalar curvature of these geometries is

$$R = -\frac{3\theta^2 - 4(z+3)\theta + 2\left(z^2 + 3z + 6\right)}{b_0} u^{-\theta}. \tag{3}$$

The geometries are flat when $\theta = 2$ and $z = 0, 1$. The geometry is Ricci flat when $\theta = 4$ and $z = 3$. The geometry is in Rindler coordinates when $\theta = 0$ and $z = 1$. Usually, the above special solutions violate the Gubser bound conditions [25]. In addition, the pure Lifshitz case is related to $\theta = 0$.

By using a radical redefinition

$$u = (2 - z)\, r^{1/(2-z)} \tag{4}$$

and rescaling t and x^i, we have the following metric:

$$\begin{aligned} ds^2 &\sim r^{(\theta-2)/(2-z)} \left[-f(r)\, dt^2 + \frac{dr^2}{f(r)} + dx^i dx^i \right], \\ f(r) &= f_0 r^{2(1-z)/(2-z)}, \end{aligned} \tag{5}$$

with $f_0 = (2 - z)^{2(1-z)}$.

In the presence of hyperscaling violations, the energy scale is

$$E \simeq u^{(\theta-2z)/2} \simeq r^{(\theta-2z)/2(2-z)}. \tag{6}$$

For the generalized scaling solutions of (5), the Gubser bound conditions are as follows:

$$\begin{aligned} \frac{2z + 3(2-\theta)}{2(z-1) - \theta} &> 0, \\ \frac{z - 1}{2(z-1) - \theta} &> 0, \\ \frac{2(z-1) + 3(2-\theta)}{2(z-1) - \theta} &> 0. \end{aligned} \tag{7}$$

Also, to consider the thermodynamic stability, one needs

$$\frac{z}{2(z-1) - \theta} > 0. \tag{8}$$

More discussions about other generalized Lifshitz geometries can be found in [25].

The generalizations of (5) to include finite temperature can be written as

$$\begin{aligned} ds^2 &\sim \left(\frac{r}{\ell}\right)^{-\alpha} \left[-f(r)\, dt^2 + \frac{dr^2}{f(r)} + dx^i dx^i \right], \\ f(r) &= f_0 \left(\frac{r}{\ell}\right)^{2\beta} h, \\ h &= 1 - \left(\frac{r}{r_h}\right)^{\gamma}, \end{aligned} \tag{9}$$

where $\alpha = (\theta - 2)/(z - 2)$, $\beta = (z - 1)/(z - 2)$, and $\gamma = (2z + 3(2 - \theta))/2(2 - z)$.

The Hawking temperature is

$$T = \frac{f_0}{8\pi\ell} \left(\frac{r_h}{\ell}\right)^{z/(z-2)} \left| \frac{2z - 3\theta + 6}{z - 2} \right|. \tag{10}$$

3. Heavy Quark Potential

In the holographic description, the heavy quark potential is given by the expectation value of the static Wilson loop

$$W(C) = \frac{1}{N} \mathrm{Tr} P e^{i \int A_\mu dx^\mu}, \tag{11}$$

where C is a closed loop in a 4-dimensional space time and the trace is over the fundamental representation of the SU(N) group. A_μ is the gauge potential and P enforces the path ordering along the loop C. The heavy quark potential can be extracted from the expectation value of this rectangular Wilson loop in the limit $\mathcal{T} \to \infty$:

$$\langle W(C) \rangle \sim e^{-\mathcal{T} V}. \tag{12}$$

On the other hand, the expectation value of Wilson loop in (12) is given by

$$\langle W(C) \rangle \sim e^{-S_c}, \tag{13}$$

where S_c is the regularized action. Therefore, the heavy quark potential can be expressed as

$$V = \frac{S_c}{\mathcal{T}}. \tag{14}$$

We now analyze the heavy quark potential using the metric of (9). The string action can reduce to the Nambu-Goto action:

$$S = -\frac{1}{2\pi\alpha'} \int d\tau\, d\sigma \sqrt{-\det g_{\alpha\beta}}, \tag{15}$$

where g is the determinant of the induced metric on the string world sheet embedded in the target space; that is,

$$g_{\alpha\beta} = G_{\mu\nu} \frac{\partial X^\mu}{\partial \sigma^\alpha} \frac{\partial X^\nu}{\partial \sigma^\beta}, \tag{16}$$

where X^μ and $G_{\mu\nu}$ are the target space coordinates and the metric, and σ^α with $\alpha = 0, 1$ parameterize the world sheet.

Using the parametrization $X^\mu = (t, x, 0, 0, r)$, $\sigma = x$, $\tau = t$ and $r = r(x)$, we extremize the open string worldsheet attached to a static quark at $x = +L/2$ and an antiquark at $x = -L/2$. Then the induced metric of the fundamental string is given by

$$g_{\alpha\beta} = b(r) \begin{pmatrix} -f(r) & 0 \\ 0 & 1 + \dfrac{\dot{r}^2}{f(r)} \end{pmatrix}, \tag{17}$$

with $b(r) = (r/\ell)^{-\alpha}$, $\dot{r} = dr/dx$.

Plugging (17) into (15), the Euclidean version of Nambu-Goto action in (9) becomes

$$S = \frac{\mathcal{T}}{2\pi\alpha'} \int dx \sqrt{b^2(r)\left[f(r) + \dot{r}^2\right]}. \tag{18}$$

We now identify the Lagrangian as

$$\mathcal{L} = \sqrt{b^2(r)\left[f(r) + \dot{r}^2\right]}. \tag{19}$$

Note that $\mathcal{L}$ does not depend on x explicitly, so the corresponding Hamiltonian will be a constant of motion; that is,

$$H = \frac{\partial \mathcal{L}}{\partial \dot{r}} \dot{r} - \mathcal{L} = \text{Constant} = C. \tag{20}$$

This constant can be found at special point $r(0) = r_c$, where $r_c' = 0$, as

$$H = -\sqrt{f(r_c)\, b^2(r_c)}, \tag{21}$$

and then a differential equation is derived:

$$\dot{r} = \sqrt{\frac{f^2(r)\, b^2(r) - f(r)\, f(r_c)\, b^2(r_c)}{f(r_c)\, b^2(r_c)}}, \tag{22}$$

with

$$f(r_c) = f_0 \left(\frac{r_c}{\ell}\right)^{2\beta} h_1,$$
$$h_1 = 1 - \left(\frac{r_c}{r_h}\right)^{\gamma}, \tag{23}$$
$$b(r_c) = \left(\frac{r_c}{\ell}\right)^{-\alpha}.$$

By integrating (22) the separation length $L(\theta, z)$ of quark-antiquark pair becomes

$$L(\theta, z) = 2 \int_0^{r_c} dr \sqrt{\frac{f(r_c)\, b^2(r_c)}{f^2(r)\, b^2(r) - f(r)\, f(r_c)\, b^2(r_c)}}. \tag{24}$$

On the other hand, plugging (22) into the Nambu-Goto action of (18), one finds the action of the heavy quark pair:

$$S = \frac{\mathcal{T}}{\pi\alpha'} \int_0^{r_c} dr b^2(r) \sqrt{\frac{f(r)}{f(r)\, b^2(r) - f(r_c)\, b^2(r_c)}}. \tag{25}$$

This action is divergent, but the divergences can be avoided by subtracting the inertial mass of two free quarks, given by

$$S_0 = \frac{\mathcal{T}}{\pi\alpha'} \int_0^{r_h} dr b(r). \tag{26}$$

Subtracting this self-energy, the regularized action is obtained:

$$S_c = S - S_0. \tag{27}$$

Applying (14), we end up with the heavy quark potential with hyperscaling violation:

$$V(\theta, z) = \frac{1}{\pi\alpha'} \int_0^{r_c} dr \cdot \left[b^2(r) \sqrt{\frac{f(r)}{f(r)\, b^2(r) - f(r_c)\, b^2(r_c)}} - b(r) \right] - \frac{1}{\pi\alpha'} \int_{r_c}^{r_h} dr b(r). \tag{28}$$

Note that the potential $V(z)$ in the Lifshitz space-time [45, 46] can be derived from (28) if we neglect the effect of the hyperscaling violation exponent by plugging $\theta = 0$ in (28). Also, in the limit ($\theta = 0$, $z = 1$), (28) can reduce to the finite temperature case in [34, 35].

Before evaluating the heavy quark potential of (28), we should pause here to determine the allowed region for z and θ at hand. The space boundary is considered at $r = 0$, consequently $\alpha > 0$. To avoid (28) being ill-defined, it is required that $\gamma > 0$. Moreover, one should consider the

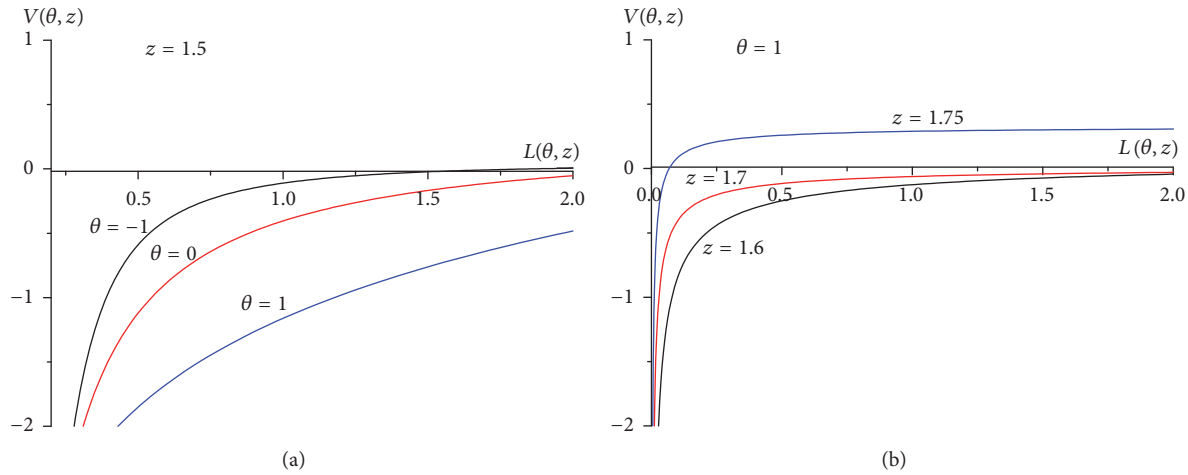

Figure 1: Plots of $V(\theta, z)$ versus $L(\theta, z)$. (a) $z = 1.5$; from top to bottom $\theta = -1, 0, 1$, respectively; (b) $\theta = 1$; from top to bottom $z = 1.75, 1.7, 1.6$, respectively.

Gubser conditions of (7) and the thermodynamic stability condition of (8). With these restrictions, one finds

$$1 < z < 2,$$
$$\theta < 2, \tag{29}$$
$$\theta < z,$$

and then one can choose the values of z and θ in such a range.

In Figure 1, we plot the potential $V(\theta, z)$ versus distance $L(\theta, z)$ with different z, θ. In Figure 1(a), the dynamical exponent is $z = 1.5$ and from top to bottom the hyperscaling violation exponent is $\theta = -1, 0, 1$, respectively. In Figure 1(b), $\theta = 1$ and from top to bottom $z = 1.75, 1.7, 1.6$, respectively. From the figures, we can see clearly that by increasing θ the potential decreases. One finds also that increasing z leads to increasing the potential. In other words, increasing z and θ had different effects on the potential. Then one can change the potential by changing the values of these parameters. Therefore, the heavy quark potential depends on the nonrelativistic parameters.

To study how the potential changes with the temperature T, we show $V(\theta, z)$ as a function of $L(\theta, z)$ with $z = 1.6$, $\theta = 1$ in Figure 2. From (10), we can see that T is a decreasing function of z_h for $z = 1.6$. So one finds in Figure 2 that increasing T (or decreasing z_h) leads to increasing the potential. This result is consistent with the finding of [34, 35].

Moreover, to see the short distance behavior of the potential, we take the limit $L(\theta, z)T \to 0$ and find the following approximate formula:

$$L(\theta, z) \simeq \frac{2 f_0^{-1/2}}{\alpha - 2\beta + 1} r_c^{1-\beta},$$
$$V(\theta, z) \simeq \frac{\sqrt{\lambda}}{\pi (1-\alpha)} r_c^{1-\alpha}, \tag{30}$$

which yields

$$V(\theta, z) \propto L(\theta, z)^{\theta - z}. \tag{31}$$

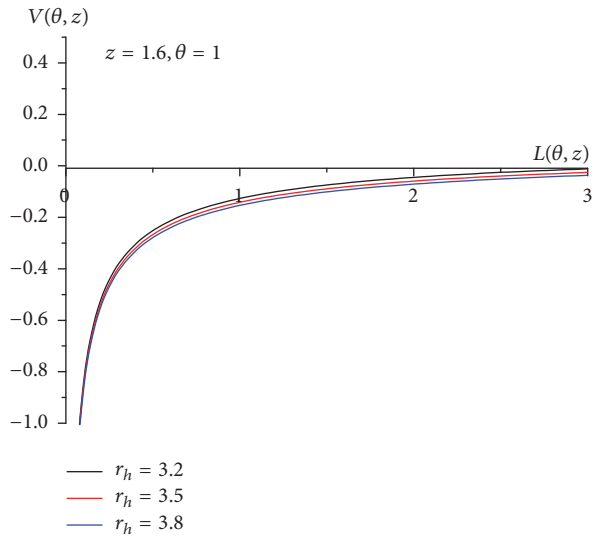

Figure 2: Plots of $V(\theta, z)$ versus $L(\theta, z)$ with $z = 1.6$, $\theta = 1$. From top to bottom $r_h = 3.2, 3.5, 3.8$, respectively.

One can see that the potential is dependent on z and θ. In the special case of $\theta = 0$, $z = 1$ (or $\alpha = 2$, $\beta = 0$), one finds that the potential is of Coulomb type:

$$V(\theta, z) \simeq -\frac{\sqrt{\lambda}}{1.5\pi L(\theta, z)}, \tag{32}$$

but for other cases, the potential may not be Coulombian.

4. Effect of Constant Electric Field

In this section, we study the effect of a constant electric field on the heavy quark potential following the method proposed in [12]. The constant B-field is along the x^1 and x^2 directions. As the field strength is involved in the equations of motion, this ansatz could be a good solution to supergravity as well as

a simple way of studying the B-field correction. The constant B-field is added to the metric of (9) by the following form:

$$B = B_{01} dt \wedge dx^1 + B_{12} dx^1 \wedge dx^2, \tag{33}$$

where B_{01} and B_{12} are assumed to be constants with $B_{01} = E$ being the NS-NS antisymmetric electric field and $B_{12} = H$ being the NS-NS antisymmetric magnetic field.

The constant B-field considered here is only turned on x^1 direction, which implies $H = 0$. After adding an electric field to this background metric of (9), the string action is given by

$$S = -\frac{1}{2\pi\alpha'} \int d\tau\, d\sigma \sqrt{-\det\left(g + b\right)_{\alpha\beta}}, \tag{34}$$

where $g_{\alpha\beta}$ is given in (17). $b_{\alpha\beta} = B_{\mu\nu}\partial_\alpha X^\mu \partial_\beta X^\nu$ is obtained as

$$b_{\alpha\beta} = \begin{pmatrix} 0 & 0 \\ 0 & \xi \end{pmatrix}, \tag{35}$$

and then the string action in (34) reads

$$S = \frac{\mathcal{T}}{2\pi\alpha'} \int dx \sqrt{b^2(r) f(r) + b(r) f(r) \xi + b^2(r) \dot{r}^2}. \tag{36}$$

Parallel to the case of the previous section, we have

$$\dot{r} = \sqrt{\frac{A^2(r) - A(r) A(r_c)}{A(r_c) b^2(r)}}, \tag{37}$$

with

$$\begin{aligned} A(r) &= b^2(r) f(r) + b(r) f(r) \xi, \\ A(r_c) &= b^2(r_c) f(r_c) + b(r_c) f(r_c) \xi. \end{aligned} \tag{38}$$

We call again the separation length and the heavy quark potential as L and V, respectively. One finds

$$\begin{aligned} L &= 2 \int_0^{r_c} dr \sqrt{\frac{A(r_c) b^2(r)}{A^2(r) - A(r) A(r_c)}}, \\ V &= \frac{1}{\pi\alpha'} \int_0^{r_c} dr \left[\sqrt{\frac{A(r) b^2(r)}{A(r) - A(r_c)}} - b(r) \right] \\ &\quad - \frac{1}{\pi\alpha'} \int_{r_c}^{r_h} dr b(r). \end{aligned} \tag{39}$$

To see the effect of the constant electric field ξ on the heavy quark potential in the backgrounds with hyperscaling violation, we plot the heavy quark potential as a function of the interdistance for $z = 1.7$, $\theta = 1$ with three different ξ in Figure 3. In the plots from top to bottom $\xi = 3.0, 1.5, 0.1$, respectively. From the figures, we can see that the heavy quark potential increases with increasing ξ. In other words, the presence of the constant electric field leads to a smaller screening radius. This result can be understood by considering the relation between the potential and the viscosity of the medium. It was argued [47] that, increasing the viscosity, the screening of the potential due to the thermal medium weakens and so the potential decreases. On the other hand, the presence of the constant electric field tends to weaken the viscosity [12]. Thus, increasing the constant electric field leads to weakening the viscosity or increasing the potential.

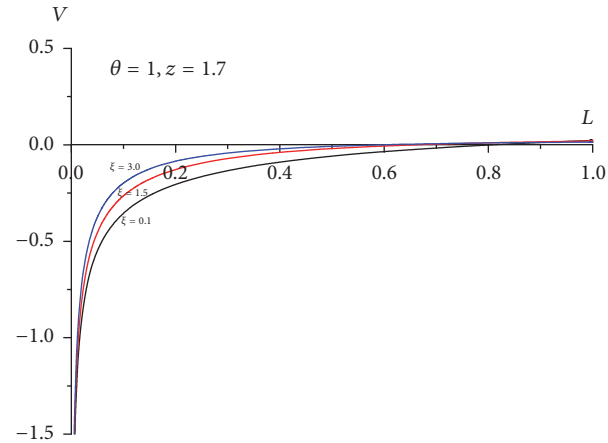

Figure 3: Plots of V versus L with different ξ. Here $z = 1.7$ and $\theta = 1$. From top to bottom $\xi = 3.0, 1.5, 0.1$, respectively.

5. Conclusion and Discussion

In this paper, we have investigated the heavy quark potential in the backgrounds with hyperscaling violation at finite temperature. These theories are strongly coupled with anisotropic scaling symmetry in the time and a spatial direction. Although the theories are not directly applicable to QCD, the features of them are similar to QCD. Therefore one can expect that the results obtained from these theories provide qualitative insights into analogous questions in QCD. In addition, an understanding of how the heavy quark potential changes by these theories may be useful for theoretical predictions.

In Section 3, we used the holographic description to calculate the heavy quark potential at finite temperature. We considered the space boundary at $r = 0$ and discussed the potential for a certain range of z and θ which satisfies the Gubser conditions and the thermodynamic stability condition. In is shown that increasing z and θ had different effects: the potential increases as z increases but it decreases as θ increases. As a result, the heavy quark potential depends on the nonrelativistic parameters. In Section 4, we added a constant electric field to the background metrics and study its effect on the heavy quark potential. We observed that the potential rises as the constant electric field increases. In other words, the presence of the constant electric field leads to increasing the heavy quark potential.

Finally, it is interesting to mention that the drag force [4] can also be studied in the backgrounds with hyperscaling violation. We will leave this for further study.

Competing Interests

The authors declare that they have no competing interests.

Acknowledgments

This research is partly supported by the Ministry of Science and Technology of China (MSTC) under the 973 Project no. 2015CB856904(4). Zi-qiang Zhang and Gang Chen are supported by the NSFC under Grant no. 11475149. De-fu Hou is supported by the NSFC under Grant nos. 11375070 and 11521064.

References

[1] J. Maldacena, "The large-N limit of superconformal field theories and supergravity," *International Journal of Theoretical Physics*, vol. 38, no. 4, pp. 1113–1133, 1999.

[2] S. Gubser, I. Klebanov, and A. Polyakov, "Gauge theory correlators from non-critical string theory," *Physics Letters B*, vol. 428, no. 1-2, pp. 105–114, 1998.

[3] O. Aharony, S. S. Gubser, J. Maldacena, H. Ooguri, and Y. Oz, "Large N field theories, string theory and gravity," *Physics Reports. A Review Section of Physics Letters*, vol. 323, no. 3-4, pp. 183–386, 2000.

[4] C. P. Herzog, A. Karch, P. Kovtun, C. Kozcaz, and L. G. Yaffe, "Energy loss of a heavy quark moving through $N = 4$ supersymmetric Yang-Mills plasma," *Journal of High Energy Physics*, vol. 2006, no. 7, 2006.

[5] C. P. Herzog, "Energy loss of a heavy quark from asymptotically AdS geometries," *Journal of High Energy Physics*, vol. 2006, no. 9, article no. 032, 2006.

[6] M. Ali-Akbari and U. Gürsoy, "Rotating strings and energy loss in non-conformal holography," *Journal of High Energy Physics*, vol. 2012, no. 1, 2012.

[7] S. S. Gubser, "Drag force in AdS/CFT," *Physical Review. D. Third Series*, vol. 74, 2006.

[8] E. Caceres and A. Guijosa, "Drag force in a charged $\mathcal{N} = 4$ SYM plasma," *Journal of High Energy Physics*, vol. 2006, no. 11, article 077, 2006.

[9] J. Sadeghi and B. Pourhassan, "Drag force of moving quark at $\mathcal{N} = 2$ supergravity," *Journal of High Energy Physics*, vol. 2008, no. 12, article no. 026, 2008.

[10] K. B. Fadafan and H. Soltanpanahi, "Energy loss in a strongly coupled anisotropic plasma," *Journal of High Energy Physics*, vol. 2012, no. 10, article no. 085, 2012.

[11] M. Chernicoff, J. A. Garcia, and A. Guijosa, "The energy of a moving quark-antiquark pair in an $\mathcal{N} = 4$ SYM plasma," *Journal of High Energy Physics*, vol. 2006, no. 9, article 068, 2006.

[12] T. Matsuo, D. Tomino, and W. Wen, "Drag force in SYM plasma with B field from AdS/CFT," *Journal of High Energy Physics*, vol. 2006, no. 10, article no. 055, 2006.

[13] R. Cai, S. Chakrabortty, S. He, and L. Li, "Some aspects of QGP phase in a hQCD model," *Journal of High Energy Physics*, vol. 2013, no. 2, article no. 068, 2013.

[14] M. Ali-Akbari and K. B. Fadafan, "Rotating mesons in the presence of higher derivative corrections from gauge-string duality," *Nuclear Physics B*, vol. 835, no. 1-2, pp. 221–237, 2010.

[15] U. Gürsoy and E. Kiritsis, "Exploring improved holographic theories for QCD: part I," *Journal of High Energy Physics*, vol. 2008, no. 2, article no. 032, 2008.

[16] T. Azeyanagi, W. Li, and T. Takayanagi, "On string theory duals of Lifshitz-like fixed points," *Journal of High Energy Physics*, vol. 2009, no. 6, article 084, 2009.

[17] K. Balasubramanian and K. Narayan, "Lifshitz spacetimes from AdS null and cosmological solutions," *Journal of High Energy Physics*, vol. 2010, no. 8, article 14, 2010.

[18] H. Singh, "Lifshitz/Schrödinger Dp-branes and dynamical exponents," *Journal of High Energy Physics*, vol. 2012, no. 7, article 82, 2012.

[19] K. Narayan, "Lifshitz scaling and hyperscaling violation in string theory," *Physical Review D*, vol. 85, no. 10, Article ID 106006, 2012.

[20] P. Dey and S. Roy, "Intersecting D-branes and Lifshitz-like space-time," *Physical Review D*, vol. 86, 2012.

[21] B. Goutéraux and E. Kiritsis, "Generalized holographic quantum criticality at finite density," *Journal of High Energy Physics*, vol. 2011, no. 12, article no. 036, 2011.

[22] E. Perlmutter, "Domain wall holography for finite temperature scaling solutions," *Journal of High Energy Physics*, vol. 2011, no. 2, article 013, 2011.

[23] M. Alishahiha and H. Yavartanoo, "On holography with hyperscaling violation," *Journal of High Energy Physics*, vol. 2012, no. 11, 2012.

[24] J. Sadeghi, B. Pourhassan, and F. Pourasadollah, "Thermodynamics of Schrodinger black holes with hyperscaling violation," *Physics Letters. B. Particle Physics, Nuclear Physics and Cosmology*, vol. 720, no. 1–3, pp. 244–249, 2013.

[25] E. Kiritsis, "Lorentz violation, gravity, dissipation and holography," *Journal of High Energy Physics*, vol. 2013, no. 1, article 030, 2013.

[26] E. J. Brynjolfsson, U. H. Danielsson, L. Thorlacius, and T. Zingg, "Holographic superconductors with Lifshitz scaling," *Journal of Physics. A. Mathematical and Theoretical*, vol. 43, Article ID 065401, 2010.

[27] S. Sin, S. Xu, and Y. Zhou, "Holographic superconductor for a lifshitz fixed point," *International Journal of Modern Physics A*, vol. 26, no. 26, pp. 4617–4631, 2011.

[28] Y. Bu, "Holographic superconductors with $z = 2$ Lifshitz scaling," *Physical Review D*, vol. 86, no. 4, Article ID 046007, 2012.

[29] Q. Pan and S.-J. Zhang, "Revisiting holographic superconductors with hyperscaling violation," *The European Physical Journal C*, vol. 76, article 126, 2016.

[30] J. Sadeghi and S. Heshmatian, "Jet quenching parameter with hyperscaling violation," *The European Physical Journal C*, vol. 74, no. 9, 2014.

[31] J. Sadeghi and S. Heshmatian, "Decay widths of large-spin mesons from the noncritical string/gauge duality," *Physical Review D*, vol. 84, no. 12, 2011.

[32] K. B. Fadafan and F. Saiedi, "Holographic Schwinger effect in non-relativistic backgrounds," *The European Physical Journal C*, vol. 75, no. 12, 2015.

[33] J. M. Maldacena, "Wilson loops in large N field theories," *Physical Review Letters*, vol. 80, no. 22, pp. 4859–4862, 1998.

[34] A. Brandhuber, N. Itzhaki, J. Sonnenschein, and S. Yankielowicz, "Wilson loops in the large N limit at finite temperature," *Physics Letters B*, vol. 434, no. 1-2, pp. 36–40, 1998.

[35] S. Rey, S. Theisen, and J. Yee, "Wilson-Polyakov loop at finite temperature in large-N gauge theory and anti-de Sitter supergravity," *Nuclear Physics B*, vol. 527, no. 1-2, pp. 171–186, 1998.

[36] S. Chu, D. Hou, and H. Ren, "The subleading term of the strong coupling expansion of the heavy-quark potential in a $\mathcal{N} = 4$ super Yang-Mills vacuum," *Journal of High Energy Physics*, vol. 2009, 2009.

[37] Z. Zhang, D. Hou, H. Ren, and L. Yin, "The subleading term of the strong coupling expansion of the heavy-quark potential in a $\mathcal{N} = 4$ super Yang-Mills plasma," *Journal of High Energy Physics*, vol. 2011, no. 7, article 35, 2011.

[38] O. Andreev and V. I. Zakharov, "On heavy-quark free energies, entropies, Polyakov loop, and AdS/QCD," *Journal of High Energy Physics*, vol. 2007, no. 4, article no. 100, 2007.

[39] S. He, M. Huang, and Q. Yan, "Logarithmic correction in the deformed AdS5 model to produce the heavy quark potential and QCD beta function," *Physical Review D*, vol. 83, no. 4, Article ID 045034, 2011.

[40] J. Greensite and P. Olesen, "Remarks on the heavy quark potential in the supergravity approach," *Journal of High Energy Physics*, vol. 1998, 1998.

[41] F. Bigazzi, A. L. Cotrone, L. Martucci, and L. A. Pando Zayas, "Wilson loop, Regge trajectory, and hadron masses in a Yang-Mills theory from semiclassical strings," *Physical Review D—Particles, Fields, Gravitation and Cosmology*, vol. 71, no. 6, Article ID 066002, 2005.

[42] L. Martucci, "Semiclassical strings on confining backgrounds," *Fortschritte der Physik. Progress of Physics*, vol. 53, no. 7-8, pp. 936–942, 2005.

[43] Y. Kinar, E. Schreiber, and J. Sonnenschein, "$\overline{QQ}$ potential from strings in curved space-time—classical results," *Nuclear Physics. B*, vol. 566, no. 1-2, pp. 103–125, 2000.

[44] S. He, M. Huang, and Q. Yan, "Heavy quark potential and QCD beta function from a deformed AdS5 model," *Progress of Theoretical Physics Supplement*, vol. 186, pp. 504–509, 2010.

[45] U. H. Danielsson and L. Thorlacius, "Black holes in asymptotically Lifshitz spacetime," *Journal of High Energy Physics*, vol. 2009, 2009.

[46] J. Klusoň, "Open string in a nonrelativistic background," *Physical Review D*, vol. 81, no. 10, Article ID 106006, 8 pages, 2010.

[47] J. Noronha and A. Dumitru, "Heavy quark potential as a function of shear viscosity at strong coupling," *Physical Review D*, vol. 80, Article ID 014007, 2009.